Photochemical Generation of Alkyl and Acyl Radicals and their Application in Synthetic Organic Chemistry

Dissertation

zur Erlangung des Doktorgrades der Naturwissenschaften

(Dr. rer. nat.)

an der Fakultät für Chemie und Pharmazie

der Universität Regensburg

vorgelegt von

Tobias Emanuel Schirmer

aus Starnberg

2021

The experimental work of this thesis was carried out between January 2018 and December 2020 at the University of Regensburg, Institute of Organic Chemistry, group of Prof. König, and from June to November 2021 at *Sorbonne Université - Campus Pierre et Marie Curie,* Paris, group of Prof. Fensterbank. The thesis was supervised by Prof. König.

Date of submission: 13.12.2021

Date of colloquium: 28.01.2022

Board of examiners:

Prof. Dr. Julia Rehbein	(chair)
Prof. Dr. Burkhard König	(1st referee)
Prof. Dr. Louis Fensterbank	(2nd referee)
Prof. Dr. Robert Wolf	(examiner)

Table of Contents

CHAPTER I

Stereoselective Transformations of Ion Pairs in Photoredox Catalysis

Author Contributions:

Tobias Schirmer chose the topic of this theoretical chapter, drafted the conceptual framework, and wrote the draft. Burkhard König supervised the project.

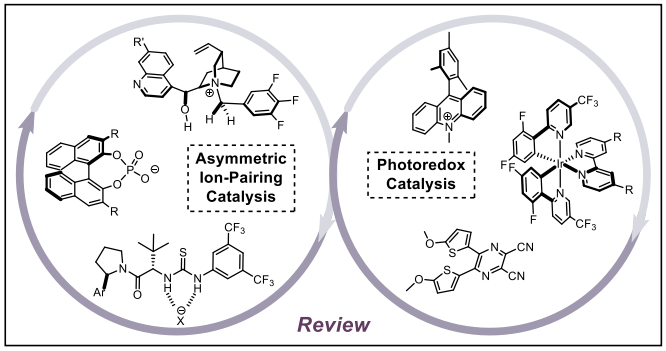

ABSTRACT

With the rapid development of photoredox catalysis, numerous concepts for asymmetric induction were successfully and broadly adapted from polar two-electron transformations to radical chemistry. While this truly applies to organo-catalysis or transition metal chemistry, asymmetric ion-pairing catalysis remains a niche application within the realm of photoredox catalysis as of today. This chapter gives an overview of recent examples, strategies, and their application in stereoselective transformations at the interface of ion-pairing and photoredox catalysis.

1.1 Introduction

In recent years, photoredox catalysis has furnished an incredible number of new transformations and facilitated access to novel molecules, structural motives, or shortened synthetic routes drastically.[1] The combination of photoredox chemistry with other modes of catalysis turned out to be particularly powerful.[2] The great value of dual catalysis lies not only in the combination of orthogonal reactivities, therefore multiplying the potential follow-up reaction of a photogenerated species, but also in generating a handle for stereo induction.[3] Chiral ligands on metals,[4] amine organocatalysts,[5] Lewis acids[6,] and hydrogen bonding catalysts[7] are frequently used for this purpose. As photoredox chemistry evolved from merely being a new tool for radical generation and trapping to being a highly sophisticated toolbox with access to various types of reaction intermediates, new exciting applications of ion-pairing catalysis and its subdisciplines cation/anion-directed catalysis and cation/anion-binding catalysis emerged (Scheme 1).[8]

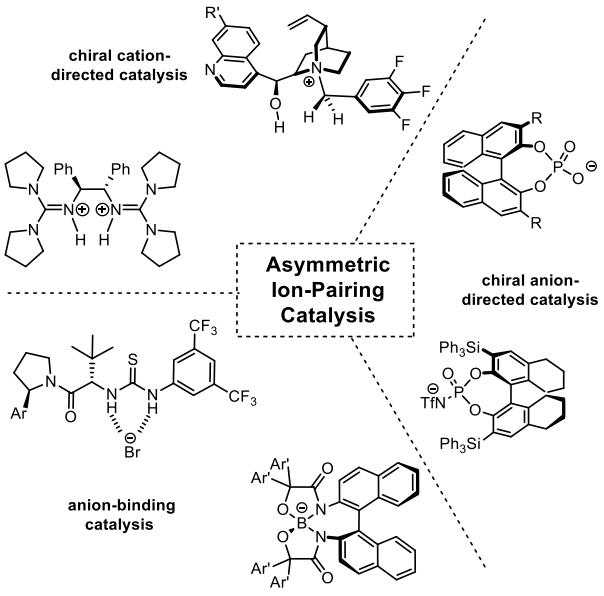

Scheme 1: Ion-pairing catalysis and its subclasses according to *Jacobsen*. (Cation-binding omitted).[8c]

Not long ago, these strategies were exclusively applied in two-electron processes and ions originating from proton transfer, iminium formation, or elimination, to name a few.[8c, 9] Through the rapid development of one-electron processes in the past decade, radical cations and anions became suddenly easily accessible from various abundant precursors. In consequence, new applications of asymmetric ion-pairing catalysis appeared. Photocatalysis offers multiple options for substrate activation. The most prominent is single electron transfer (SET), by which a molecule is either oxidized or reduced by the excited state photocatalyst ***PC**. Assuming the substrate is neutral, a radical cation or anion would be generated. These species can exhibit both radical (e.g., radical-radical

coupling, radical addition to an olefin) and polar (e.g., the addition of a nucleophile or electrophile) reactivity. In the latter, the radical remains, which can be reduced or oxidized to the respective ion, enabling net reductions or oxidations. Either way, both reaction types offer a chance for the chemist to apply counter ions to facilitate a stereoselective transformation.

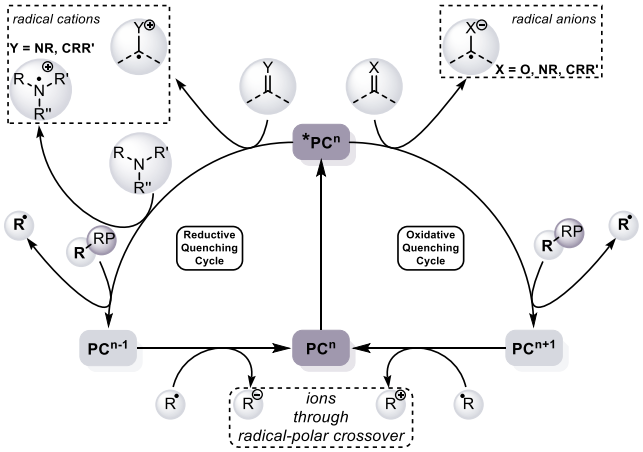

Scheme 2: Oxidative and reductive quenching pathways of excited state photocatalysts with exemplary substrates and charged intermediates.

If the substrate exhibits a radical progenitor (RP), fragmentation can be induced by SET to furnish the desired radical. The radical subsequently undergoes further reactions (not shown), including but not limited to homocoupling, radical-radical cross-coupling, or trapping by radical acceptors such as olefins (radical relay). If the previously generated radical species is again engaged by the photocatalyst, a radical-polar crossover occurs.[10] By either oxidizing or reducing the neutral radical, a cation or anion forms, respectively, and undergoes subsequent two-electron processes with yet another potential implementation of counterion catalysis. Depending on the reaction design and the other reactants, the depicted exemplary redox events might as well be induced by $\mathbf{PC^{n-1}}$ or $\mathbf{PC^{n+1}}$ rather than by the excited state ***PC** (Scheme 2).

In the context of ion-pairing catalysis, the charge of the photocatalyst should be considered throughout its catalytic cycle to avoid competitive pairing with the substrate. Ideally, the catalyst converts to a neutral form after (photoinduced) electron transfer to or from the substrate, which is now charged and designated to interact with a chiral counterion. Through this charge shift, rather than a charge separation, as it would occur with a neutral catalyst and substrate, electrostatic interactions between the two species are avoided.[11] In consequence, one commonly seen strategy is to employ photocatalysts with chiral counterions.[3a] This also avoids potential ion scrambling during the reaction processes. Other modes of substrate activation include but are not limited to electron transfer within EDA complexes,[12] direct irradiation of the substrate, or energy transfer.

In this article, we would like to give a brief overview of the current strategies which allow stereoselective transformations via counterions and showcase the respective key ionic interaction of the substrate or reaction intermediate with the catalyst. Beyond that, counterions, in general, can have a massive influence on the reaction, its kinetics, and the physicochemical properties of catalysts or substrates.[13] Albeit being important to the field, it is beyond the scope of this article.

1.2 Cation-Directed Catalysis

In 2015, the Ooi Group disclosed the asymmetric photocatalytic coupling of aldimines (**1**) with *N*-arylaminomethanes (**2**).[14]

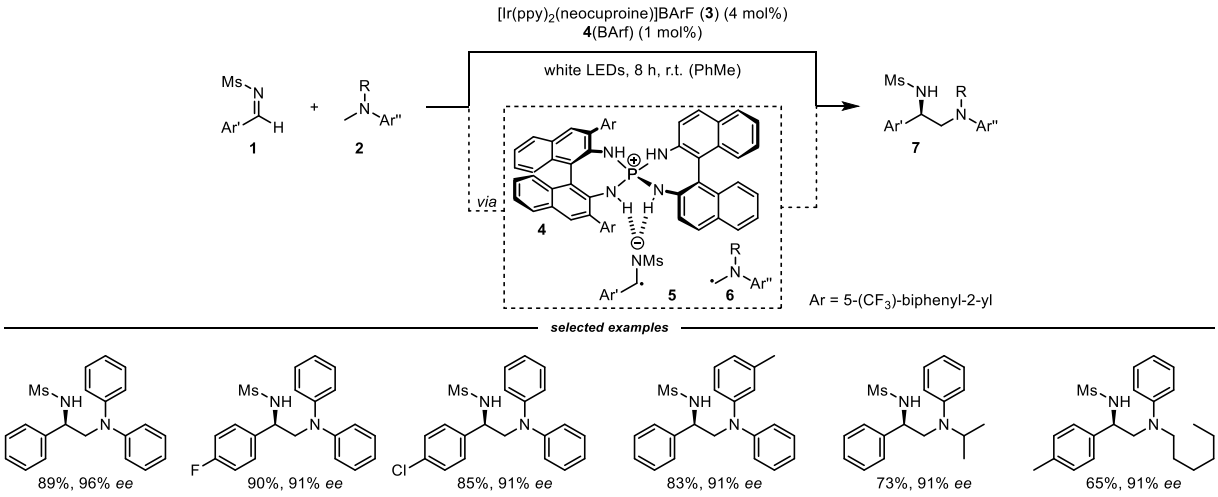

Scheme 3: Ooi's asymmetric α-coupling of *N*-arylaminomethanes with aldimines.[14]

To facilitate the rather challenging radical-radical coupling in an enantioselective manner, the Ooi group identified radical anion **5**, generated by single-electron reduction of **1**, as an ideal target for asymmetric ion-pairing catalysis. Initial investigations quickly revealed that hydrogen bonding of the catalyst to the radical anion **5** is required for the reaction to proceed to the desired product instead of homocoupling and other side products. Tetraaminophosphonium catalyst **4** was the optimal catalyst for this transformation, which is initiated by the reductive quenching of iridium catalyst **3** excited state by the *N*-arylaminomethane **2**. Deprotonation of the resulting radical cation to the aminomethyl radical **6** provides one coupling partner. The reduced photocatalyst then transfers its excess electron to *N*-sulfonylaldimine **1**, generating **5**. Strict stereo control during the radical combination to product **7** is ensured by both ionic interactions and hydrogen bonding between chiral catalyst **4** and substrate **5**. A complementary study, inverting the photocatalytic cycle to an oxidative quenching one, was later published by the same group.[15] The interchanging of the single-

electron reduction and oxidation steps of substrates **1** and **2** did not influence the overall transformation outcome described above.

Jiang employed a chiral diiminium catalyst **8** in the stereoselective reduction of benzils (**9**) to benzoins (**13**).[16] The reaction proceeds via two consecutive single-electron reductions via **10·8** and protonations, where the last protonation of ion pair **11·12** is the enantiodetermining step. Notably, most substrates can be converted without the **DPZ** photocatalyst with very similar results, as the employed THIQ reductant forms an EDA complex with the benzil (**10**).

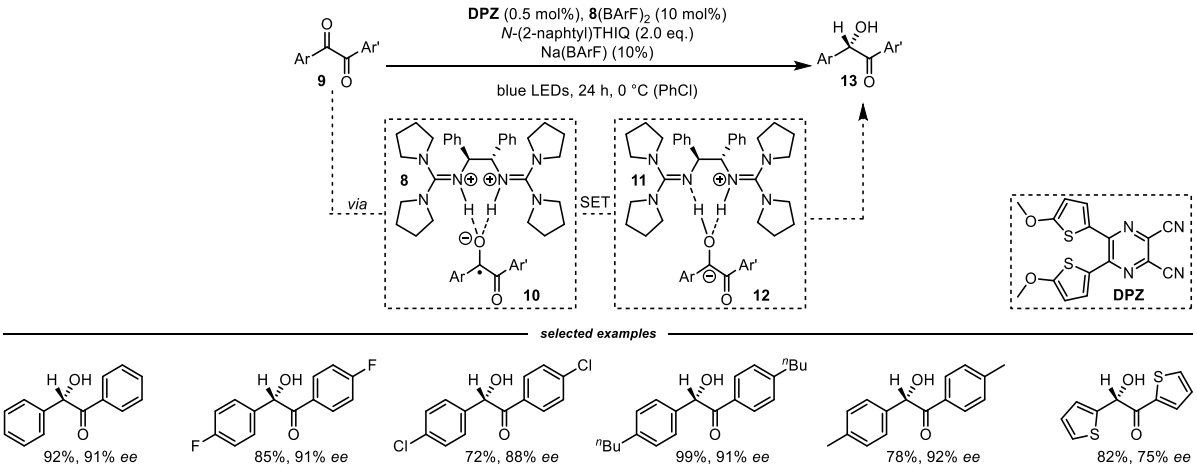

Scheme 4: Jiang's asymmetric reduction of benzils.[16]

Additionally, ketimines can be reduced under slightly altered reaction conditions with a non-ionic hydrogen bonding catalyst. A later work of the same group discloses a related reductive dehalogenation of α-halo ketones with a similar enantioselective protonation step.[17] This transformation is catalyzed by a chiral squaramide-tertiary amine hydrogen bonding catalyst.

1.3 Phase-Transfer-Catalysis (PTC)

While previously introduced ion pairs originate from photochemically generated species, the preformation of such salts prior to the photochemical step enables new strategies in reaction design. The formation of ion pairs from the starting material with catalytic amounts of a counter ion ensures a chiral environment and selective reaction of the active salt, rather than the uncoordinated, prochiral substrate, which, ideally, is completely unreactive in its neutral form. The group of Meng and Gao employed this PTC strategy from 2012 onwards to achieve the enantioselective photooxygenation of β-ketoesters (**15**).[18]

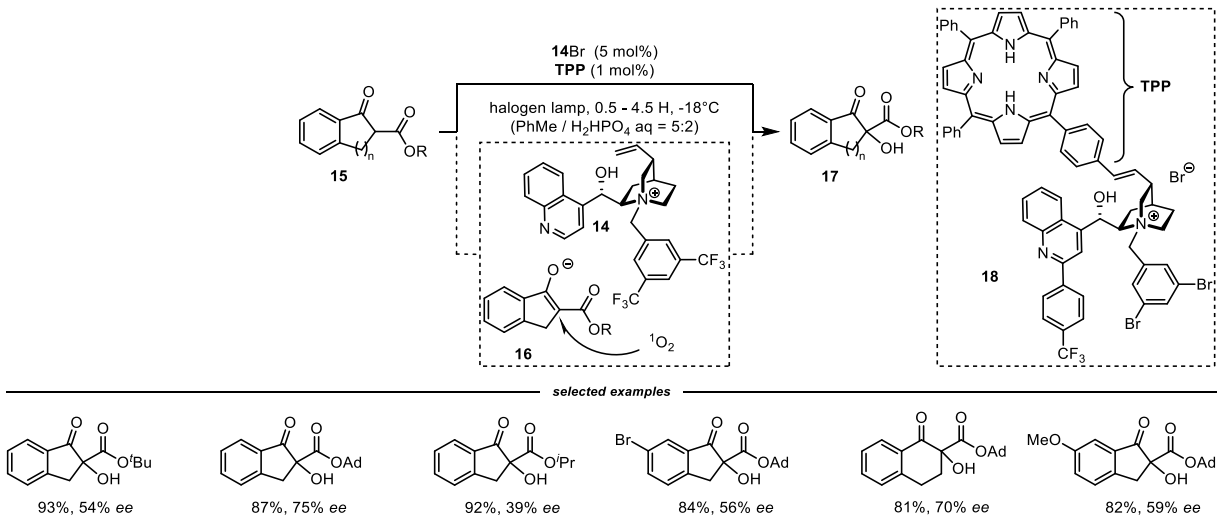

Scheme 5: Meng and Gao's first asymmetric photooxygenation of *β*-ketoesters.[18]

They initially hypothesized that cinchona-alkaloid derived phase transfer catalyst **14** (PTC) forms the enolate-PTC complex **16·14** upon treatment of the *β*-ketoesters (**15**) with base. Further, they envisioned the use of air as an abundant oxygen source. The electron-rich enolate-PTC complex thereby serves as a trap for the highly reactive and electrophilic singlet oxygen generated by photosensitization.

The group revisited their work several times and designed new iterations of their cinchona-alkaloid-based PTC catalyst with improved stereoselectivity, expanded the scope to *β*-keto amides, and adapted the reaction in flow.[19] Most notably, a combined PC-PTC catalyst was developed by coupling tetraphenylporphyrin (TPP) to various positions of the cinchona-alkaloid PTC. Thereby, the group was able to identify **18** as an efficient bifunctional catalyst.[20] A different concept led the Coeffard group to a similar BODIPY-quinine derived catalyst.[21] Unlike precedent in previous reports on PTC-photooxygenation of the Meng group, the Coeffard group did not quarternize the quinuclidine moiety of the cinchona-alkaloid derivative. The design plan, termed *On/Off photooxygenation*, proposed that the free nitrogen lone pair serves as a quencher of singlet oxygen produced by the proximate BODIPY unit if not interacting with the substrate. This would precisely deliver the reactive species to the substrate in a stereo-controlled environment or otherwise quench it to triplet oxygen. While high yields were generally achieved with this catalytic system, the *ee* did not exceed 40% under optimized conditions.

Inspired by Melchiorre's work[22] (Scheme 5), who introduced enolate-PTC complex **19a·16** as photocatalytic species, the Meng group applied this concept to their transformation.[23] While in the latter case, the enolate-PTC complex is proposed to serve as a sensitizer for the generation of singlet

oxygen, Melchiorre used **19a·16** as a donor in an EDA complex with perfluoroalkyl iodides (Scheme 6). Electron transfer to the perfluoroalkyl iodides initiates a radical chain reaction wherein the enolate-PTC complexes trap the perfluoroalkyl radicals in an enantioselective manner.

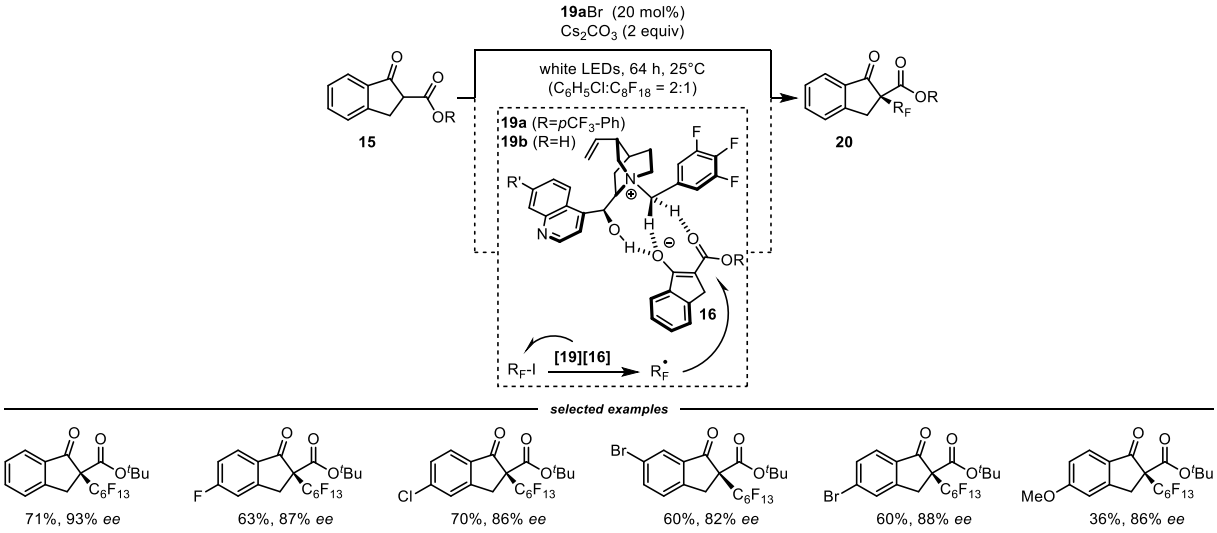

Scheme 6: Melchiorre's asymmetric perfluoroalkylation of *β*-ketoesters.[22]

19·16 depicts a conformational relatively accurate ion pair according to the DFT calculations of the Li group.[24] Their study investigated several potential enolate-PTC ion pairs with different conformations and interactions of the quininium ion **19b** with the enolate **16.** Interestingly, neither the electron-poor quinoline nor the electron-deficient trifluorobenzyl moiety undergo mixed π-π interactions with the electron-rich enolate. Instead, the key to the high enantioselectivity of Melchiorre's reaction lies in both the ^{quininium}O–H···O^{enolate} and in the ^{quininium}C–H···O^{enolate} interactions. These insights should contribute to more PTC-photoredox dual catalysis, as the examples of this PTC-type dual catalysis are relatively rare and mostly limited to *β*-keto carbonyls and cinchona-alkaloid derived phase transfer catalysts.

The Xiao group achieved asymmetric photooxygenation (Scheme 5) and perfluoroalkylation (Scheme 6) via asymmetric photo-Lewis acid dual catalysis.[25]

1.4 Anion-Directed Catalysis

Alkyl- or aryl olefins are particularly suitable and abundant substrates for single-electron oxidation to the respective radical cations. Latter species displays both radical and ionic reactivity depending on the available reaction partners and overall conditions.

The Luo group communicated an example of such an ionic reaction pathway.[26] The cooperation of strongly oxidizing acridinium photocatalyst **Mes-Arc** with chiral phosphate **21** as a combined catalyst enabled the intramolecular hydroesterification of alkenol substrate **22** with moderate enantiomeric excess.

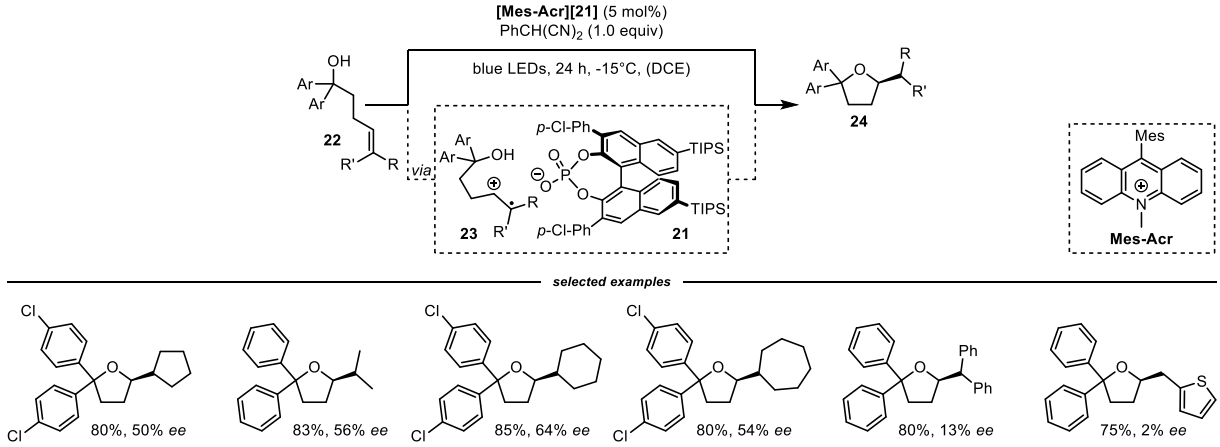

Scheme 7: Luo's asymmetric hydroetherification of alkenols.[26]

Reductive quenching of the excited **Mes-Acr*** by the olefin to a neutral **Mes-Acr**-radical and radical cation **23** leads to the chiral substrate-catalyst ion pair **23·21** shown below (Scheme 7). Nucleophilic addition of the alcohol in this chiral environment and subsequent hydrogen atom abstraction by the tertiary alkyl radical from the phenylmalononitrile furnish the enantioenriched tetrahydrofuran product **24**. Alkyl substituents on the olefin are crucial for higher stereoselectivity but not for the overall yield of the reaction.

The Tang group employed an analogous catalytic system to develop an asymmetric version of their photochemical 1,2,4-triazoline synthesis from 2*H*-azrine **25** and azodicarboxylate **26**.[27]

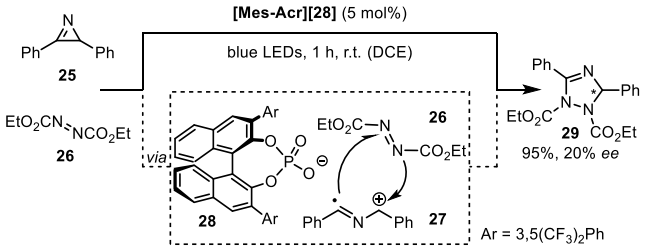

Scheme 8: Tang's asymmetric version of the 1,2,4-triazolines synthesis from 2*H*-azrine.[27]

The reaction is proposed to proceed via single-electron oxidation of **25** to furnish ring-opened radical cation **27**, which undergoes [3+2] cycloaddition with **25**. After applying combined

photocatalyst-chiral anion **Mes-Acr·28**, the reaction proceeded with stereo induction and yielded the product (**29**) in 95% with 20% *ee* (Scheme 8).

The Nicewicz group envisioned an asymmetric photo-Diels-Alder reaction via asymmetric ion-pairing catalysis.[28] They identified pyrilium salt **TP·30** with a chiral *N*-triflyl phosphoramide as a suitable catalytic system for this reaction.

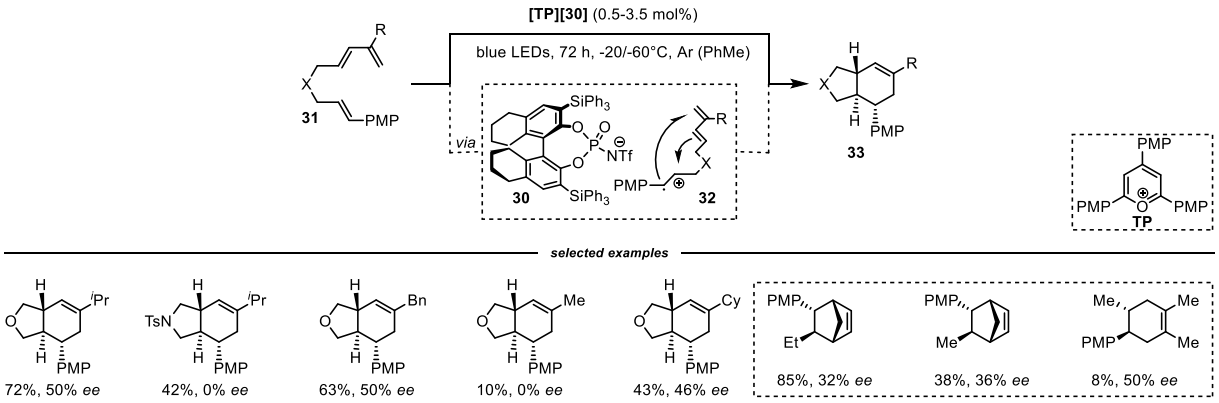

Scheme 9: Nicewicz' asymmetric photo-Diels-Alder reaction.[28]

Like previously discussed mechanisms, single-electron oxidation of **31** and ion exchange at the phosphoramide anion **30** give rise to chiral ion pair **32·30**, providing the stereo information for the subsequent intramolecular cyclization to the Diels-Alder-product **33**. The methodology provides generally good yields with moderate enantiomeric excess in most intra- and intermolecular applications (Scheme 9). Small R-groups, such as a methyl group or nitrogen within the tether, inexplicably lead to a racemic product.

Knowles reported an asymmetric dearomatization of tryptamine derivatives (**34**) and their transformation to pyrroloindolines (**35**).[29] Photooxidation of the indole ring gives rise to radical cation **36**. This step is facilitated by the phosphate base **37**, as a detailed mechanistic investigation revealed. However, DFT calculations determined the proton to be covalently bound to the indole rather than to the phosphate and thus the formation of ion pair **36·37**. Stereoselective nucleophilic attack of the tethered amide and diastereoselective trapping of the benzylic radical with TEMPO furnish adduct **35**, which serves as bench stable and masked radical equivalent: Cation **38** can be accessed by another single-electron oxidation of *N*-Boc-**35,** and diastereoselectively adds various kinds of nucleophiles to form products **39**.

Zhang and You abbreviated this two-step procedure.[30] Direct *in situ* oxidation of the benzylic radical to cation **38** rather than trapping the former with TEMPO is proposed to enable the dearomative difunctionalization of indoles with the tethered amide and *N*-hydroxycarbamates. As molecular

oxygen is used as an oxidant, the respective peroxide adduct might serve as analogs of **35** and react similarly by masking the radical temporarily *in situ*. An iridium photocatalyst-free version was achieved by Xia through direct photoexcitation of TEMPO.[31]

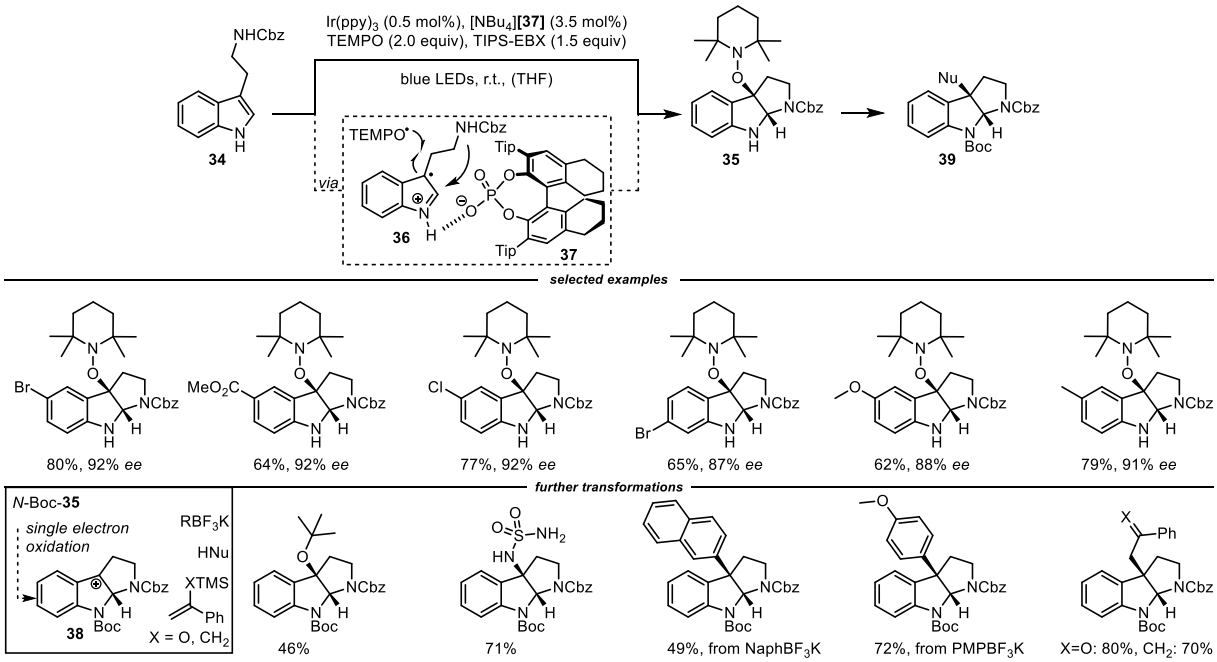

Scheme 10: Knowles' dearomatization of indoles.[29]

1.5 Strict Ion Pairs Derived from Brønsted Acids

Brønsted-acid catalysis is, as List argues, a *specific case of asymmetric counteranion-directed catalysis*.[9b] It exhibits various possible activation modes referred to as hydrogen bonding catalysis, hydrogen-bonding-assisted ion pair- and counter ion catalysis. As the lines between these modes of activation blur and often are not distinguishable by simple theoretical analysis, determining the true nature of the interaction between the catalyst and the substrate requires rather detailed NMR or *in silico* studies.[9c, 32] To limit the scope of this perspective on ion pairs and in consideration of the increasing number of photoredox-Brønsted-acid dual catalysis, only strict ion pairs derived from Brønsted acids will be discussed below. Other modes of activation, such as protonation of a substrate (hydrogen-bonding-assisted ion pair) and hydrogen bonding from Brønsted acids to one or multiple substrates (non-ionic interactions), are beyond the scope. These strategies often applied in Minisci-type reactions, have been extensively and comprehensively reviewed elsewhere.[33]

As Rueping points out, a strict ion pair can form from a parent acid *in situ* by facilitating the loss of a leaving group such as water from a neutral species. In this case, the use of phosphate salts, as shown in the preceding examples, is not necessarily required for ion pair formation.[9c]

The enantioselective synthesis of 2,4-diaryl-4*H*-chromenes (**41**) from 2-hydroxychalcones (**40**) by Rueping can serve as an illustration for such a case.[34] The reaction itself is Brønsted acid co-catalyzed, yet a chiral phosphate ion pair is crucial for the stereoselectivity of the transformation (Scheme 11). After Brønsted acid-assisted E/Z-photoisomerization and cyclization of chalcone **40** to hemiacetal **42**, protonation by the acid and loss of water give rise to the chiral and reactive benzopyrylium phosphate **43·44**. This key intermediate is transformed into product **41** by hydride transfer from **HEH**. The overall transformation of intermediate **42** to product **41** does not require irradiation.

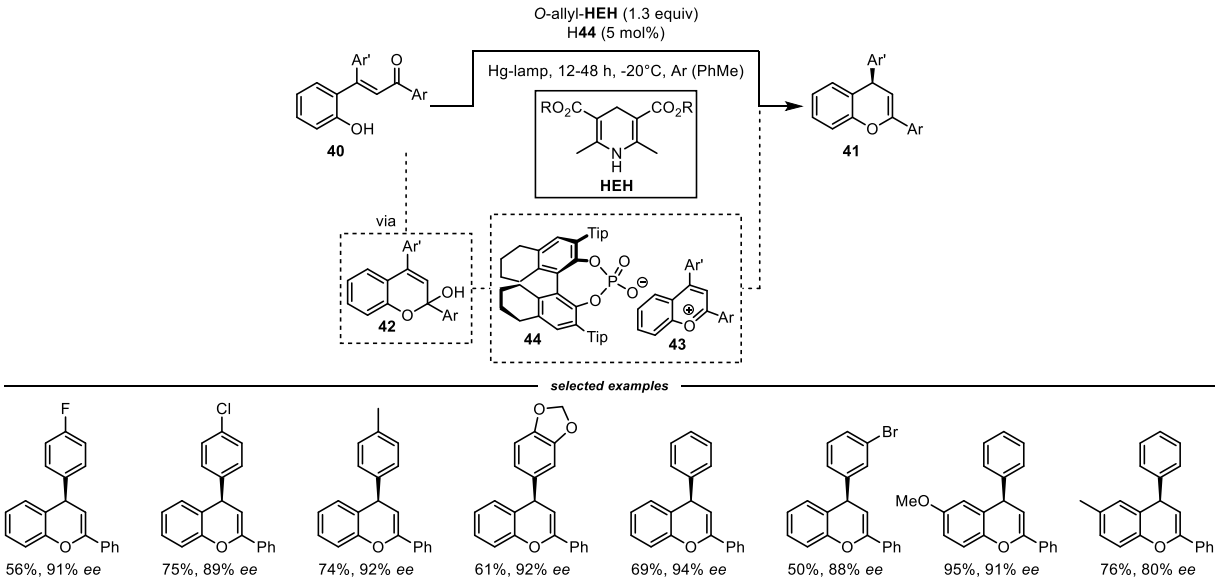

Scheme 11: Rueping's synthesis of 2,4-diaryl-4*H*-chromenes from 2-hydroxychalcones.[34]

Adapting the reaction design to 2-aminochalcones **45**, Rueping gained access to 2-aryltetrahydroquinolines (**46**) via a quinolin-1-ium phosphate ion pair **47·48**.[35]

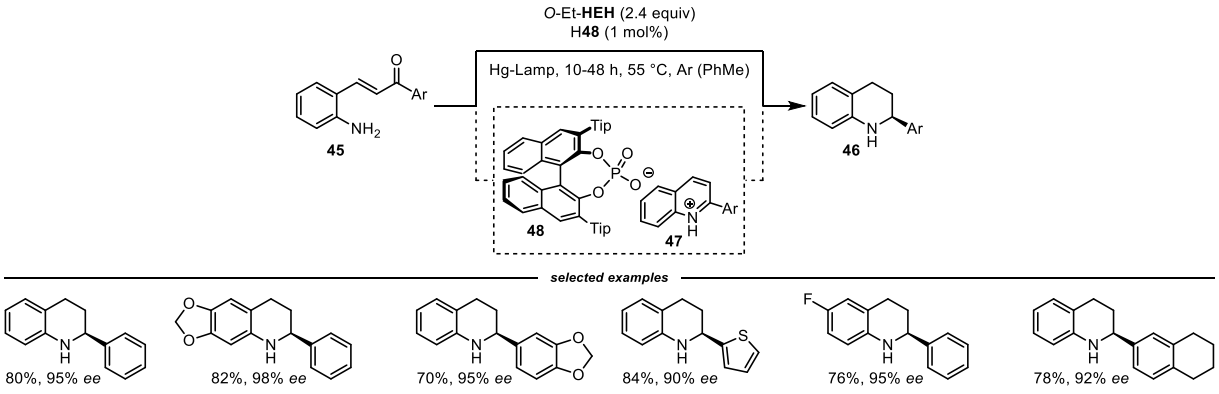

Scheme 12: Rueping's synthesis of 2-aryltetrahydrochinolines.[35]

In contrast to the previous example, the *N*-heterocycle is fully reduced in the presence of a Hantzsch-ester. Additionally, the transformation can be run under photo-flow conditions with equally high yields and stereocontrol.[36] The same reaction was later optimized for visible light LED irradiation, easing the access to enantiopure 2-aryltetrahydrochinolines even further.[37]

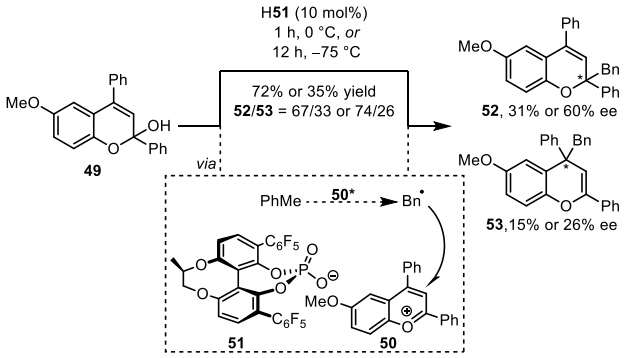

Scheme 13: Terada's asymmetric benzylation of benzopyrylium ions.[38]

Terada's recently published work goes one step further and uses chiral pyrilium phosphate ion pair **50·51** as both photocatalyst for radical generation and as a radical trap.[38] The reaction proceeds via photooxidation of toluene by photoexcited benzopyrylium cation **50*** while ground state **50·51** serves as a radical trap. Although the asymmetric version of this reaction suffers from low regioselectivity and, depending on the conditions, either from low *ee* or low yield, it is certainly adding an interesting example to the relatively rare, photoactive, and substrate derived ion pairs.

Only very recently, the Bach group disclosed the photosensitized [2+2] photocycloaddition of chiral iminium phosphate ion pairs.[39]

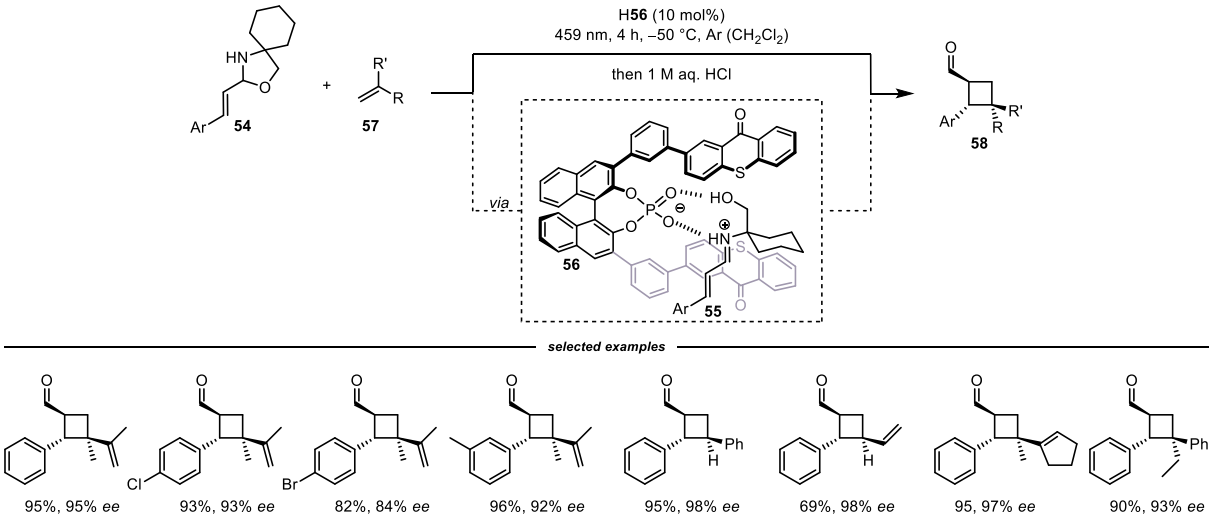

Scheme 14: Bach's asymmetric [2+2] photocycloaddition of iminium ions.[39]

The reaction was envisioned to proceed via Brønsted acid-catalyzed opening of *α,β*-unsaturated aldehyde derived *N,O*-acetals **54** to yield iminium ion **55**. The tightly bonded phosphate **56** provides the chiral environment for the addition of **57** and delivers the light energy for the reaction through the attached thioxanthone chromophore sensitizing **55**. Densely substituted cyclobutane carbaldehydes (**58**) are accessible with high enantiomeric excess and significantly improved diastereocontrol compared to the racemic variant. The Gschwind group contributed very detailed NMR studies to this project and confirmed the formation of a hydrogen-bonded iminium phosphate ion pair. It originates from a 2:1 mixture of the closed *N,O*-acetal and its open imine form. These thorough investigations shall serve as a prime example of the power of NMR studies in determining the true nature of reaction intermediates and their interactions.

1.6 Anion Binding Catalysis

To the best of our knowledge, the earliest example of anion binding photoredox dual catalysis was disclosed by Stephenson and Jacobsen.[40] In their two-step procedure, **59** is photochemically *α*-chlorinated. After solvent exchange and the addition of anion binding catalyst **61** and silyl enol ether **62**, the formation of the depicted ion pair **63·61** is promoted, and it is engaged in a Mannich reaction with silyl enol ether **62** in a stereoselective fashion to yield alkylated **64**.

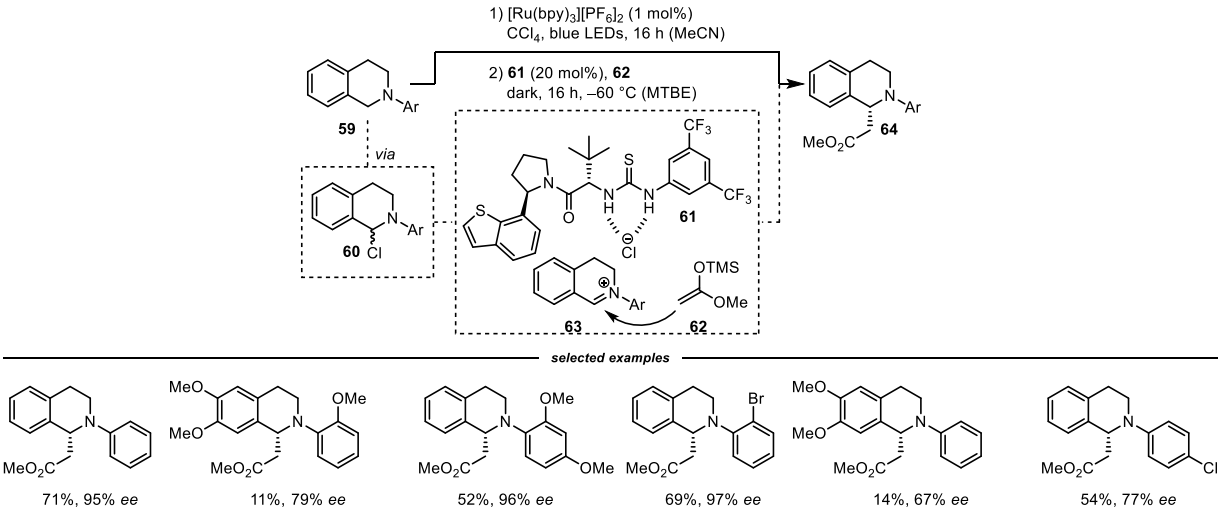

Scheme 15: Stephenson and Jacobsen's enantioselective synthesis of *β*-amino esters.[40]

A different approach to anion binding catalysis was only very recently disclosed by the Ooi group for a formal [3+2] cycloaddition *of N*-cyclopropyl amine derivative **65**.[41]

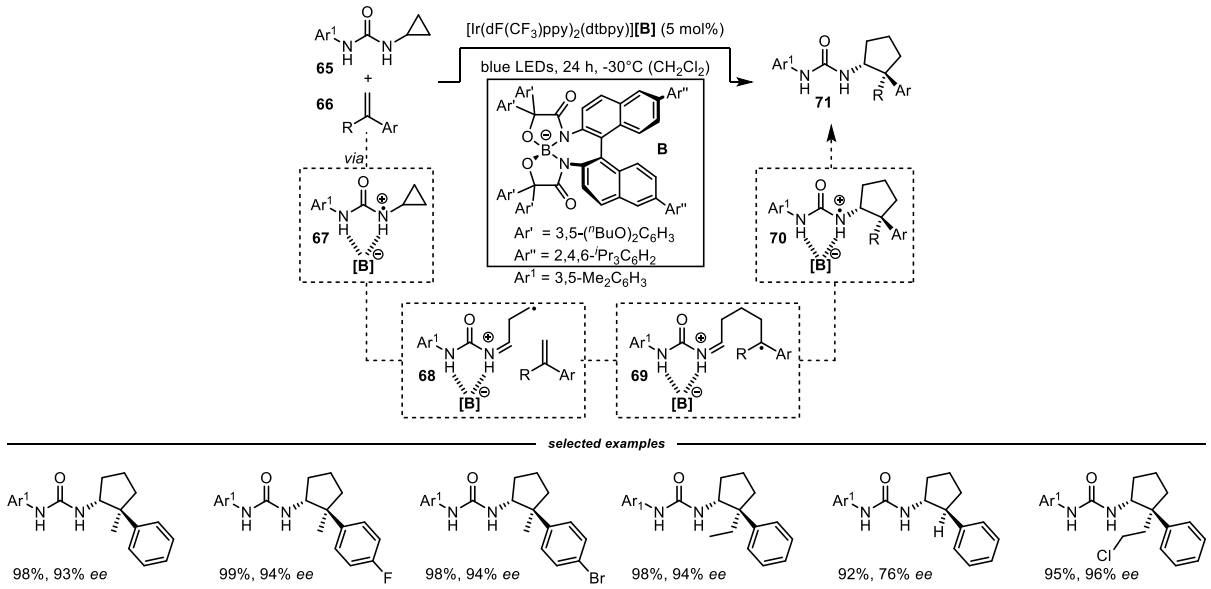

Scheme 16: Ooi's urea directed [3 + 2]-cycloaddition of cyclopropylamines and α-alkylstyrenes.[41]

Instead of using a chiral anion binding catalyst, the group designed the urea moiety of the substrate specifically to act as an anion recognition site. It promotes the preorganization of the substrate to the chiral counterion of the photocatalyst. Hence, substrate, anion **B,** and the iridium catalyst can be anticipated near each other before any photochemical event. Photoexcitation of the iridium complex and electron transfer from the substrate yield a neutral iridium complex, while its former counterion **B** and radical cation **67** form a chiral supramolecular ion pair. This assembly is maintained throughout the cyclopropane ring-opening (**68·B**), the radical addition to styrene **66**, and most importantly, the enantioselective bond-forming event. Reduction of **70·B** by the reduced catalyst reestablishes the initial catalytic system and yields the product **71**. The urea directing group can easily be removed to access the free cyclopentylamines without losing enantiomeric purity. The authors then expanded the substrate scope from styrenes to acrylates, elegantly granting access to alicyclic α-quaternary β-amino acids after removing the urea moiety and saponification of the former acrylate.[42]

1.7 Related Transformations

Not only strict ion pairs can lead to stereoselective transformations. The following two examples illustrate how interactions between charged acids and bases could be exploited to control a reaction's stereochemistry. An interesting observation concerning the diastereoselectivity of the Giese reaction between *N*-Boc-pyrrolidine (**72**) and ethyl 2-phenylacrylate (**73**) was made by the Ooi group during their study of a zwitterionic HAT-catalyst (**74**).[43] Commonly used HAT catalysts such as tetra-*n*-butylammonium decatungstate (TBADT) and benzophenone yielded the product in 1.3:1

and 1.5:1 diastereomeric ratio, respectively. However, with **74** as HAT catalyst, the reaction can be conducted with high diastereoselectivity (d.r. = 20:1).

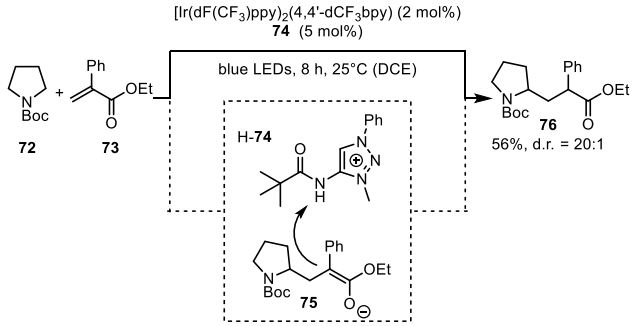

Scheme 17: Ooi's diastereoselective C–H alkylation catalyzed by a zwitterionic HAT-catalyst.[43]

Based on this result and the quantum yield of the reaction, the authors suspect *N*-protonated **74** to be involved in the protonation of enolate **75** and thereby controlling the stereochemical outcome of that reaction step. A similar Giese-reaction with protected *α*-amino acrylates as substrates and TBADT as catalyst was later published as an asymmetric version: A chiral spiro phosphoric acid achieves the enantioselective protonation.[44]

A difference in the interaction between chiral radical cations and a chiral phosphate base was exploited by Knowles to deracemize cyclic *N*-aryl ureas.[45]

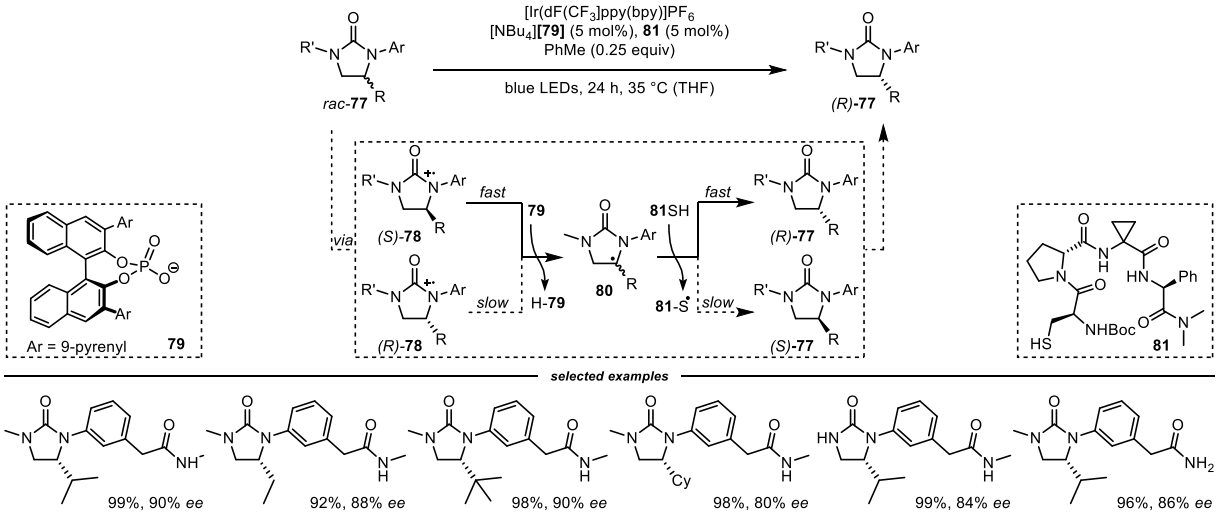

Scheme 18: Knowles' photochemical deracemization of cyclic *N*-aryl ureas.[45]

The reaction proceeds *via* single-electron oxidation of racemate *rac*-**77**. Unfavorable interactions between the *R*-enantiomer *(R)*-**77** and phosphate **79** lead to significantly slower deprotonation than the *S*-enantiomer. Therefore, the electron back transfer from the photocatalyst to *(R)*-**77** is favored, while *(S)*-**77** is depleted due to its relatively fast conversion to radical **80**. Hydrogen abstraction by

prochiral radical **80** from a thiol catalyst restores the starting material.By discriminating one enantiomer during the deprotonation, enantiomeric ratios up to 86:14 (72% *ee*) can be achieved with a racemic thiol catalyst. *Vice versa*, achiral diphenyl phosphates in combination with chiral thiol **81** yield enantiomeric ratios of up to 79:21 (58% *ee*) *via* enantioselective hydrogen abstraction by **80**. By combining the two independent stereoselective steps and brief subsequent optimization, the enantiomeric excess was increased to 92% *ee* (e.r. = 96:4).

1.8 Summary and Outlook

The few examples of photoredox ion-pairing catalysis compiled in this article can inspire the synthetic chemist and hopefully encourage to experiment with the rather powerful strategy of counter ion catalysis. Charged intermediates have never been more accessible through photoredox catalysis as today and can be found in many racemic transformations. Counter-anion-directed catalysis might be the most readily applicable approach due to the abundance of chiral phosphates, the number of precedents of the related photo-Brønsted-acid dual catalysis, and the many examples in polar chemistry. Additionally, combining cationic photocatalysts such as iridium complexes or Fukuzumi dyes with chiral anions or incorporation of the photocatalyst into the phosphate enables the development of highly efficient catalytic systems, as Nicewicz' and Luo's work foreshadowed, and Bach, as well as Ooi, confirmed.[26, 28, 39, 41] To this date, anion-binding catalysis only finds niche applications in combination with photoredox catalysis. The Ooi group's transition from chiral anion-binding catalysts to an achiral recognition site incorporated in the substrate, combined with a chiral anion, proved very powerful by directing the photocatalyst to the designated reaction site.[41] This change in concept could enable the activation and stereoselective transformation of more challenging substrates or reaction sites with potentially higher selectivity. After careful literature research, we could not find a recent example for cation-binding catalysis combined with synthetic photochemistry.[46] In contrast, phase-transfer catalysis finds some application in the functionalization of β-keto carbonyls. The groundbreaking findings in this field were contributed by Melchiorre with the use of an ion pair as an electron donor to initiate a radical reaction photochemically.[22] However, so far, almost exclusively indanones are used as substrates, and the reactions of PTC ion pairs, oxygenation and radical alkylation are somewhat limited and have room for expansion. Without PTC, examples for cation-directed-catalysis within the realm of photoredox chemistry are relatively rare. Both examples in this review additionally exploit hydrogen bonding from the cationic catalyst to the anion. Hydrogen bonding is often sufficient to impose stereocontrol on the substrate anion's bond-forming event. The Jiang group's reduction of benzils is a prime example in

that matter: The reduction of benzils is facilitated by a cationic hydrogen bonding catalyst, while the reduction of benzoylacetyl and ketimines is realized with a neutral hydrogen bonding catalyst in the very same study.[16] In another study, the same group showed that a Brønsted-acid hydrogen bonding catalyst facilitates radical additions to the very same benzil radical anion, once again exemplifying how these concepts are interlinked.[47] Currently, cation-directed catalysis merely supports hydrogen bonding catalysis with electrostatic attractions in addition to hydrogen bonding.

With the continuous development of racemic photochemical transformation, we are confident that new opportunities in ion-pairing catalysis for stereo induction will be identified and implemented. We hope this article supports this quest by providing an overview of current strategies and examples.

1.9 References

[1] (a) Petzold, D.; Giedyk, M.; Chatterjee, A.; König, B., *Eur. J. Org. Chem.* **2020**, *2020*, 1193-1244; (b) Romero, N. A.; Nicewicz, D. A., *Chem. Rev.* **2016**, *116*, 10075-10166; (c) Prier, C. K.; Rankic, D. A.; MacMillan, D. W., *Chem. Rev.* **2013**, *113*, 5322-5363.

[2] (a) Skubi, K. L.; Blum, T. R.; Yoon, T. P., *Chem. Rev.* **2016**, *116*, 10035-10074; (b) Twilton, J.; Le, C.; Zhang, P.; Shaw, M. H.; Evans, R. W.; MacMillan, D. W. C., *Nat. Rev. Chem.* **2017**, *1*; (c) Milligan, J. A.; Phelan, J. P.; Badir, S. O.; Molander, G. A., *Angew. Chem. Int. Ed.* **2019**, *58*, 6152-6163.

[3] (a) Genzink, M. J.; Kidd, J. B.; Swords, W. B.; Yoon, T. P., *Chem. Rev.* **2021**; (b) Saha, D., *Chem. Asian J.* **2020**, *15*, 2129-2152; (c) Rigotti, T.; Aleman, J., *Chem. Commun.* **2020**, *56*, 11169-11190; (d) Prentice, C.; Morrisson, J.; Smith, A. D.; Zysman-Colman, E., *Beilstein J. Org. Chem.* **2020**, *16*, 2363-2441; (e) Hong, B. C., *Org. Biomol. Chem.* **2020**; (f) Jiang, C.; Chen, W.; Zheng, W. H.; Lu, H., *Org. Biomol. Chem.* **2019**, *17*, 8673-8689; (g) Silvi, M.; Melchiorre, P., *Nature* **2018**, *554*, 41-49; (h) Garrido-Castro, A. F.; Maestro, M. C.; Aleman, J., *Tetrahedron Lett.* **2018**, *59*, 1286-1294; (i) Brenninger, C.; Jolliffe, J. D.; Bach, T., *Angew. Chem. Int. Ed.* **2018**, *57*, 14338-14349; (j) Skubi, K. L.; Blum, T. R.; Yoon, T. P., *Chem. Rev.* **2016**, *116*, 10035-10074; (k) Hopkinson, M. N.; Sahoo, B.; Li, J. L.; Glorius, F., *Chem. Eur. J.* **2014**, *20*, 3874-3886.

[4] Lu, F. D.; Chen, J.; Jiang, X.; Chen, J. R.; Lu, L. Q.; Xiao, W. J., *Chem. Soc. Rev.* **2021**.

[5] Liu, Y.-Y.; Liu, J.; Lu, L.-Q.; Xiao, W.-J., *Top. Curr. Chem.* **2019**, *377*, 1-15.

[6] (a) Huang, X.; Meggers, E., *Acc. Chem. Res.* **2019**, *52*, 833-847; (b) Yoon, T. P., *Acc. Chem. Res.* **2016**, *49*, 2307-2315.

[7] Burg, F.; Bach, T., *J. Org. Chem.* **2019**, *84*, 8815-8836.

[8] (a) Proctor, R. S. J.; Colgan, A. C.; Phipps, R. J., *Nat. Chem.* **2020**, *12*, 990-1004; (b) Bhattacharyya, A.; De Sarkar, S.; Das, A., *ACS Catal.* **2020**, *11*, 710-733; (c) Brak, K.; Jacobsen, E. N., *Angew. Chem. Int. Ed.* **2013**, *52*, 534-561.

[9] (a) Phipps, R. J.; Hamilton, G. L.; Toste, F. D., *Nat. Chem.* **2012**, *4*, 603-614; (b) Mahlau, M.; List, B., *Angew. Chem. Int. Ed.* **2013**, *52*, 518-533; (c) Parmar, D.; Sugiono, E.; Raja, S.; Rueping, M., *Chem. Rev.* **2014**, *114*, 9047-9153.

[10] (a) Wiles, R. J.; Molander, G. A., *Isr. J. Chem.* **2020**, *60*, 281-293; (b) Donabauer, K.; Konig, B., *Acc. Chem. Res.* **2021**, *54*, 242-252; (c) Pitzer, L.; Schwarz, J. L.; Glorius, F., *Chem. Sci.* **2019**, *10*, 8285-8291.

[11] Legros, B.; Vandereecken, P.; Soumillion, J. P., *J. Phys. Chem.* **2002**, *95*, 4752-4761.

[12] Crisenza, G. E. M.; Mazzarella, D.; Melchiorre, P., *J. Am. Chem. Soc.* **2020**, *142*, 5461-5476.

[13] Farney, E. P.; Chapman, S. J.; Swords, W. B.; Torelli, M. D.; Hamers, R. J.; Yoon, T. P., *J. Am. Chem. Soc.* **2019**, *141*, 6385-6391.

[14] Uraguchi, D.; Kinoshita, N.; Kizu, T.; Ooi, T., *J. Am. Chem. Soc.* **2015**, *137*, 13768-13771.

[15] Kizu, T.; Uraguchi, D.; Ooi, T., *J. Org. Chem.* **2016**, *81*, 6953-6958.

[16] Lin, L.; Bai, X.; Ye, X.; Zhao, X.; Tan, C. H.; Jiang, Z., *Angew. Chem. Int. Ed.* **2017**, *56*, 13842-13846.

[17] Hou, M.; Lin, L.; Chai, X.; Zhao, X.; Qiao, B.; Jiang, Z., *Chem. Sci.* **2019**, *10*, 6629-6634.

[18] Lian, M.; Li, Z.; Cai, Y.; Meng, Q.; Gao, Z., *Chem. Asian. J.* **2012**, *7*, 2019-2023.

[19] (a) Tang, X. F.; Zhao, J. N.; Wu, Y. F.; Zheng, Z. H.; Feng, S. H.; Yu, Z. Y.; Liu, G. Z.; Meng, Q. W., *Org. Biomol. Chem.* **2019**, *17*, 7938-7942; (b) Wang, Y.; Zheng, Z.; Lian, M.; Yin, H.; Zhao, J.; Meng, Q.; Gao, Z., *Green Chem.* **2016**, *18*, 5493-5499; (c) Wang, Y.; Yin, H.; Tang, X.; Wu, Y.; Meng, Q.; Gao, Z., *J. Org. Chem.* **2016**, *81*, 7042-7050.

[20] Tang, X.-f.; Feng, S.-h.; Wang, Y.-k.; Yang, F.; Zheng, Z.-h.; Zhao, J.-n.; Wu, Y.-f.; Yin, H.; Liu, G.-z.; Meng, Q.-w., *Tetrahedron* **2018**, *74*, 3624-3633.

[21] Fischer, J.; Mele, L.; Serier-Brault, H.; Nun, P.; Coeffard, V., *Eur. J. Org. Chem.* **2019**, *2019*, 6352-6358.

[22] Wozniak, L.; Murphy, J. J.; Melchiorre, P., *J. Am. Chem. Soc.* **2015**, *137*, 5678-5681.

[23] Tang, X. F.; Zhao, J. N.; Wu, Y. F.; Feng, S. H.; Yang, F.; Yu, Z. Y.; Meng, Q. W., *Adv. Synth. Catal.* **2019**, *361*, 5245-5252.

[24] Yang, C.; Zhang, W.; Li, Y. H.; Xue, X. S.; Li, X.; Cheng, J. P., *J. Org. Chem.* **2017**, *82*, 9321-9327.

[25] (a) Ding, W.; Lu, L.-Q.; Zhou, Q.-Q.; Wei, Y.; Chen, J.-R.; Xiao, W.-J., *J. Am. Chem. Soc.* **2017**, *139*, 63-66; (b) Liu, J.; Ding, W.; Zhou, Q. Q.; Liu, D.; Lu, L. Q.; Xiao, W. J., *Org. Lett.* **2018**, *20*, 461-464.

[26] Yang, Z.; Li, H.; Li, S.; Zhang, M.-T.; Luo, S., *Org. Chem. Front.* **2017**, *4*, 1037-1041.

[27] Wang, H.; Ren, Y.; Wang, K.; Man, Y.; Xiang, Y.; Li, N.; Tang, B., *Chem. Commun.* **2017**, *53*, 9644-9647.

[28] Morse, P. D.; Nguyen, T. M.; Cruz, C. L.; Nicewicz, D. A., *Tetrahedron* **2018**, *74*, 3266-3272.

[29] Gentry, E. C.; Rono, L. J.; Hale, M. E.; Matsuura, R.; Knowles, R. R., *J. Am. Chem. Soc.* **2018**, *140*, 3394-3402.

[30] Cheng, Y. Z.; Zhao, Q. R.; Zhang, X.; You, S. L., *Angew. Chem. Int. Ed.* **2019**, *58*, 18069-18074.

[31] Liang, K.; Tong, X.; Li, T.; Shi, B.; Wang, H.; Yan, P.; Xia, C., *J. Org. Chem.* **2018**, *83*, 10948-10958.

[32] (a) Rothermel, K.; Melikian, M.; Hioe, J.; Greindl, J.; Gramuller, J.; Zabka, M.; Sorgenfrei, N.; Hausler, T.; Morana, F.; Gschwind, R. M., *Chem. Sci.* **2019**, *10*, 10025-10034; (b) Sorgenfrei, N.; Hioe, J.; Greindl, J.; Rothermel, K.; Morana, F.; Lokesh, N.; Gschwind, R. M., *J. Am. Chem. Soc.* **2016**, *138*, 16345-16354.

[33] (a) Proctor, R. S. J.; Phipps, R. J., *Angew. Chem. Int. Ed.* **2019**, *58*, 13666-13699; (b) Lv, X.; Xu, H.; Yin, Y.; Zhao, X.; Jiang, Z., *Chin. J. Chem.* **2020**, *38*, 1480-1488; (c) Yin, Y.; Zhao, X.; Qiao, B.; Jiang, Z., *Org. Chem. Front.* **2020**, *7*, 1283-1296.

[34] Hsiao, C. C.; Liao, H. H.; Sugiono, E.; Atodiresei, I.; Rueping, M., *Chem. Eur. J.* **2013**, *19*, 9775-9779.

[35] Liao, H. H.; Hsiao, C. C.; Sugiono, E.; Rueping, M., *Chem. Commun.* **2013**, *49*, 7953-7955.

[36] Sugiono, E.; Rueping, M., *Beilstein J. Org. Chem.* **2013**, *9*, 2457-2462.

[37] Xiong, W.; Li, S.; Fu, B.; Wang, J.; Wang, Q. A.; Yang, W., *Org. Lett.* **2019**, *21*, 4173-4176.

[38] Kikuchi, J.; Kodama, S.; Terada, M., *Org. Chem. Front.* **2021**.

[39] Pecho, F.; Sempere, Y.; Gramuller, J.; Hormann, F. M.; Gschwind, R. M.; Bach, T., *J. Am. Chem. Soc.* **2021**, *143*, 9350-9354.

[40] Bergonzini, G.; Schindler, C. S.; Wallentin, C. J.; Jacobsen, E. N.; Stephenson, C. R., *Chem. Sci.* **2014**, *5*.

[41] Uraguchi, D.; Kimura, Y.; Ueoka, F.; Ooi, T., *J. Am. Chem. Soc.* **2020**, *142*, 19462-19467.

[42] Kimura, Y.; Uraguchi, D.; Ooi, T., *Org. Biomol. Chem.* **2021**, *19*, 1744-1747.

[43] Ohmatsu, K.; Suzuki, R.; Furukawa, Y.; Sato, M.; Ooi, T., *ACS Catal.* **2019**, *10*, 2627-2632.

[44] Dai, Z. Y.; Nong, Z. S.; Song, S.; Wang, P. S., *Org. Lett.* **2021**, *23*, 3157-3161.

[45] Shin, N. Y.; Ryss, J. M.; Zhang, X.; Miller, S. J.; Knowles, R. R., *Science* **2019**, *366*, 364-369.

[46] Oliveira, M. T.; Lee, J.-W., *ChemCatChem* **2017**, *9*, 377-384.

[47] Liu, Y.; Liu, X.; Li, J.; Zhao, X.; Qiao, B.; Jiang, Z., *Chem. Sci.* **2018**, *9*, 8094-8098.

CHAPTER II

Photo-Nickel Dual Catalytic Benzoylation of Aryl Bromides

Reproduced from:

T.E. Schirmer, A. Wimmer, F. W. C. Weinzierl, B. König, *Chem. Commun.* **2019**, *55*, 10796-10799.

Author Contributions:

T.E.S. initiated the project, wrote the first draft, conducted the mechanistic experiments, and isolated the products with the help of his colleague A.W. (compounds **3b-e**, **3h**, **3j**, **3k**) and with the help of his research intern F.W.C.W. All authors contributed to the final manuscript. B.K. supervised the project.

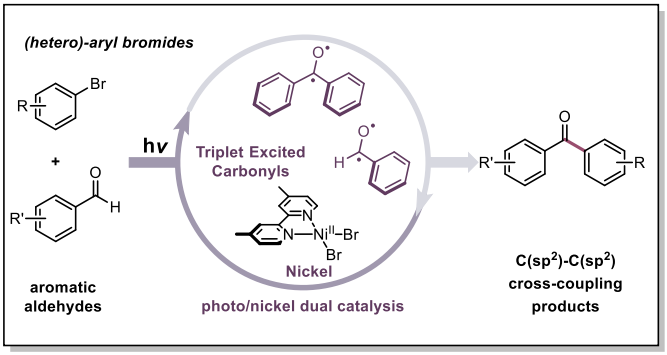

ABSTRACT

The dual catalytic arylation of aromatic aldehydes by aryl bromides using UV-irradiation and a nickel catalyst is reported. The reaction product serves as photocatalyst and hydrogen atom transfer agent (HAT) of this transformation.

2.1 Introduction

Photoredox catalysis has emerged as a powerful tool for C–H activation.[1] In particular, merging photo- and nickel catalysis enabled the functionalization of a wide range of C–H bonds.[2] As the field of photocatalysis develops, expensive iridium catalysts are successively replaced by novel organic dyes.[3] At the same time, long known photocatalysts such as benzophenones regain interest due to their ability to act as efficient triplet sensitizers or photoinduced hydrogen atom transfer catalysts.[4]

In his recent work on C(sp^3)–H functionalization, *Martin* demonstrated the efficiency of a carefully designed benzophenone in dual catalytic transformations.[5] A similar approach was later independently reported by *Hashmi*[6] and *Rueping,*[7] employing benzaldehyde and benzophenones, respectively, as combined HAT-photocatalyst and sensitizer for nickel catalyzed C(sp^3)–H arylations. Besides their utility in recent synthetic applications and classical photochemistry, diaryl ketones are a ubiquitous motive in pharmaceuticals, making their synthesis an attractive target of ongoing research.[8]

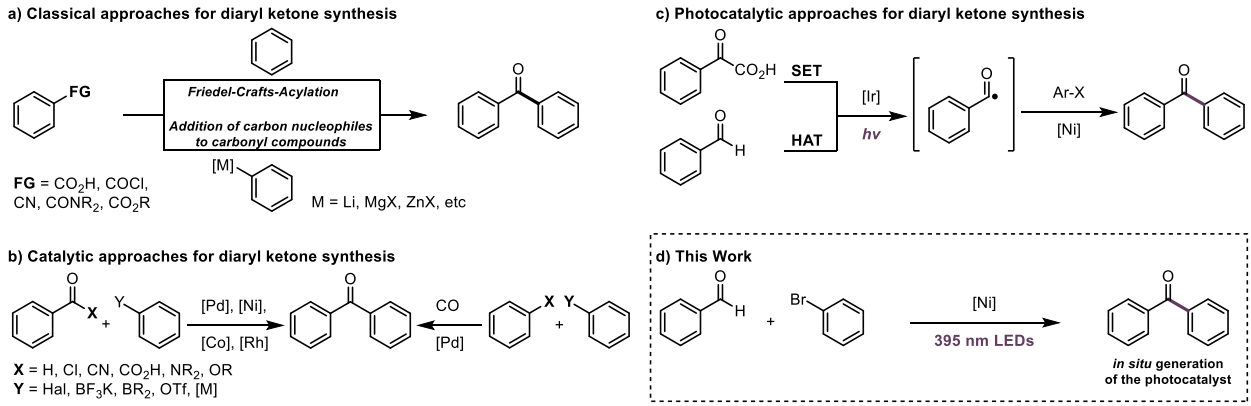

Scheme 1: Synthesis of benzophenones. (a) Classical and (b) catalytic methods for the synthesis of diaryl ketones and novel dual catalytic approaches (c and d).

As non-catalytic approaches such as the Friedel-Craft acylation often lack regioselectivity and the addition of organometallic reagents to carbonyls either require prefunctionalization or reoxidation (Scheme 1a), catalytic methods have been continuously developed over the years.[9] Both different acyl surrogates, and aldehydes have been employed together with transition metals such as palladium,[10] rhodium,[11] nickel,[12] and cobalt[13] to furnish benzophenones. The use of CO as a carbonyl source is likewise well established (Scheme 1b).[14] Recent developments in photoredox catalysis allow access to the acyl radical in a mild and selective manner (Scheme 1c). However, current photochemical methods for synthesizing ketones by C–H activation focused mainly on the coupling of

aliphatic aldehydes.[2e] To extend the catalytic approach to aromatic aldehydes, we envisioned a nickel-based dual catalytic methodology, which exploits the ability of diaryl ketones to act as sensitizers and HAT-catalysts (Scheme 1d).

2.2 Results and Discussion

We started our investigation with the coupling of 4-chlorobenzaldehyde (**1a**) with 4-bromobenzonitrile (**2a**). Gratifyingly, the respective ketone **3a** was observed under various conditions, revealing acetone as the optimal solvent, (4,4'-dimethyl-2,2'-bipyridyl)nickel(II) bromide as the most efficient precatalyst, and sodium carbonate as the best base during the screening (Table 1).

Table 1: Optimization and control reactions. The reactions were carried out with 4-bromobenzonitrile (0.5 mmol), 4-chlorobenzaldehyde (0.75 mmol), Na_2CO_3 (1.0 mmol), and Ni(dmbpy)Br_2 (0.025 mmol) in dry acetone (0.25 M) under irradiation with UV-LEDs (395 nm) and under an N_2-atmosphere for 8 h at 25 °C. [a]Yield determined by calibrated GC-FID analysis with 1,3,5-trimethoxybenzene as internal standard. [b]Isolated yield

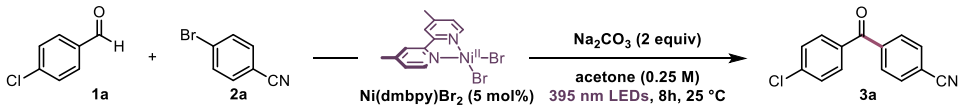

entry	deviation from standard condition	yield[a] (%)
1	None	93% (86%)[b]
2	Ni(dtbbpy)Br_2	40%
3	DMSO	0%
4	MeCN	50%
5	PhH	8%
6	Cs_2CO_3	61%
7	K_2CO_3	71%
8	K_2HPO_4	2%
9	no base	8%
10	$NiBr_2$-glyme as catalyst	0%
11	4,4'-dimethyl-2,2'-bipyridne as catalyst	0%
12	no catalyst	0%
13	in the dark or	0%
14	55°C in the dark	0%
15	455 nm LEDs	0%

After performing the control experiments and confirming the essential contribution of all reaction components to the product's formation, we explored the scope of this transformation.

The reaction of electron-deficient aryl bromides gave cyano-, trifluoromethyl-, sulfonyl- and ester-substituted benzophenones (**3a**, **3g**, **3i**, **3j**, **3l**) in good to excellent yields. Dihalogenated ketones (**3d**, **3h**) were obtained in moderate to good yields. The reaction is not limited to phenyl bromides. For example, Benzothiazoyl ketone **3f** was obtained in 59% yield (Scheme 2).

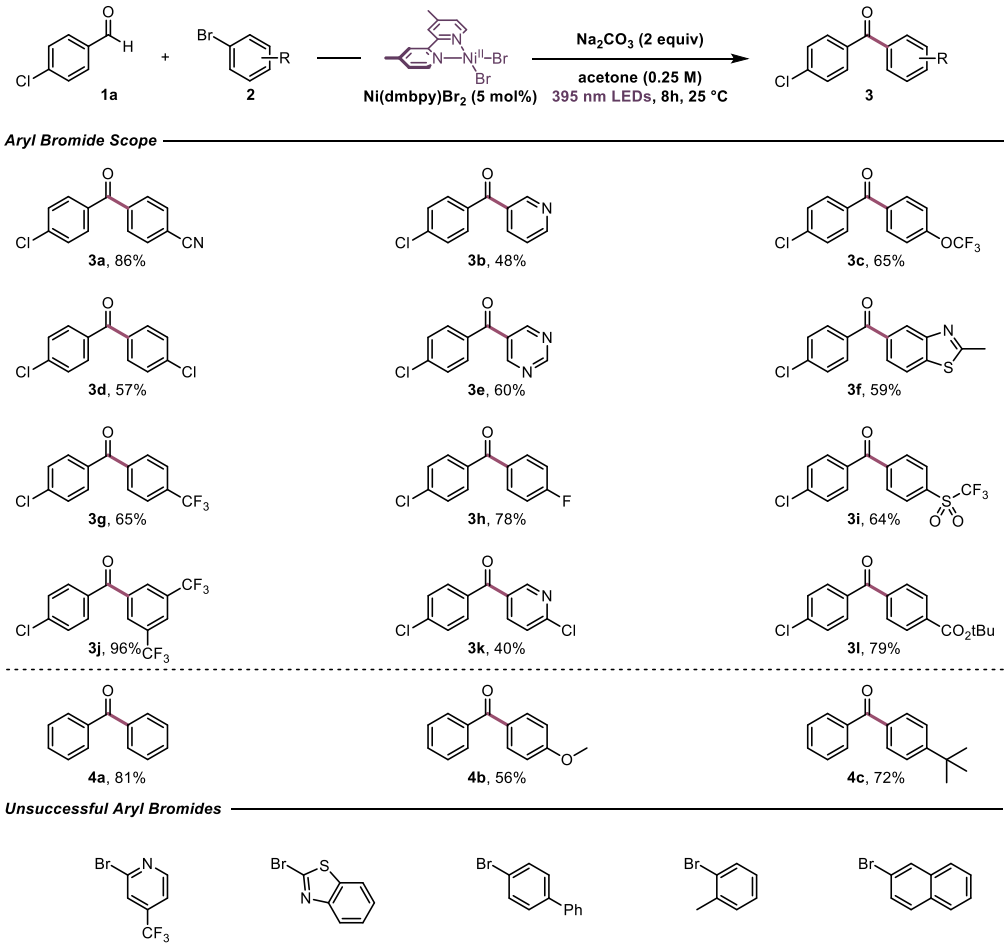

Scheme 2: Aryl bromide scope. All reactions were carried out with aryl bromide (0.5 mmol), 4-chlorobenzaldehyde or benzaldehyde (0.75 mmol), Na_2CO_3 (1.0 mmol), and Ni(dmbpy)Br_2 (0.025 mmol) in dry acetone (0.25 M) under irradiation with UV-LEDs (395 nm) and an N_2-atmosphere for 8 h at 25 °C. Isolated yield after purification by column chromatography.

Heteroaryl ketones (**3b**, **3e**, **3k**) were formed from bromopyridines and bromopyrimidine in moderate yields. However, neither 2-bromo-4-(trifluoromethyl)pyridine nor 2-bromobenzothiazole furnished significant amounts of product. The same was observed for 4-bromobiphenyl, 2-bromotoluene, and 2-bromonaphthalene (Scheme 2).[15] Using benzaldehyde as a coupling partner allowed benzoylation of bromobenzene and electron-rich aryl bromides in moderate to good yields (**4a-c**). After establishing the aryl bromide scope, we investigated the aldehyde scope, using 4-bromobenzonitrile as the coupling partner (Scheme 3). Benzaldehyde reacted smoothly under the

developed reaction conditions and afforded **5a** in excellent yield. Fluorinated benzaldehydes formed the respective ketones in good to excellent yields (**5e**, **5i**-**k**). Both very electron-poor benzophenones (**5b**-**e**, **5k**) as well as "*push-pull*" systems (**5f**-**i**), bearing an electron-donating on one side and one electron-withdrawing substituent on the other, were synthesized in good to excellent yields (**5f**-**i**). While benzoyl-protected hydroxybenzaldehyde was transformed into ketone **5l** in good yield, neither 4-hydroxybenzaldehyde nor 4-aminobenzaldehyde reacted to yield the respective ketones.[40]

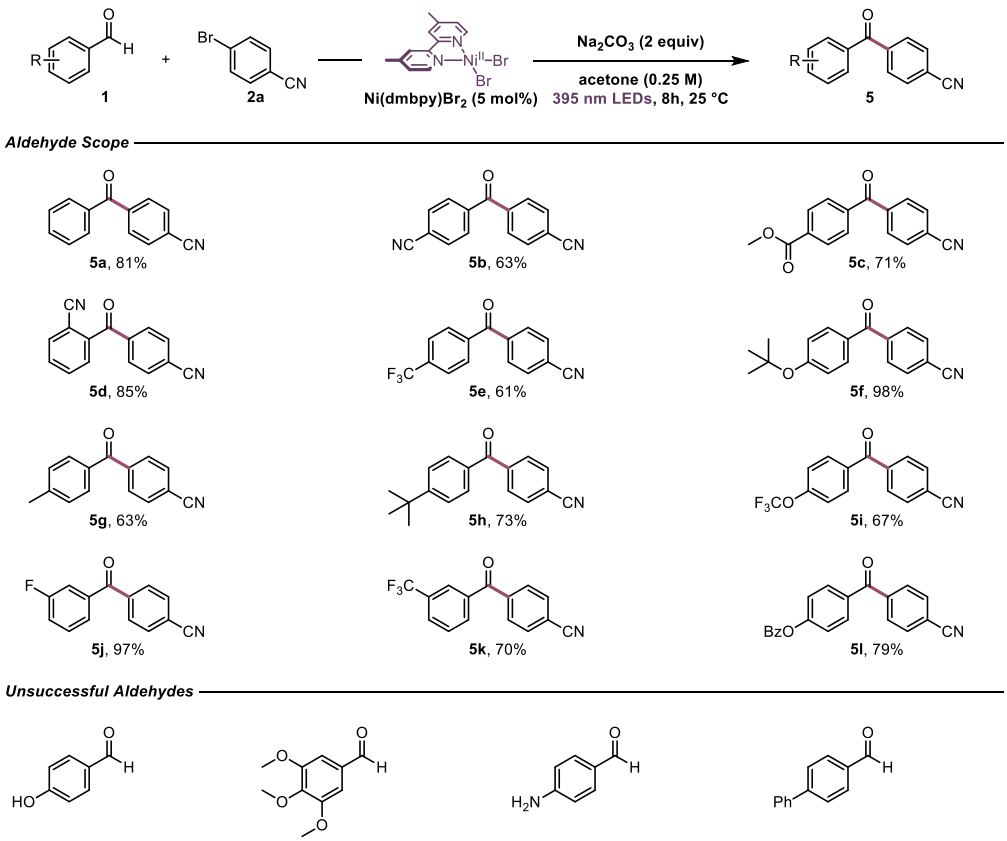

Scheme 3: Aldehyde scope. All reactions were carried out with 4-bromobenzonitrile (0.5 mmol), aldehyde (0.75 mmol), Na_2CO_3 (1.0 mmol), and Ni(dmbpy)Br_2 (0.025 mmol) in dry acetone (0.25 M) under irradiation with UV-LEDs (395 nm) and under an N_2-atmosphere for 8 h at 25 °C. Isolated yield after purification by column chromatography.

The mechanism of different nickel-based metalla-photocatalyzed reactions has been investigated in computations and experimental studies.[5, 16] Different modes of C-H activation are discussed, including σ-bond metathesis by a sensitized nickel(II)-aryl bromide complex (complex **B,** scheme 4) and HAT by bromine radicals that form upon homolytic fragmentation of the same excited complex. The use of benzophenones (**BP***) as a photocatalyst, however, opens a new potential reaction pathway, as triplet excited **BP*** can serve as a sensitizer to facilitate energy transfer-based pathways

but additionally can act as HAT catalyst itself.[17] A plausible mechanism based on the latter property is shown below.

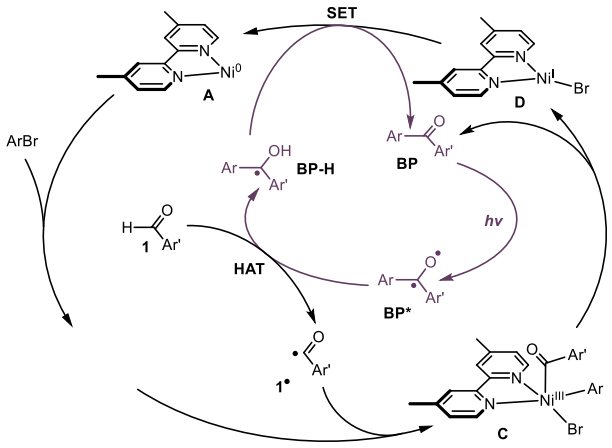

Scheme 4: Plausible mechanism.

The photocatalytic cycle starts with benzophenone **BP** absorbing a photon to reach its triplet-state **BP***, enabling it to abstract a hydrogen atom from aldehyde **1** to form both the acyl radical **1**· and radical **BP-H**. The oxidative addition of the nickel(0)-complex **A** into the aryl bromide bond furnishes nickel(II) species **B**, which serves as radical-trap for acyl radical **1**·. The formed nickel(III) species **C** is believed to undergo reductive elimination to benzophenone **BP** and complex **D**. Single electron transfer (SET) from **BP-H** to the nickel(I) bromide **D** is closing the catalytic cycle, furnishing both nickel(0) complex **A** and the ground state benzophenone **BP**.

However, the formation of the first photocatalytically active species remains elusive. Attempted photoreduction of the precatalyst with a mixture of benzaldehyde and sodium carbonate allows the observation of an air-sensitive species formed after already a few minutes of irradiation (see experimental section). GC-MS analysis of the mixture revealed traces of different products known to form upon photolysis of benzaldehyde, such as benzene, benzil, and its decarbonylation product benzophenone. We consider the latter ones together with the aldehyde capable of initiating the reaction.[18]

2.3 Conclusion

In conclusion, we have developed a photochemical, nickel catalyzed benzoylation of aryl bromides with various aldehydes. The reaction does not need the addition of a photocatalyst since the products of the reaction serve as photocatalysts after the reaction was initiated by photolysis of the respective benzaldehyde.

2.4 Experimental Section

2.4.1 General Information

All NMR spectra were recorded at room temperature using one of the following devices: Bruker Avance 300 (300 MHz for ^{1}H, 75 MHz for ^{13}C, 282 MHz for ^{19}F), Bruker Avance 400 (400 MHz for ^{1}H, 100 MHz for ^{13}C, 376 MHz for ^{19}F). All chemical shifts are reported on the δ-scale in parts per million (ppm) (multiplicity, coupling constant *J* in Hertz (Hz), number of protons) relative to the solvent residual peaks as the internal standard.[19]. Abbreviations used for signal multiplicity are br = broad, s = singlet, d = doublet, t = triplet, q = quartet, m = multiplet, and combinations thereof. High-resolution mass spectra (HRMS) were obtained from the institute's central analytic mass spectrometry department. The spectra were recorded on one of the following devices: Finnigan MAT 95, Thermo Quest Finnigan TSQ 7000, Finnigan MATSSQ 710 A, or Agilent Q-TOF 6540 UHD. For GC-FID measurements, a GC 7890 from Agilent Technologies was used, the analysis of the data was performed with Agilent ChemStation Rev.C.01.04. [35]. IR-Spectra were recorded on an Agilent Cary 630 FTIR Spectrometer. Uncorrected melting points were determined using the Stanford Research System OptiMelt MPA 100. The temperature was ranged from 30 °C to 300 °C with a heating rate of 2.5 °C/min. Analytical TLC was performed on silica gel-coated alumina plates (MN TLC plates ALUGRAM® Xtra SIL G/UV254). Detection was done by UV light (254 or 366 nm). Compounds were purified by automated column chromatography with silica gel 60 M (40-63 µm, 230-440 mesh, Merck) on a Biotage® Isolera TM Spektra One device. Benzoylation Reactions were irradiated with 395 nm LEDs (*LED Engin*, LZ4-40UB00-00U5 (λ = 395 nm, 14.5 V, 700 mA, 3.8 W light flux), 400 nm LEDs (*Edison,* EDEV-SLC1-03, λ = 395 - 410 nm, 3.5 V, 700 mA, 350 mW light flux), 385 nm LEDs (*Opulent Americas*, LST1-01G01-UV02-00, λ = 385 nm, 3.4 V, 350 mA, 1.015 W light flux) and 365 nm LEDs (*Seoul VIOSYS,* SSC VIOSYS CUN66A1B λ = 365 nm, 3.6 V, 700 mA, 0.92 - 1.25 W light flux). Emission spectra of the LEDs were recorded with an Ocean Optics HR4000CG UV NIR spectrometer running Ocean View software (V1.6.5) for data acquisition. All chemicals and solvents were obtained from commercial sources if not otherwise stated. Dry acetone was purchased from *Acros Organics* (Acetone, 99.8%, Extra Dry, AcroSeal®). 4-Formylphenyl benzoate was synthesized according to the reported procedure.[20] Solid aldehydes were used as received; liquid ones were purified by distillation under reduced pressure prior to use.

2.4.2 Synthesis of the Nickel Catalysts

(4,4'-dimethyl-2,2'-bipyridyl)nickel(II) bromide was synthesized adapting the literature procedure for $NiBr_2$·dtbbpy (4,4'-di-*tert*-butyl-2,2'-bipyridyl)nickel(II) bromide.[21] A 50 mL crimp cap vial was charged with nickel(II) bromide glyme complex (480 mg, 1.56 mmol, 1.0 equiv), 4,4'-dimethyl-2,2'-bipyridin (287 mg, 1.56 mmol, 1.0 equiv) and dry THF (25 mL). A bright green precipitate formed as the mixture was stirred at 55 °C for 2 h under a nitrogen atmosphere. The solid was filtered off and washed with dry THF (3 × 10 mL) and ether. After drying *in vaccuo,* the complex was received as green solid (610 mg, 97%) and used without further purification. For the catalyst screening, nickel-complexes with different ligands were synthesized accordingly at 156 mmol scale.

2.4.3 General Procedure for the Benzoylation of Aryl Bromides

A crimp cap vial was charged with (4,4'-dimethyl-2,2'-bipyridyl)nickel(II) bromide (10 mg, 25.0 µmol, 0.05 equiv), sodium carbonate (106 mg, 1.0 mmol, 2.0 equiv), solid aryl bromides (0.5 mmol, 1.0 equiv), solid aldehydes (0.75 mmol, 1.5 eqiuv) and a stirring bar. The vial was sealed and flushed with dried nitrogen (3×) before adding dry acetone (2 mL). Liquid reactants were added at this point by syringe through the septum. The mixture was degassed by two *freeze-pump-backfill-thaw* cycles. The reaction mixture was irradiated for 8 h at 25 °C, diluted with acetone (3-4 mL) filtered through a glass frit, concentrated, and submitted to automated column chromatography (20 g to 50 g SiO_2, pentane/ethyl acetate = 100/0 → 90/10 or 75/25, detection at 254 nm).

2.4.4 Photoreduction of the Nickel Catalyst

A mixture of benzaldehyde (0.375 mmol), Na_2CO_3 (0.5 mmol), and Ni(dmbpy)Br_2 (12.5 µmol) in acetone (1 mL) was irradiated for 1, 5, 10, 15, and 30 min and subsequently exposed to air. The experiment was prepared as described in the general procedure at half scale without adding aryl bromide.

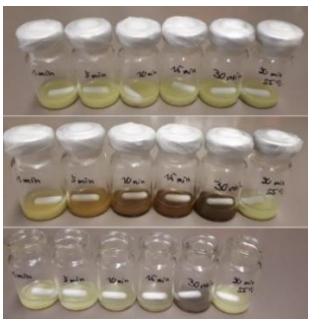

Figure 1: Photoreduction experiment. (top) samples before irradiation. (middle) samples after irradiation. (bottom) samples after exposition to air.

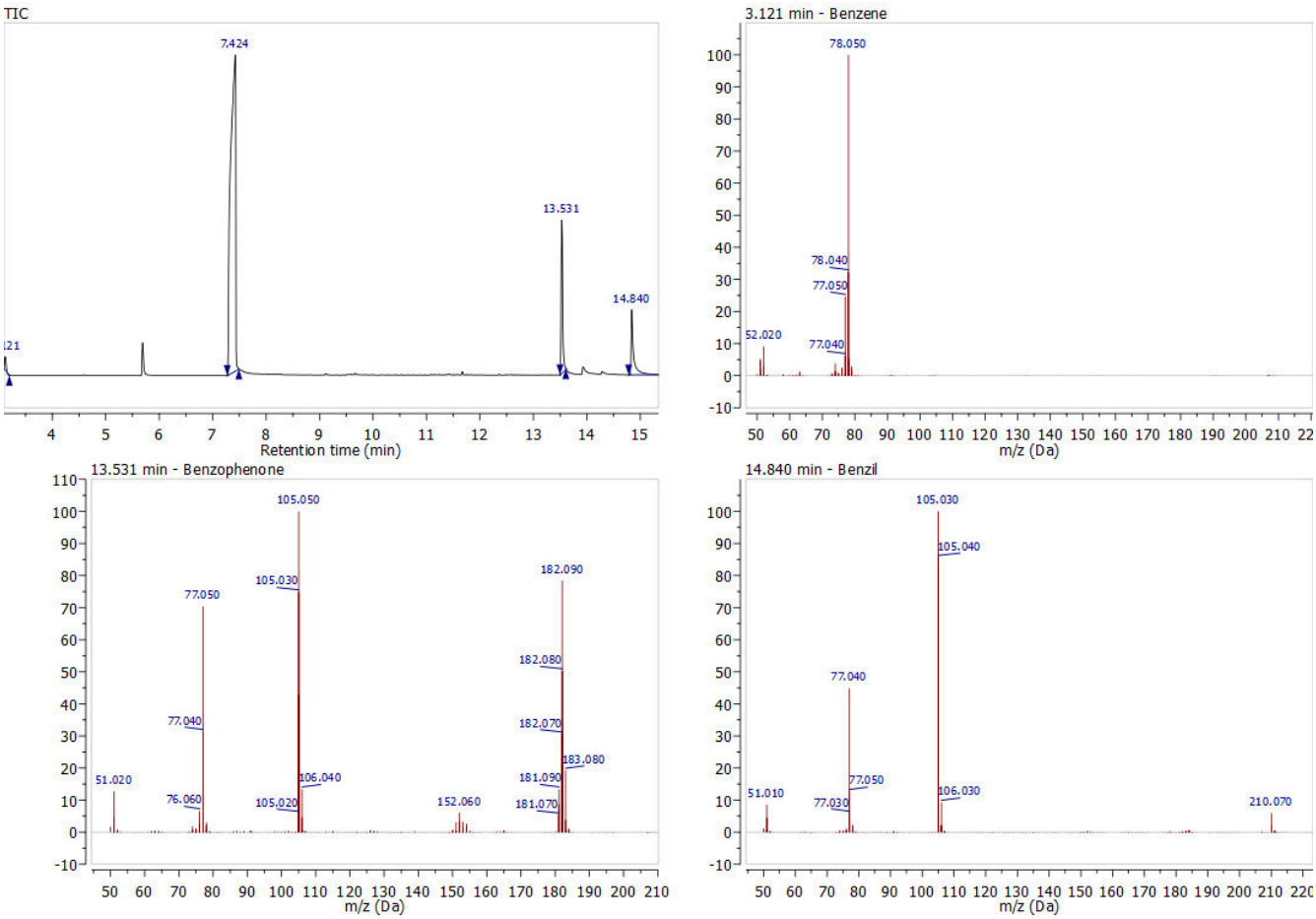

Figure 2: GC-MS analysis of the photoreduction experiment after 30 min upon irradiation with 395 nm LEDs. Benzene (3.121 min), benzophenone (13.531 min), and benzil (14.840) are formed from benzaldehyde (7.424 min).

2.4.5 Optimization of the Reaction Conditions

Table 2: Optimization of the reaction conditions. The reactions were carried out with 4-bromobenzonitrile (1.0 equiv), 4-chlorobenzaldehyde (1.5 equiv), base (2.0 equiv), and nickel complex (5 mol%) in indicated solvent (0.25 M) under irradiation with UV-LEDs and under N_2-atmosphere at 25 °C. The yield was determined by calibrated GC-FID analysis with 1,3,5-trimethoxybenzene as internal standard. [a]0.25 mmol scale. [b]0.5 mmol scale.

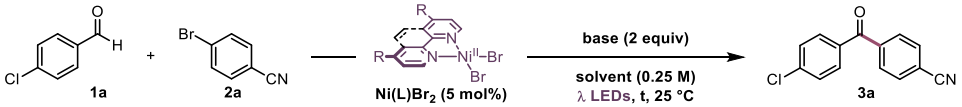

entry	nickel salt	λ (nm)	time (h)	solvent	base	yield (%)
1[a]	Ni(bpy)Br_2	400	16 h	$PhCF_3$	Na_2CO_3	25%
2[a]	Ni(dmbpy)Br_2	400	16 h	**$PhCF_3$**	Na_2CO_3	**28%**
3[a]	Ni(4,4' –$(OMe)_2$bpy)Br_2	400	16 h	$PhCF_3$	Na_2CO_3	24%
4[a]	Ni(dtbbpy)Br_2	400	16 h	$PhCF_3$	Na_2CO_3	20%
5[a]	Ni(phen)Br_2	400	16 h	$PhCF_3$	Na_2CO_3	21%
6[a]	Ni(dmbpy)Br_2	395	4 h	$PhCF_3$	Na_2CO_3	25%
7[a]	Ni(dmbpy)Br_2	**395**	**8 h**	**$PhCF_3$**	**Na_2CO_3**	**40%**
8[a]	Ni(dmbpy)Br_2	385	16 h	$PhCF_3$	Na_2CO_3	45%
9[a]	Ni(dmbpy)Br_2	365	16 h	$PhCF_3$	Na_2CO_3	33%
10[b]	Ni(dmbpy)Br_2	395	8h	Ph	Na_2CO_3	8%
11[b]	Ni(dmbpy)Br_2	395	8h	DMSO	Na_2CO_3	0%
12[b]	Ni(dmbpy)Br_2	**395**	**8h**	**acetone**	**Na_2CO_3**	**93%**
13[b]	Ni(dmbpy)Br_2	395	8h	MeCN	Na_2CO_3	50%
14[b]	Ni(dmbpy)Br_2	395	8h	DMA	Na_2CO_3	2%
15[b]	Ni(dmbpy)Br_2	395	8h	THF	Na_2CO_3	0%
16[b]	Ni(dmbpy)Br_2	395	8h	acetone	Cs_2CO_3	61%
17[b]	Ni(dmbpy)Br_2	395	8h	acetone	K_2CO_3	71%
18[b]	Ni(dmbpy)Br_2	395	8h	acetone	K_2HPO_4	2%
19[b]	Ni(dmbpy)Br_2	395	8h	acetone	Na_2HPO_4	1%
20[b]	Ni(dmbpy)Br_2	395	8h	acetone	DABCO	0%
21[b]	Ni(dmbpy)Br_2	395	8h	acetone	DIPEA	19%
22[b]	Ni(dmbpy)Br_2	395	8h	acetone	DBU	0%

2.4.6 Mechanistic Experiments

Table 3: Radical inhibitor/trapping experiments. The reactions were carried out according to the general procedure with 2 equivalents of additive.

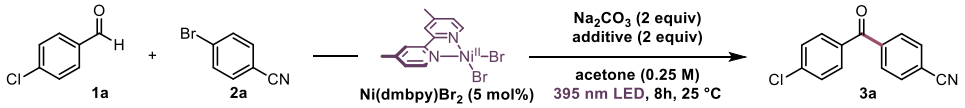

entry	additive	yield (%)
1	1,1-diphenylethylene	0%
2	2,2,6,6-tetramethyl piperidinyloxy (TEMPO)	0%
3	3,5-di-tert-butyl-4-hydroxytoluene (BHT)	9%
4	ethyl acrylate	44%

1,1-Diphenylethylene completely shuts down the reaction. As GC-FID analysis showed no conversion, we assume that 1,1-diphenylethylene, in this case, acts as a triplet quencher rather than as a radical inhibitor or radical trap (see table 4, entry 7).[22] The addition of 2 equiv of TEMPO shuts down the product formation without furnishing a GC-MS detectable benzoyl-adduct. However, TEMPO is a potential poison to the nickel catalyst, as discussed in the literature, limiting the significance of this experiment.[23] BHT as an additive reduces the yield of the reaction to 9%. Ethyl acrylate was added to trap the potential benzoyl radical; however, no such product could be detected by GC-MS. This reaction proceeded with lower efficiency and furnished **3a** in 44% yield.

2.4.7 Experiments with Complex B-1

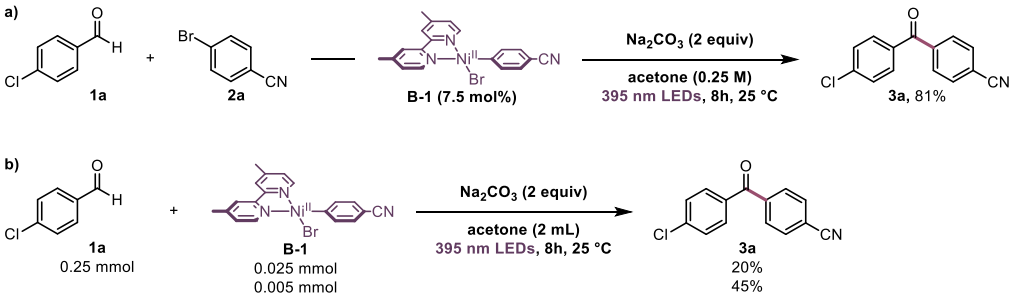

Scheme 5: Experiments with complex B-1. (a) Using **B-1** as precatalysts and potential intermediate of the reaction furnishes the product in 81% yield based on both **2a** and **B-1**. (B) Using **B-1** as a stoichiometric reactant yields product **3a** in 20% to 45%, favoring lower concentrations of B-1. Yields determined by calibrated GC.

2.4.8 Remarks on Unsuccessful Substrates

Aryl Bromides: Benzophenone has been used to sensitize both 2-bromonaphtalene[24] and 4-bromobiphenyl[25] to study the triplet state reactions of the excited aromatic compounds. Compiled

triplet-energies of aldehydes, benzophenones and aryl bromides indicate that both 2-bromonaphtalene and 4-bromobiphenyl could serve as triplet quenchers to proposed photoactive species.

Table 4: Triplet energies of substrates.

entry	substrate	E_T
1	benzaldehyde	301 kJ/mol[26]
2	4-chlorobenzaldehyde	299 kJ/mol[26]
3	benzophenone	289 kJ/mol[27]
4	4,4'-dichlorobenzophenone	285 kJ/mol[28]
5	4-bromobiphenyl	272 kJ/mol[29]
6	2-bromonaphtalene	252 kJ/mol[30]
7	1,1-diphenylethylene	247 kJ/mol[22]

Further, it was observed that 2-bromo pyridines did not undergo benzoylation; however, 3-bromopyridines (example **3b**, **3k**) and 5-bromo pyrimidine (example **3e**) did. The neighboring heteroatom seems to be not compatible with our conditions.

Aldehydes: We believe that the aldehyde plays a crucial part in the initiation of the reaction. It could either act as the first active catalyst upon excitation[6] or undergo photolysis to furnish other species such as benzil or benzophenones to be the active catalysts. Despite the broad emission of used 395 nm LEDs, aromatic aldehydes hardly absorb in this region, which might be one reason for unsuccessful reactions. Lowering the wavelength to overcome this issue leads to a drastic loss in efficiency of the transformation due to vastly increased side reactions. If all species (aldehyde and photolysis products) cannot initiate the reaction, the reaction might already fail at this point.

2.4.9 Synthesis of Ni(dmbpy)(4-CN-Ph)Br (B-1)

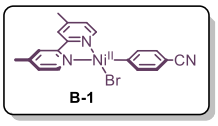

B-1

Following the literature procedure,[5] an oven-dried crimp vial (50 mL) was charged with $Ni(cod)_2$ (275 mg, 1.00 mmol) and 4,4'-dimethyl-2,2'-bipyridine (194 mg, 1.05 mmol) under the nitrogen atmosphere of a glovebox. The vial was sealed, moved outside the glovebox, and filled with 10 mL THF (dry and degassed). The mixture was stirred for 3 h at room temperature to form a deep purple solution which was then treated with a solution of 4-bromobenzonitrile (910 mg, 5.00 mmol) in THF (3 mL) to give a bright reddish-orange precipitate. After one hour at room temperature, pentane (10 mL) was added, and the product was filtered under nitrogen atmosphere, washed with THF (10 mL) and pentane (5 mL) before the frit was moved into the glovebox to obtain the complex in 95% yield (401 mg) as red solid. The complex is hardly soluble in THF, decomposes quickly in DMSO, and is water sensitive. The poor

solubility allows to obtain a proton spectrum; however, it prevents the acquisition of a carbon spectrum. **^{1}H NMR** (400 MHz, THF-d_8) δ 9.24 (s, 1H), 8.04 (s, 2H), 7.74 (d, *J* = 7.8 Hz, 2H), 7.40 (s, 1H), 7.08 (m, *J* = 7.8 Hz, 4H), 2.48 (s, 3H), 2.40 (s, 3H). **HRMS** (ESI+) Calc. for $C_{19}H_{16}N_3Ni^+$ [M-Br]$^+$: 344.0692 Found: 344.0700. Calc. for $C_{12}H_{12}BrN_2Ni^+$ [M-C_7H_4N]$^+$: 320.9532 Found: 320.9541.

2.4.10 Characterization Data for Benzoylation Products

4-(4-chlorobenzoyl)benzonitrile (3a)

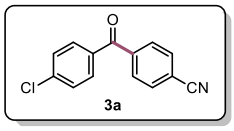

^{1}H NMR (300 MHz, $CDCl_3$) δ (ppm) 7.85 (d, *J* = 8.7 Hz, 2H), 7.80 (d, *J* = 8.7 Hz, 2H), 7.76 – 7.71 (m, 2H), 7.53 – 7.47 (m, 2H). **^{13}C NMR** (75 MHz, $CDCl_3$) δ (ppm) 194.0, 141.0, 140.1, 134.7, 132.4, 131.6, 130.3, 129.2, 118.0, 116.0. **HRMS** (EI+) Calc. for $C_{14}H_8ClNO^{\bullet+}$ [M$^{\bullet+}$]: 241.0289. Found: 241.0293. The data match reported literature values.[13]

(4-chlorophenyl)(pyridin-3-yl)methanone (3b)

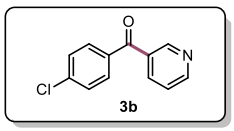

^{1}H NMR (400 MHz, $CDCl_3$) δ (ppm) 8.97 (dt, *J* = 2.2, 1.0 Hz, 1H), 8.82 (dd, *J* = 4.9, 1.8 Hz, 1H), 8.10 (dt, *J* = 7.9, 2.0 Hz, 1H), 7.81 – 7.73 (m, 2H), 7.54 – 7.46 (m, 2H), 7.46 (ddd, *J* = 7.8, 4.9, 0.9 Hz, 1H). **^{13}C NMR** (101 MHz, $CDCl_3$) δ (ppm) 193.8, 153.2, 150.9, 139.9, 137.2, 135.1, 133.0, 131.5, 129.2, 123.6. **HRMS** (APCI) Calc. for $C_{12}H_9ClNO^+$ [M+H$^+$]: 218.0367. Found: 218.0372. The data match reported literature values.[31]

(4-chlorophenyl)(4-(trifluoromethoxy)phenyl)methanone (3c)

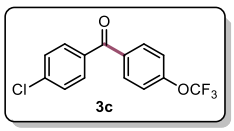

^{1}H NMR (400 MHz, $CDCl_3$) δ (ppm) 7.86 – 7.81 (m, 2H), 7.74 (d, *J* = 8.3 Hz, 2H), 7.48 (d, *J* = 8.3 Hz, 2H), 7.35 – 7.31 (m, 2H). **^{13}C NMR** (101 MHz, $CDCl_3$) δ (ppm) 194.0, 152.4 (q, *J* = 1.7 Hz), 139.4, 135.6, 135.6, 132.0, 131.5, 128.9, 120.5, 120.5 (q, *J* = 258.8 Hz). **^{19}F NMR** (376 MHz, $CDCl_3$) δ (ppm) -58.10. **HRMS** (EI+) Calc. for $C_{14}H_8ClF_3O_2^{\bullet+}$ [M$^{\bullet+}$]: 300.0159. Found: 300.0159. The data match reported literature values.[32]

bis(4-chlorophenyl)methanone (3d)

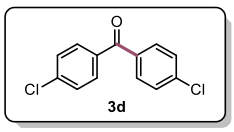

^{1}H NMR (300 MHz, $CDCl_3$) δ (ppm) 7.77 – 7.70 (m, 4H), 7.51 – 7.44 (m, 4H). **^{13}C NMR** (75 MHz, $CDCl_3$) δ (ppm) 194.4, 139.3, 135.7, 131.5, 128.9. **HRMS** (EI+) Calc. for $C_{13}H_8Cl_2O^{\bullet+}$ [M$^{\bullet+}$]: 249.9947. Found: 249.9948. The data match reported literature values.[10b]

(4-chlorophenyl)(pyrimidin-5-yl)methanone (3e)

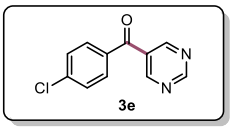

^{1}H NMR (300 MHz, $CDCl_3$) δ (ppm) 9.39 (s, 1H), 9.08 (s, 2H), 7.81 – 7.71 (m, 2H), 7.57 – 7.48 (m, 2H). **^{13}C NMR** (75 MHz, $CDCl_3$) δ (ppm) 191.5, 161.0, 157.7, 140.7, 134.2, 131.4, 130.8, 129.5. **HRMS** (EI+) Calc. for $C_{11}H_7ClN_2O^{\bullet+}$ [$M^{\bullet+}$]: 218.0236. Found: 218.0237.

(4-chlorophenyl)(2-methylbenzo[d]thiazol-5-yl)methanone (3f)

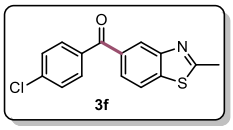

^{1}H NMR (300 MHz, $CDCl_3$) δ (ppm) 8.30 (d, *J* = 1.6 Hz, 1H), 7.95 (dd, *J* = 8.4, 0.6 Hz, 1H), 7.85 (dd, *J* = 8.4, 1.6 Hz, 1H), 7.81 – 7.75 (m, 2H), 7.50 – 7.44 (m, 2H), 2.87 (s, 3H). **^{13}C NMR** (75 MHz, $CDCl_3$) δ (ppm) 195.0, 168.9, 153.1, 140.5, 139.1, 136.0, 135.4, 131.6, 128.8, 125.9, 124.6, 121.8, 20.5. **HRMS** (EI+) Calc. for $C_{15}H_{10}ClNOS^{\bullet+}$ [$M^{\bullet+}$]: 287.0166. Found: 287.0165. **FTIR** (ν / cm^{-1}): 1644, 1580, 1412, 1159, 898, 842, 749. **MP**.: 101 °C.

(4-chlorophenyl)(4-(trifluoromethyl)phenyl)methanone (3g)

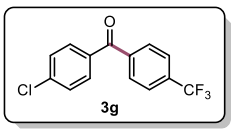

^{1}H NMR (400 MHz, $CDCl_3$) δ (ppm) 7.87 (d, *J* = 8.1 Hz, 2H), 7.80 – 7.72 (m, 4H), 7.52 – 7.46 (m, 2H).**^{13}C NMR** (101 MHz, $CDCl_3$) δ (ppm) 194.4, 140.5, 139.8, 135.1, 134.1 (q, *J* = 32.8 Hz), 131.6, 130.2, 129.1, 125.6 (q, *J* = 3.8 Hz), 123.7 (q, *J* = 272.7 Hz). **^{19}F NMR** (377 MHz, $CDCl_3$) δ -63.57. **HRMS** (EI+) Calc. for $C_{14}H_8ClF_3O^{\bullet+}$ [$M^{\bullet+}$]: 284.0210. Found: 284.0208. The data match reported literature values.[31]

(4-chlorophenyl)(4-fluorophenyl)methanone (3h)

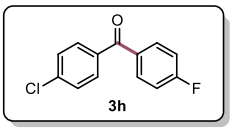

^{1}H NMR (300 MHz, $CDCl_3$) δ (ppm) 7.85 – 7.78 (m, 2H), 7.75 – 7.70 (m, 2H), 7.49 – 7.44 (m, 2H), 7.21 – 7.13 (m, 2H). **^{13}C NMR** (75 MHz $CDCl_3$) δ (ppm) 194.2, 165.6 (d, *J* = 254.7 Hz), 139.1, 135.9, 133.6 (d, *J* = 3.1 Hz), 132.7 (d, *J* = 9.2 Hz), 131.4, 128.9, 115.8 (d, *J* = 21.8 Hz). **^{19}F NMR** (377 MHz, $CDCl_3$) δ (ppm) -105.89. **HRMS** (EI+) Calc. for $C_{13}H_8ClFO^{\bullet+}$ [$M^{\bullet+}$]: 234.0242. Found: 243.0246. The data match reported literature values.[10b]

(4-chlorophenyl)(4-((trifluoromethyl)sulfonyl)phenyl)methanone (3i)

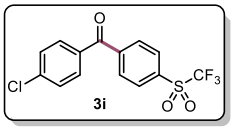

^{1}H NMR (400 MHz, $CDCl_3$) δ (ppm) 8.19 (d, *J* = 8.2 Hz, 2H), 8.00 (d, *J* = 8.4 Hz, 2H), 7.79 – 7.74 (m, 2H), 7.54 – 7.50 (m, 2H). **^{13}C NMR** (101 MHz, $CDCl_3$) δ (ppm) 193.5, 144.5, 140.6, 134.6 (d, *J* = 1.4 Hz), 134.3, 131.7, 131.1, 130.7, 129.4, 119.8 (q, *J* = 326.0 Hz). **^{19}F NMR** (282 MHz, $CDCl_3$) δ (ppm) -78.4. **HRMS** (ESI+) Calc. for $C_{14}H_9ClF_3O_3S^{+}$ [M+H^{+}]: 348.9908. Found: 348.9911. **FTIR** (ν / cm^{-1}): 1669, 1588, 1372, 1271, 1215, 1133, 1073, 1013, 928, 760, 715, 670. **MP**.: 113 °C.

(3,5-bis(trifluoromethyl)phenyl)(4-chlorophenyl)methanone (3j)

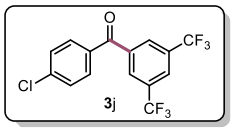

3j

^{1}H NMR (300 MHz, $CDCl_3$) δ (ppm) 8.20 (s, 2H), 8.11 (s, 1H), 7.78 – 7.70 (m, 2H), 7.57 – 7.50 (m, 2H). **^{13}C NMR** (101 MHz, $CDCl_3$) δ (ppm) 192.5, 140.5, 139.2, 134.3, 132.4 (q, *J* = 34.1 Hz), 131.5, 129.8 (d, *J* = 3.7 Hz), 126.0 (sept, *J* = 3.7 Hz), 123.0 (q, *J* = 273.0 Hz). **^{19}F NMR** (377 MHz, $CDCl_3$) δ (ppm) -63.46. **HRMS** (EI+) Calc. for $C_{15}H_7ClF_6O^{\bullet+}$ [$M^{\bullet+}$]: 352.0084. Found: 352.0083. The data match reported literature values.[33]

(4-chlorophenyl)(6-chloropyridin-3-yl)methanone (3k)

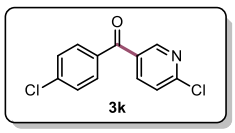

3k

^{1}H NMR (300 MHz, $CDCl_3$) δ (ppm) 8.73 (dd, *J* = 2.5, 0.8 Hz, 1H), 8.07 (dd, *J* = 8.3, 2.4 Hz, 1H), 7.77 – 7.71 (m, 2H), 7.53 – 7.46 (m, 3H). **^{13}C NMR** (75 MHz, $CDCl_3$) δ (ppm) 192.5, 155.3, 151.1, 140.2, 139.8, 134.8, 131.8, 131.4, 129.2, 124.6. **HRMS** (EI+) Calc. for $C_{12}H_7Cl_2NO^{\bullet+}$ [$M^{\bullet+}$]: 250.9894. Found: 250.9893. The data match reported literature values.[34]

***tert*-butyl 4-(4-chlorobenzoyl)benzoate (3l)**

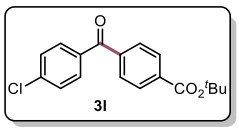

3l

^{1}H NMR (300 MHz, $CDCl_3$) δ (ppm) 8.13 – 8.07 (m, 2H), 7.82 – 7.77 (m, 2H), 7.77 – 7.72 (m, 2H), 7.50 – 7.44 (m, 2H), 1.62 (s, 9H). **^{13}C NMR** (101 MHz, $CDCl_3$) δ (ppm) 195., 165.0, 140.6, 139.6, 135.5, 135.5, 131.6, 129.7, 129.6, 128.9, 82.0, 28.3. **HRMS** (ESI+) Calc. for $C_{18}H_{18}ClO_3^{+}$ [M+H^{+}]: 317.0939. Found: 317.0945. **FTIR** (ν / cm^{-1}): 1711, 1651, 1584, 1384, 1289, 1163, 1103, 931, 848, 738, 704. **MP**.: 148 °C.

Benzophenone (4a)

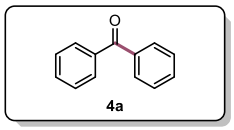

4a

^{1}H NMR (300 MHz, $CDCl_3$) δ (ppm) 7.86 – 7.76 (m, 4H), 7.63 – 7.56 (m, 2H), 7.52 – 7.45 (m, 4H). **^{13}C NMR** (101 MHz, $CDCl_3$) δ (ppm) 196.9, 137.7, 132.6, 130.2, 128.4. **HRMS** (EI+) Calc. for $C_{13}H_{10}O^{\bullet+}$ [$M^{\bullet+}$]: 182.0726. Found: 182.0731. The data match reported literature values.[10i]

(4-methoxyphenyl)(phenyl)methanone (4b)

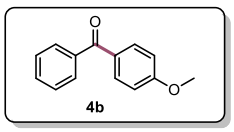

4b

^{1}H NMR (400 MHz, $CDCl_3$) δ (ppm) 7.87 – 7.80 (m, 2H), 7.79 – 7.73 (m, 2H), 7.60 – 7.53 (m, 1H), 7.51 – 7.43 (m, 2H), 7.00 – 6.94 (m, 2H), 3.89 (s, 3H). **^{13}C NMR** (101 MHz, $CDCl_3$) δ (ppm) 195.7, 163.4, 138.4, 132.7, 132.0, 130.3, 129.9, 128.3, 113.7, 55.6. **HRMS** (EI+) Calc. for $C_{14}H_{12}O_2^{\bullet+}$ [$M^{\bullet+}$]: 212.0832. Found: 212.0837. The data match reported literature values.[10i]

(4-(tert-butyl)phenyl)(phenyl)methanone (4c)

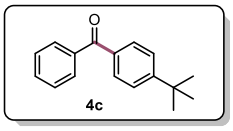

^{1}H NMR (300 MHz, $CDCl_3$) δ (ppm) 7.83 – 7.79 (m, 2H), 7.79 – 7.74 (m, 2H), 7.57 (m, 1H), 7.53 – 7.44 (m, 4H), 1.37 (s, 9H). **^{13}C NMR** (75 MHz, $CDCl_3$) δ (ppm) 196.6, 156.3, 138.1, 134.9, 132.3, 130.3, 130.1, 128.3, 125.4, 35.3, 31.3. **HRMS** (EI+) Calc. for $C_{17}H_{18}O^{\bullet+}$ [$M^{\bullet+}$]: 238.1352. Found: 238.1354. The data match reported literature values.[10i]

4-Benzoylbenzonitrile (5a)

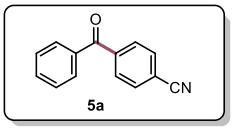

^{1}H NMR (400 MHz, $CDCl_3$) δ (ppm) 7.91 – 7.85 (m, 2H), 7.82 – 7.76 (m, 4H), 7.67 – 7.60 (m, 1H), 7.52 (dd, *J* = 8.3, 7.1 Hz, 2H). **^{13}C NMR** (101 MHz, $CDCl_3$) δ (ppm) 195.2, 141.4, 136.4, 133.5, 132.3, 130.4, 130.2, 128.8, 118.2, 115.8. **HRMS** (EI+) Calc. for $C_{14}H_9NO^{\bullet+}$ [$M^{\bullet+}$]: 207.0679. Found: 207.0684. The spectroscopic data matches reported values.[10b]

4,4'-carbonyldibenzonitrile (5b)

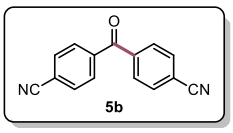

^{1}H NMR (400 MHz, $CDCl_3$) δ (ppm) 7.87 (d, *J* = 8.6 Hz, 1H), 7.82 (d, *J* = 8.6 Hz, 1H). **^{13}C NMR** (101 MHz, $CDCl_3$) δ (ppm) 193.6, 139.9, 132.6, 130.4, 117.8, 116.7. **HRMS** (EI+) Calc. for $C_{15}H_8N_2O^{\bullet+}$ [$M^{\bullet+}$]: 232.0631. Found: 232.0624. The spectroscopic data matches reported values.[10a]

Methyl 4-(4-cyanobenzoyl)benzoate (5c)

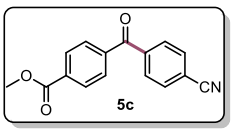

^{1}H NMR (400 MHz, $CDCl_3$) δ (ppm) 8.18 (d, *J* = 8.3 Hz, 2H), 7.89 (d, *J* = 8.2 Hz, 2H) 7.85 – 7.79 (m, 4H), 3.98 (s, 3H). **^{13}C NMR** (101 MHz, $CDCl_3$) δ (ppm) 194.5, 166.1, 140.6, 140.0, 134.2, 132.5, 130.4, 130.0, 129.9, 118.0, 116.4, 52.8. **HRMS** (EI+) Calc. for $C_{16}H_{11}NO_3^{\bullet+}$ [$M^{\bullet+}$]: 265.0733. Found: 265.0734. The spectroscopic data matches reported values.[35]

2-(4-cyanobenzoyl)benzonitrile (5d)

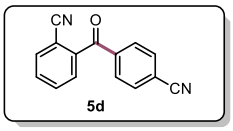

^{1}H NMR (400 MHz, $CDCl_3$) δ (ppm) 7.93 – 7.86 (m, 3H), 7.82 (d, *J* = 8.3 Hz, 2H), 7.76 – 7.71 (m, 2H), 7.66 – 7.63 (m, 1H). **^{13}C NMR** (101 MHz, $CDCl_3$) δ (ppm) 192.5, 140.2, 139.4, 134.7, 132.7, 132.6, 132.4, 130.6, 130.3, 117.8, 117.2, 116.9, 112.3. **HRMS** (EI+) Calc. for $C_{15}H_8N_2O^{\bullet+}$ [$M^{\bullet+}$]: 232.0631. Found: 232.0636. **FTIR** (ν / cm^{-1}): 2225, 1669, 1271, 928, 861, 790, 760. **MP**.: 135 °C.

4-(4-(trifluoromethyl)benzoyl)benzonitrile (5e)

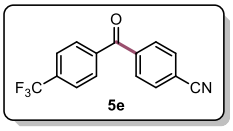

^{1}H NMR (400 MHz, $CDCl_3$) δ (ppm) 7.91 – 7.86 (m, 4H), 7.84 – 7.80 (m, 2H), 7.79 (d, *J* = 8.3 Hz, 2H). **^{13}C NMR** (101 MHz, $CDCl_3$) δ (ppm) 194.0, 140.3, 139.5, 134.7 (q, *J* = 32.9 Hz), 132.5, 130.4, 130.3, 125.8 (q, *J* = 3.7 Hz), 123.6 (q, *J* = 272.9 Hz), 117.9, 116.5. **^{19}F NMR** (377 MHz, $CDCl_3$) δ (ppm) -63.7. The spectroscopic data matches reported values.[31]

4-(4-(tert-butoxy)benzoyl)benzonitrile (5f)

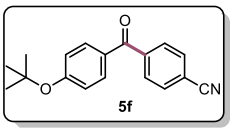

^{1}H NMR (300 MHz, $CDCl_3$) δ (ppm) 7.87 – 7.82 (m, 2H), 7.80 – 7.72 (m, 4H), 7.11 – 7.03 (m, 2H), 1.45 (s, 9H). **^{13}C NMR** (75 MHz, $CDCl_3$) δ (ppm) 194.1, 161.0, 142.0, 132.2, 131.9, 130.3, 130.1, 122.1, 118.2, 115.3, 80.1, 29.0. **HRMS** (EI+) Calc. for $C_{18}H_{17}NO_2^{\bullet+}$ [$M^{\bullet+}$]: 279.1254. Found: 279.1247. **FTIR** (ν / cm^{-1}): 2981, 2229, 1640, 1591, 1502, 1367, 1312, 1256, 1140, 857, 767, 678. **MP**.: 128 °C.

4-(4-methylbenzoyl)benzonitrile (5g)

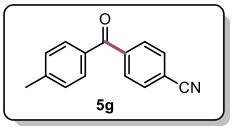

^{1}H NMR (300 MHz, $CDCl_3$) δ (ppm) 7.88 – 7.82 (m, 2H), 7.80 – 7.76 (m, 2H), 7.72 – 7.67 (m, 2H), 7.33 – 7.28 (m, 2H), 2.45 (s, 3H). **^{13}C NMR** (75 MHz, $CDCl_3$) δ (ppm) 194.9, 144.5, 141.8, 133.8, 132.3, 130.4, 130.3, 129.5, 118.2, 115.5, 21.9. **HRMS** (EI+) Calc. for $C_{15}H_{11}NO$ [$M^{\bullet+}$]: 221.0835. Found: 221.0831. The spectroscopic data matches reported values.[13]

4-(4-(*tert*-butyl)benzoyl)benzonitrile (5h)

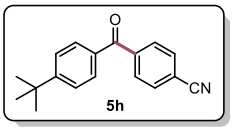

^{1}H NMR (400 MHz, $CDCl_3$) δ (ppm) 7.89 – 7.85 (m, 2H), 7.80 – 7.77 (m, 2H), 7.75 –7.72 (m, 2H), 7.54 – 7.50 (m, 2H), 1.37 (s, 9H). **^{13}C NMR** (101 MHz, $CDCl_3$) δ (ppm) 194.8, 157.4, 141.8, 133.7, 132.2, 130.3, 125., 118.2, 115.6, 35.4, 31.2. **HRMS** (EI+) Calc. for $C_{18}H_{17}NO^{\bullet+}$ [$M^{\bullet+}$]: 263.1305. Found: 263.1305. The spectroscopic data matches reported values.[10e] **HRMS** (EI+) Calc. for $C_{15}H_8F_3NO^{\bullet+}$ [$M^{\bullet+}$]: 275.0553. Found: 275.0554. The spectroscopic data matches reported values.[31]

4-(4-(trifluoromethoxy)benzoyl)benzonitrile (5i)

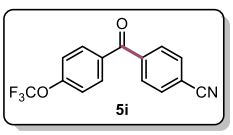

^{1}H NMR (300 MHz, $CDCl_3$) δ (ppm) 7.89 – 7.78 (m, 6H), 7.40 – 7.29 (m, 2H). **^{13}C NMR** (75 MHz, $CDCl_3$) δ (ppm) 193.6, 152.9 (q, *J* = 1.9 Hz), 140.8, 134.6, 132.4, 132.2, 130.3, 120.6, 118.7 (q, *J* = 259 Hz), 118.0, 116.1. **^{19}F NMR** (282 MHz, $CDCl_3$) δ (ppm) -58.1. **HRMS** (EI+) Calc. for $C_{15}H_8F_3NO_2$ [$M^{\bullet+}$]: 291.0502. Found: 291.0499.

4-(3-(fluorobenzoyl)benzonitrile (5j)

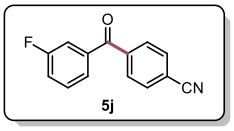

^{1}H NMR (400 MHz, CDCl3) δ (ppm) 7.90 – 7.85 (m, 2H), 7.83 – 7.79 (m, 2H), 7.54 (dt, J = 7.7, 1.4 Hz, 1H), 7.53 – 7.46 (m, 2H), 7.34 (tdd, J = 8.2, 2.6, 1.3 Hz, 1H). **^{13}C NMR** (101 MHz, CDCl3) δ (ppm) 193.8, 162.6 (d, J = 249.2 Hz), 140.7, 138.5 (d, J = 6.4 Hz), 132.4, 130.5 (d, J = 7.8 Hz), 130.3, 126.0 (d, J = 3.1 Hz), 120.5 (d, J = 21.5 Hz), 118.0, 116.9 (d, J = 22.6 Hz), 116.2. **^{19}F NMR** (377 MHz, CDCl3) δ (ppm) -111.6. **HRMS** (EI+) Calc. for Cl_4H_8FNO [M•+]: 225.0584. Found: 225.0583. The spectroscopic data matches reported values.[36]

4-(3-(trifluoromethyl)benzoyl)benzonitrile (5k)

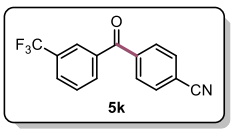

^{1}H NMR (400 MHz, $CDCl_3$) δ (ppm) 8.05 (s, 1H), 7.96 (d, *J* = 7.6 Hz, 1H), 7.92 – 7.86 (m, 3H), 7.83 (d, *J* = 8.3 Hz, 2H), 7.67 (t, *J* = 7.8 Hz, 1H). **^{13}C NMR** (101 MHz, $CDCl_3$) δ (ppm) 193.7, 140.4, 137.1, 133.2, 132.6, 131.6 (q, *J* = 33.1 Hz), 130.3, 129.8 (q, *J* = 3.6 Hz), 129.5, 126.8 (q, *J* = 3.8 Hz), 123.6 (q, *J* = 272.6 Hz), 117.9, 116.5. **^{19}F NMR** (377 MHz, $CDCl_3$) δ (ppm) -63.4. **HRMS** (EI+) Calc. for $C_{15}H_8F_3NO^{\bullet+}$ [$M^{\bullet+}$]: 275.0553. Found: 275.0548. **FTIR** (ν / cm^{-1}): 2236, 1662, 1605, 1330, 1259, 1121, 1069, 916, 857, 760, 693. **MP**.: 82 °C.

4-(4-cyanobenzoyl)phenyl benzoate (5l)

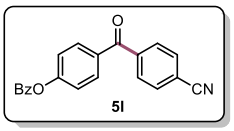

^{1}H NMR (400 MHz, $CDCl_3$) δ (ppm) 8.25 – 8.20 (m, 2H), 7.92 – 7.87 (m, 4H), 7.84 – 7.79 (m, 2H), 7.72 – 7.64 (m, 1H), 7.55 (dd, *J* = 8.4, 7.2 Hz, 2H), 7.43 – 7.37 (m, 2H). **^{13}C NMR** (101 MHz, $CDCl_3$) δ (ppm) 194.0, 164.7, 155.1, 141.3, 134.2, 134.0, 132.4, 131.9, 130.4, 130.3, 129.0, 128.9, 122.3, 118.1, 115.9. **FTIR** (ν / cm^{-1}): 2232, 1736, 1662, 1599, 1259, 1204, 1162, 1058, 931, 764, 708. **HRMS** (EI+) Calc. for $C_{21}H_{13}NO_3^{\bullet+}$ [$M^{\bullet+}$]: 327.0890. Found: 327.0887.

2.5 References

[1] (a) Twilton, J.; Le, C.; Zhang, P.; Shaw, M. H.; Evans, R. W.; MacMillan, D. W. C., *Nat. Rev. Chem.* **2017**, *1*, 0052; (b) Levin, M. D.; Kim, S.; Toste, F. D., *ACS Cent. Sci.* **2016**, *2*, 293-301; (c) Hopkinson, M. N.; Sahoo, B.; Li, J. L.; Glorius, F., *Chem. Eur. J.* **2014**, *20*, 3874-3886; (d) Skubi, K. L.; Blum, T. R.; Yoon, T. P., *Chem. Rev.* **2016**, *116*, 10035-10074.

[2] (a) Heitz, D. R.; Tellis, J. C.; Molander, G. A., *J. Am. Chem. Soc.* **2016**, *138*, 12715-12718; (b) Shields, B. J.; Doyle, A. G., *J. Am. Chem. Soc.* **2016**, *138*, 12719-12722; (c) Nielsen, M. K.; Shields, B. J.; Liu, J.; Williams, M. J.; Zacuto, M. J.; Doyle, A. G., *Angew. Chem. Int. Ed.* **2017**, *56*, 7191-7194; (d) Ackerman, L. K. G.; Martinez Alvarado, J. I.; Doyle, A. G., *J. Am. Chem. Soc.* **2018**, *140*, 14059-14063; (e) Zhang, X.; MacMillan, D. W. C., *J. Am. Chem. Soc.* **2017**, *139*, 11353-11356.

[3] (a) Romero, N. A.; Nicewicz, D. A., *Chem. Rev.* **2016**, *116*, 10075-10166; (b) Marzo, L.; Pagire, S. K.; Reiser, O.; König, B., *Angew. Chem. Int. Ed.* **2018**, *57*, 10034-10072.

[4] (a) Ravelli, D.; Fagnoni, M.; Albini, A., What For? *Chem. Soc. Rev.* **2013**, *42*, 97-113; (b) Fagnoni, M.; Dondi, D.; Ravelli, D.; Albini, A., *Chem. Rev.* **2007**, *107*, 2725-2756.

[5] Shen, Y.; Gu, Y.; Martin, R., *J. Am. Chem. Soc.* **2018**, *140*, 12200-12209.

[6] Zhang, L.; Si, X.; Yang, Y.; Zimmer, M.; Witzel, S.; Sekine, K.; Rudolph, M.; Hashmi, A. S. K., *Angew. Chem. Int. Ed.* **2019**, *58*, 1823-1827.

[7] Dewanji, A.; Krach, P. E.; Rueping, M., *Angew. Chem. Int. Ed.* **2019**, *58*, 3566-3570.

[8] Surana, K.; Chaudhary, B.; Diwaker, M.; Sharma, S., *MedChemComm* **2018**, *9*, 1803-1817.

[9] (a) Dieter, R. K., *Tetrahedron* **1999**, *55*, 4177-4236; (b) Demkiw, K.; Araki, H.; Elliott, E. L.; Franklin, C. L.; Fukuzumi, Y.; Hicks, F.; Hosoi, K.; Hukui, T.; Ishimaru, Y.; O'Brien, E.; Omori, Y.; Mineno, M.; Mizufune, H.; Sawada, N.; Sawai, Y.; Zhu, L., *J. Org. Chem.* **2016**, *81*, 3447-3456.

[10] (a) Wang, X.; Liu, F. D.; Tu, H. Y.; Zhang, A. D., *J. Org. Chem.* **2014**, *79*, 6554-6562; (b) Liu, K.; Tao, S.-W.; Qian, C.; Zhu, Y.-M., *Eur. J. Org. Chem.* **2018**, *2018*, 4769-4775; (c) Tatamidani, H.; Kakiuchi, F.; Chatani, N., *Org. Lett.* **2004**, *6*, 3597-3599; (d) Panja, S.; Maity, P.; Ranu, B. C., *J. Org. Chem.* **2018**, *83*, 12609-12618; (e) Lee, D.; Ryu, T.; Park, Y.; Lee, P. H., *Org. Lett.* **2014**, *16*, 1144-1147; (f) Ruan, J.; Saidi, O.; Iggo, J. A.; Xiao, J., *J. Am. Chem. Soc.* **2008**, *130*, 10510-10511; (g) Alvarez-Bercedo, P.; Flores-Gaspar, A.; Correa, A.; Martin, R., *J. Am. Chem. Soc.* **2010**, *132*, 466-467; (h) Flores-Gaspar, A.; Gutierrez-Bonet, A.; Martin, R., *Org. Lett.* **2012**, *14*, 5234-5237; (i) Wakaki, T.;

Togo, T.; Yoshidome, D.; Kuninobu, Y.; Kanai, M., *ACS Catal.* **2018**, 3123-3128; (j) Suchand, B.; Satyanarayana, G., *J. Org. Chem.* **2016**, *81*, 6409-6423.

[11] (a) Ishiyama, T.; Hartwig, J., *J. Am. Chem. Soc.* **2000**, *122*, 12043-12044; (b) Pucheault, M.; Darses, S.; Genet, J. P., *J. Am. Chem. Soc.* **2004**, *126*, 15356-15357.

[12] (a) Chu, L.; Lipshultz, J. M.; MacMillan, D. W., *Angew. Chem. Int. Ed.* **2015**, *54*, 7929-7933; (b) Huang, Y.-C.; Majumdar, K. K.; Cheng, C.-H., *J. Org. Chem.* **2002**, *67*, 1682-1684; (c) Gu, L. J.; Jin, C.; Zhang, H. T., *Chem. Eur. J.* **2015**, *21*, 8741-8744; (d) Vandavasi, J. K.; Hua, X.; Halima, H. B.; Newman, S. G., *Angew. Chem. Int. Ed.* **2017**, *56*, 15441-15445.

[13] Karthikeyan, J.; Parthasarathy, K.; Cheng, C. H., *Chem. Commun.* **2011**, *47*, 10461-10463.

[14] (a) Wu, X. F.; Neumann, H.; Beller, M., *Chem. Soc. Rev.* **2011**, *40*, 4986-5009; (b) He, X.; Cao, Y.; Lang, X. D.; Wang, N.; He, L. N., *ChemSusChem* **2018**, *11*, 3382-3387.

[15] Please refer to the experimental section for more information.

[16] (a) Sun, R.; Qin, Y.; Ruccolo, S.; Schnedermann, C.; Costentin, C.; Nocera, D. G., *J. Am. Chem. Soc.* **2019**, *141*, 89-93; (b) Gutierrez, O.; Tellis, J. C.; Primer, D. N.; Molander, G. A.; Kozlowski, M. C., *J. Am. Chem. Soc.* **2015**, *137*, 4896-4899.

[17] (a) Chow, Y. L.; Buono-Core, G. E.; Lee, C. W.; Scaiano, J. C., *J. Am. Chem. Soc.* **1986**, *108*, 7620-7627; (b) Wagner, P. J.; Truman, R. J.; Scaiano, J. C., *J. Am. Chem. Soc.* **1985**, *107*, 7093-7097.

[18] Berger, M.; Goldblatt, I. L.; Steel, C., *J. Am. Chem. Soc.* **1973**, *95*, 1717-1725.

[19] (a) Fulmer, G. R.; Miller, A. J. M.; Sherden, N. H.; Gottlieb, H. E.; Nudelman, A.; Stoltz, B. M.; Bercaw, J. E.; Goldberg, K. I., *Organometallics* **2010**, *29*, 2176-2179; (b) Gottlieb, H. E.; Kotlyar, V.; Nudelman, A., *J. Org. Chem.* **1997**, *62*, 7512-7515.

[20] Nasri, S.; Zahou, I.; Turowska-Tyrk, I.; Roisnel, T.; Loiseau, F.; Saint-Amant, E.; Nasri, H., *Eur. J. Inorg. Chem.* **2016**, *2016*, 5004-5019.

[21] Yahata, K.; Ye, N.; Ai, Y.; Iso, K.; Kishi, Y., *Angew. Chem. Int. Ed.* **2017**, *56*, 10796-10800.

[22] Goerner, H., *J. Phys. Chem.* **1982**, *86*, 2028-2035.

[23] Heinz, C.; Lutz, J. P.; Simmons, E. M.; Miller, M. M.; Ewing, W. R.; Doyle, A. G., *J. Am. Chem. Soc.* **2018**, *140*, 2292-2300.

[24] Scaiano, J. C.; Arnold, B. R.; McGimpsey, W. G., *J. Phys. Chem.* **1994**, *98*, 5431-5434.

[25] Wilkinson, F.; Abdel-Shafi, A. A., *J. Phys. Chem. A* **1997**, *101*, 5509-5516.

[26] Lin, Z.-P.; Aue, W. A., *Spectrochim. Acta A* **2000**, *56*, 111-117.

[27] Leigh, W. J.; Arnold, D. R., *J. Chem. Soc., Chem. Commun.* **1980**, *0*, 406-408.

[28] Arai, T.; Oguchi, T.; Wakabayashi, T.; Tsuchiya, M.; Nishimura, Y.; Oishi, S.; Sakuragi, H.; Tokumaru, K., *Bull. Chem. Soc. Jpn.* **1987**, *60*, 2937-2943.

[29] Marchetti, A. P.; Kearns, D. R., *J. Am. Chem. Soc.* **1967**, *89*, 768-777.

[30] Lewis, G. N.; Kasha, M., *J. Am. Chem. Soc.* **1944**, *66*, 2100-2116.

[31] Dohi, S.; Moriyama, K.; Togo, H., *Tetrahedron* **2012**, *68*, 6557-6564.

[32] Peng, Z.; Li, N.; Sun, X.; Wang, F.; Xu, L.; Jiang, C.; Song, L.; Yan, Z. F., *Org. Biomol. Chem.* **2014**, *12*, 7800-7809.

[33] Castello-Mico, A.; Herbert, S. A.; Leon, T.; Bein, T.; Knochel, P., *Angew. Chem. Int. Ed.* **2016**, *55*, 401-404.

[34] In, I.; Kim, S. Y., *Polym. Bull.* **2005**, *56*, 129-135.

[35] Ogawa, Y.; Saiga, A.; Mori, M.; Shibata, T.; Takagi, K., *J. Org. Chem.* **2000**, *65*, 1031-1036.

[36] Gautam, P.; Tiwari, N. J.; Bhanage, B. M., *ACS Omega* **2019**, *4*, 1560-1574.

CHAPTER III

Photocatalytic C–H Trifluoromethylthiolation by the Decatungstate Anion

Reprinted (adapted) with permission from:

T. E. Schirmer, A. B. Rolka, T. A. Karl, F. Holzhausen, B. König, *Org. Lett.* **2021**, 23, 15, 5729–5733.

Author Contributions:

T.E.S. optimized the reaction conditions for alkanes and aldehydes, contributed the compounds **2a-d**, **2g-2l**, **2r-2ak**, **2an**, **3l,** and synthesized respective starting materials. A.B.R. optimized the reaction conditions for alkoxy substrates, isolated compounds **2e-f**, **2m-q**, **2al**, **2am**, **3f**, **4f**, conducted the large-scale experiment, and synthesized respective starting materials. T.E.S. and A.B.R. wrote the first draft, which was improved through suggestions from all authors. T.A.K. synthesized the catalyst and helped to revise the manuscript. F.H. supported the isolation of thioesters during his internship under the supervision of T.E.S.. B.K. guided the project.

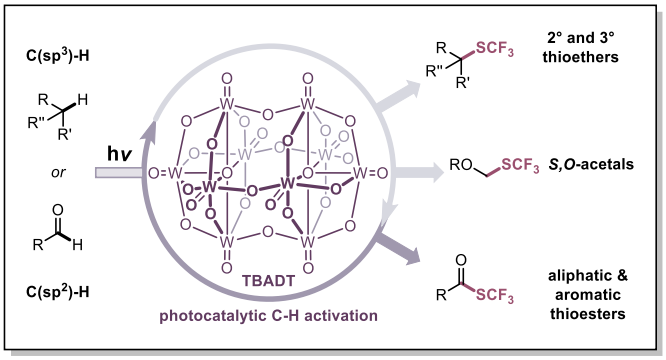

ABSTRACT

A broadly applicable method for the trifluoromethylthiolation of methylene C(sp^3)–H, methine C(sp^3)–H, α-oxygen C(sp^3)–H, and formyl C(sp^2)–H bonds is presented using the decatungstate anion as the sole catalyst. By adjusting the substrate ratio and reaction concentration, this method was applied to 40 examples in good regioselectivities, including the derivatization of natural products. Furthermore, SCF_3–drug analogs were synthesized by subsequent functionalization of the SCF_3 products, highlighting the importance of this photocatalyzed C–H functionalization.

3.1 Introduction

Straightforward access to highly valuable products from abundant starting materials is a highly desirable and mutual goal for synthetic chemists across a multitude of disciplines. To this end, the activation of inert C–H bonds has gained significant attention in chemistry over the past decades, as it represents a valuable tool for the functionalization of organic molecules with the potential for a high atom and even higher step economy.[1]

In recent years, the field of photoredox chemistry has spurred a multitude of novel hydrogen atom transfer (HAT) processes designed to facilitate such transformations. While significant success has been achieved, the vast majority of examples rely upon the functionalization of activated C–H bonds adjacent to heteroatoms or arenes.[2] The selective transformation of nonactivated bonds, on the other hand, is considerably more challenging due to the high bond dissociation energy of aliphatic C–H bonds coupled with the presence of only minor energetic differences between the multitude of similar C–H bonds typically present in a substrate of interest. [3]

Of particular focus in this field are catalysts that can serve a dual function and combine the roles of photocatalyst and HAT activation. In this context, the decatungstate anion (DT, $[W_{10}O_{32}]^{4-}$) has emerged as one of the most prominent examples of combined photo-HAT catalysts.[4] This success has been heavily influenced by a remarkably fast HAT from C(sp^3)–H centers.[5] While advances have been made in the use of DT photo-HAT catalysis in the context of C–C,[6] C–D,[7] and C–F[8] bond formation, the incorporation of the trifluoromethylthiol (–SCF_3) group by DT catalysis has thus far remained elusive.[9]

Such a development is highly desirable due to the increased application of the trifluoromethylthiol group in medicinal chemistry.[10] This surge in interest results from the motif's significant electronegativity and particularly high lipophilicity (Hansch parameter of $\pi = 1.44$), which makes the SCF_3 group a powerful handle to both adjust pharmacokinetic properties and optimize interactions of an active compound with its target.[11] While the recent development of tailored reagents[12] has allowed for both polar[13] and radical[14] transformations for the incorporation of the SCF_3 group, the use of HAT in this context is of particular interest due to its ability to selectively promote late-stage incorporation of the functionality with relatively high levels of chemoselectivity. The power of such a strategy has been demonstrated by the Glorius group using a dual catalytic system, consisting of an iridium photo- and benzoate HAT-catalyst for the selective trifluoromethylthiolation of methine and formyl C–H bonds (Scheme 1a).[15] Xie and Zhu reported a creative iteration of that approach to initiate the fragmentation of methoxymethyl ethers and thereby achieve

deoxytrifluoromethylthiolation of tertiary alcohols.[16] The same group then developed a protocol based on arene oxidation to achieve benzylic C–H trifluoromethylthiolation, which is, interestingly enough, not accessible via HAT catalysis.[15b, 17]

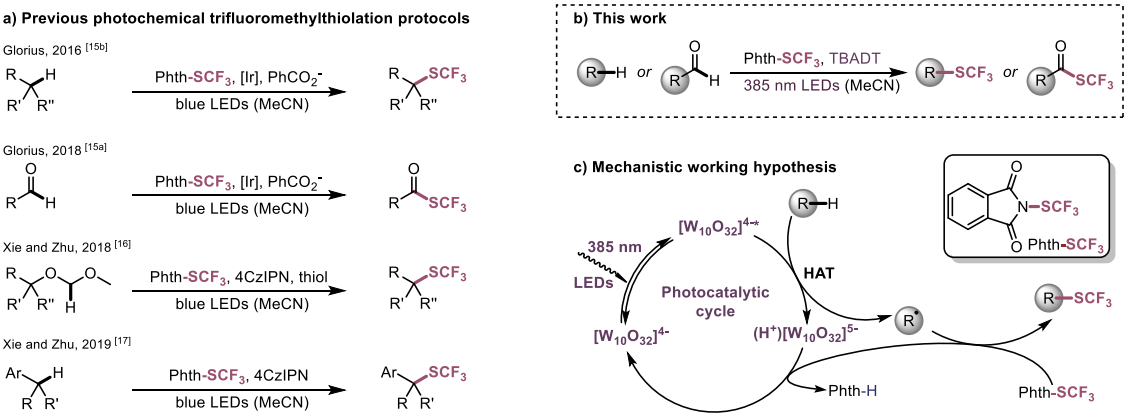

Scheme 1: Photochemical trifluoromethylthiolation reactions. (a) Photochemical trifluoromethylthiolation procedures reported in the literature. (b) Novel DT-based trifluoromethylthiolation. (c) The mechanistic rationale behind the presented work.

Given the ongoing quest for novel trifluoromethylthiolation reactions,[18] we envisioned being able to leverage the reactivity of the decatungstate anion to functionalize strong methylene C(sp^3)–H, methine-C(sp^3)–H, and C(sp^2)–H bonds with high selectivity (Scheme 1b). The development of operationally simple conditions coupled with the well-studied reactivity of the decatungstate anion and the use of a commercially available reagent would allow for widespread implementation of the procedure with a high level of predictability. Such a process would begin with the photoexcitation of DT, subsequent HAT from the substrate to the excited catalyst, and finally trapping of the radical by Munavalli's reagent (Phth-SCF_3)[19] to yield the desired trifluoromethylthiolated product while regenerating the catalyst and forming phthalimide as the side product through a formal electron and proton transfer from the reduced catalyst (Scheme 1c).

3.2 Results and Discussion

We first focused our investigations of tetra-*n*-butylammonium decatungstate (TBADT)-catalyzed trifluoromethylthiolations on the optimization of nonactivated C(sp^3)–H bonds, whose high bond dissociation energies create additional challenges in their functionalization. Using 2.0 equiv of cyclohexane (**1a**) as a model substrate (Table 1), 0.5 mol % TBADT, and Phth-SCF_3 as limiting reagent at a 0.1 mmol scale under irradiation with 385 nm LED light in dry MeCN resulted in a promising 61% crude NMR yield of the desired product **2a** (entry 1). Increasing the catalyst loading resulted in

slightly higher yields (entries 1–4) while raising the equivalents of cyclohexane from 2 to 5 produced a significant boost in yield to 82% (entry 5). Halving both the catalyst loading and amount of solvent to hold catalyst concentration constant did not reduce the yield (entries 6–8). For practical considerations, the reaction scale was increased to 0.4 mmol for these reactions and all further experiments. With optimized reaction conditions (entry 8), control experiments were run, which confirmed that the reaction requires both irradiation with light and the presence of TBADT. Based on these results, we ruled out thermal and noncatalyzed reaction pathways (entries 9–11).

Table 1: Optimization and control reactions. Reactions were run at the respective scales in anhydrous MeCN under irradiation with UV-LEDs (385 nm) and under an N_2-atmosphere for 16 h at 25 °C. [a]Yield was determined by ^{19}F-crude NMR analysis with α,α,α-trifluorotoluene as internal standard. [b]No light. [c]Run at 80 °C. [d]nd = not detected.

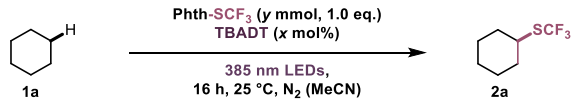

entry	TBADT (mol%)	1a (mmol)	Phth-SCF_3 (mmol)	c (M)	yield (%)
1	0.5	0.2	0.1	0.1	61
2	1.0	0.2	0.1	0.1	66
3	2.5	0.2	0.1	0.1	67
4	5	0.2	0.1	0.1	69
5	5	0.5	0.1	0.1	82
6	5	0.5	0.1	0.2	88
7	5	2.0	0.4	0.2	85
8	**2.5**	**2.0**	**0.4**	**0.2**	**83**
9[a]	2.5	2.0	0.4	0.2	nd[c]
10[a,b]	2.5	2.0	0.4	0.2	nd[c]
11	-	2.0	0.4	0.2	nd[c]

For each class of substrate used in this report, a similar optimization could be carried out by adjusting only the reaction concentration and substrate-reagent ratio, allowing all other reaction conditions to remain constant (see the experimental section). Not surprisingly, C(sp^3)–H bonds activated by an adjacent oxygen atom required a smaller excess of the substrate (2.5 equiv). In the case of aldehydes, the equivalents of the substrate could be lowered even further to 1.5 equiv. While an additional solvent screen for these activated substrates confirmed acetonitrile to be ideal, acetone was also a viable alternative (see the experimental section).

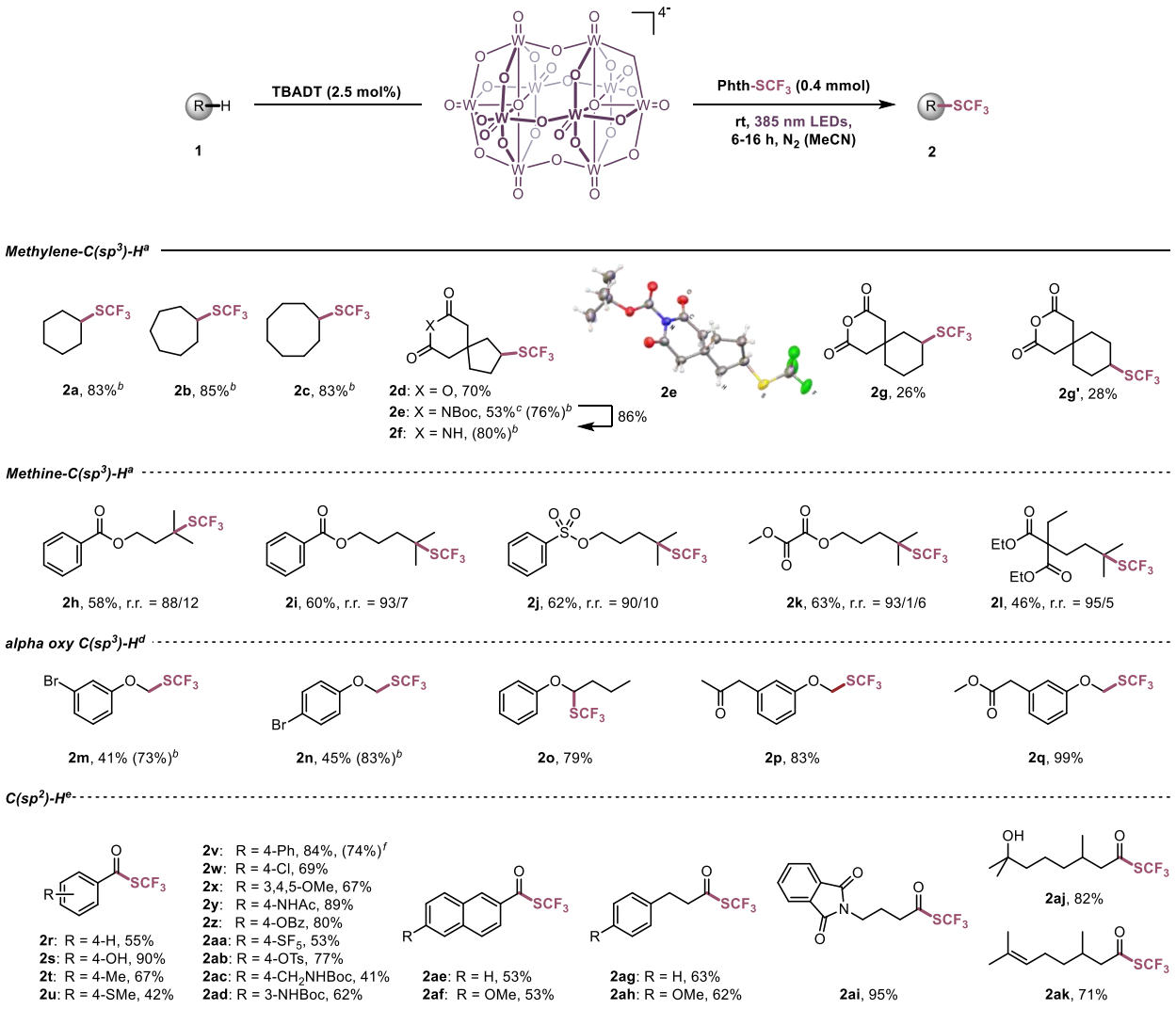

Scheme 2: Substrate scope of the decatungstate catalyzed trifluoromethylthiolation. Reactions were run at a 0.4 mmol scale in anhydrous MeCN under irradiation with UV-LEDs (385 nm) and under an N_2 atmosphere for 16 h at 25 °C. Isolated yields are given, if not stated otherwise. r.r. = regioselective ratio of isolated product. [a]5.0 equiv of the substrate was used. [b]Determined by crude 19F-NMR with α,α,α-trifluorotoluene as internal standard. [c]2.0 equiv of the substrate was used. [d]2.5 equiv of ether substrate was used at 0.4 M. [e]1.5 equiv of aldehyde was used. [f]Performed at 1.2 mmol scale (see experimental section).

With the ideal reaction conditions in hand for each class of C– H bond, the substrate scope was investigated (Scheme 2). Strong C–H bonds in the form of both methylene and methine C(sp^3)–H bonds were trifluoromethylthiolated in overall good to high yields. Selectivity in the reaction is driven both by steric accessibility and polarity matching that favors activation of the most hydridic bond present in the molecule.[5] Compound **1g** represents an exception to this high selectivity, where two methylene positions possess similar steric and electronic environments. However, these two regioisomers, **2g** and **2g'**, could be separated through column chromatography, allowing access

to two different trifluoromethylthiolated products. Additionally, the higher reactivity of spiro compound **2e** required only 2.0 equiv of the substrate to obtain a high yield, and a single-crystal X-ray structure confirmed the molecular structure. Although spiro imide **2f** can be directly trifluoromethylthiolated in 80% ^{19}F NMR yield, purification presented a challenge due to the co-elution of phthalimide. The isolation problem could be overcome by subjecting Boc-protected imide **2e** to the reaction conditions followed by a subsequent deprotection to obtain the free imide **2f**.

Next, we investigated activated α-oxy C(sp^3)–H bonds and were delighted to achieve excellent yields of up to 99%. In several examples (**2m** and **2n**), separation of the product from the starting material via silica flash chromatography was not satisfactory, but pure material could be readily achieved via Kugelrohr distillation with slightly diminished yields. In these cases, we provide the product yields determined by ^{19}F-NMR before isolation and the isolated yields following distillation.

Last, the scope of formyl C–H activation for trifluoromethylthiolation was explored. [15a, 20] We were pleased to find that aliphatic and aromatic aldehydes were functionalized in moderate to high yields. For aromatic aldehydes, electron-donating substituents on the aromatic ring increased the yield up to 90%, while electron-withdrawing groups were tolerated giving moderate to good yields (**2r–2ad**). The methodology can be upscaled to 1.2 mmol with only a minor decrease in the yield of **2v**. Expanding the aromatic system to naphthaldehydes yielded the trifluoromethylthioester in slightly decreased yields (**2ae**, **2af**). Aliphatic aldehydes worked equally well under the given reaction conditions (**2ag–2ai**).

To demonstrate the applicability of the method to the derivatization of natural products, several SCF_3-analogs were synthesized (Scheme 3a). The plant sesquiterpene lactone sclareolide (**1al**),[21] representing the class of nonactivated C(sp^3)–H bonds, was functionalized in 55% isolated yield (**2al**). The naturally occurring terpenoid ambroxide (**1am**), commonly used as a perfume ingredient,[22] contains an activated α-oxy C(sp^3)–H bond, and its SCF_3 derivative (**2am**) was obtained in good yield with a d.r. of 1:1.5. Finally, the aldehyde moiety in the 4-hydroxybenzaldehyde ester of dehydrocholic acid (**1an**) could be trifluoromethylthiolated in 45% isolated yield (**2an**), presenting an application for the activation of C(sp^2)–H bonds. Furthermore, subsequent functionalization of the SCF_3 products **2l** and **2f** gave access to trifluoromethylthiol analogs of drug molecules (Scheme 3b). SCF_3-amobarbital (**3l**), the SCF_3 derivative of the GABA receptor agonist,[23] is accessible in one step from malonate **2l** in 42% yield. We further showed that the SCF_3 analog of buspirone, which is currently used to treat anxiety disorders, can be synthesized in two high-yielding steps (overall yield of 82%) from **2f**. The synthesis of SCF_3-drug derivatives may be of interest in the context of recent investigations on the effect of SCF_3 groups in medicinal chemistry.[11b]

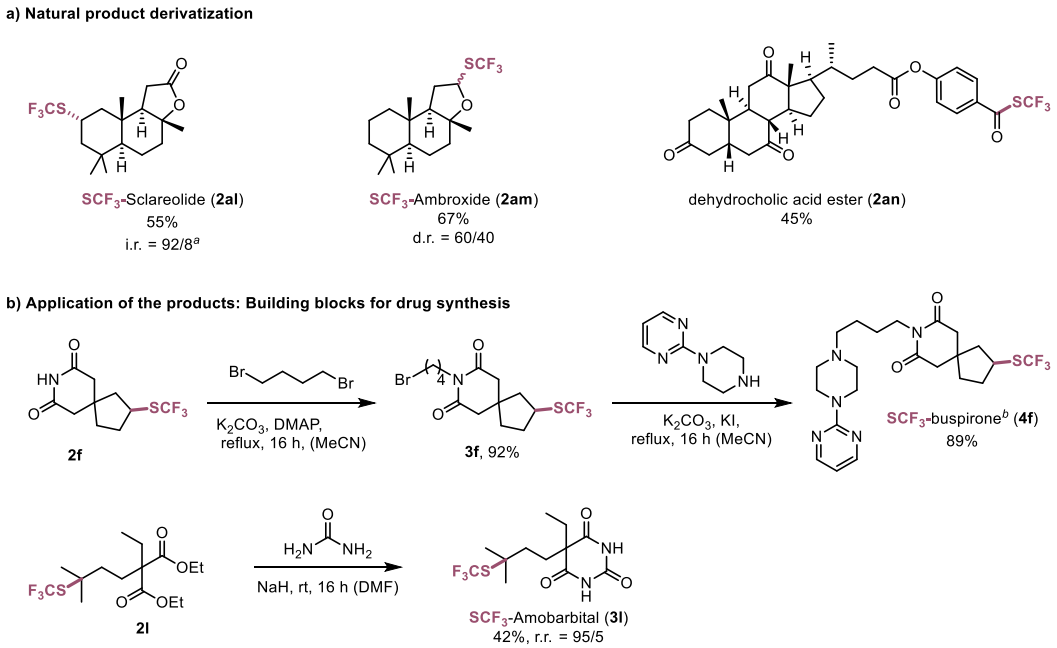

Scheme 3: Natural product derivatization and applications of the products as building blocks in the synthesis of drugs derivatives. [a]i.r. = isomeric ratio of isolated product. [b]6% of *para*-chlorinated SCF_3-buspirone was observed in the NMR-spectrum of the final isolated product, presumably introduced by using deuterated chloroform during the measurement.

3.3 Conclusion

In conclusion, we have shown that TBADT can be used as a catalyst in the photocatalyzed trifluoromethylthiolation of C–H bonds, eliminating the need for a dual catalytic system. Furthermore, we demonstrated the broad applicability of the method by functionalizing methine C(sp^3)–H, methylene C(sp^3)–H, α-oxy-C(sp^3)–H, and formyl C(sp^2)–H groups by only adjusting the ratio of substrate to reagent and concentration, while all other reaction conditions remain unchanged. The method was applied to 40 examples and gave the products in good to excellent yields. We believe that the method will prove valuable in C–H functionalization and find applications in drug discovery by improving pharmacokinetics and target binding properties of SCF_3 drugs by providing an accessible and generally applicable method for their synthesis.

3.4 Experimental Section

3.4.1 General Information

All NMR spectra were recorded at room temperature using one of the following devices: Bruker Avance 300 (300 MHz for ^{1}H, 75 MHz for ^{13}C, 282 MHz for ^{19}F), Bruker Avance 400 (400 MHz for ^{1}H, 100 MHz for ^{13}C, 376 MHz for ^{19}F). All chemical shifts are reported on the δ-scale in parts per million (ppm) (multiplicity, coupling constant *J* in Hertz (Hz), number of protons) relative to the solvent residual peaks as the internal standard.[24] Abbreviations used for signal multiplicity are br = broad, s = singlet, d = doublet, t = triplet, q = quartet, m = multiplet and combinations thereof. High-resolution mass spectra (HRMS) were obtained from the institute's central analytic mass spectrometry department. The spectra were recorded on one of the following devices: Finnigan MAT 95, Thermo Quest Finnigan TSQ 7000, Finnigan MATSSQ 710 A, or Agilent Q-TOF 6540 UHD. For GC-FID measurements, a GC 7890 from Agilent Technologies was used, the analysis of the data was performed with Agilent ChemStation Rev.C.01.04. [35]. Analytical TLC was performed on silica gel-coated alumina plates (MN TLC plates ALUGRAM® Xtra SIL G/UV254). Detection was done by UV light (254 or 366 nm). Infrared spectra were recorded neatly on an Agilent Cary 630 FT-IR Spectrometer; melting points were measured in open capillary tubes by a Stanford Research System OptiMelt MPA 100 and are uncorrected. Compounds were purified by automated column chromatography with silica gel 60 M (40-63 μm, 230-440 mesh, Merck) on a Biotage® Isolera TM Spektra One device. Trifluoromethylthiolation reactions were irradiated from the bottom (distance ca. 1 cm) with 385 nm LEDs (*Opulent Americas*, LST1-01G01-UV02-00, λ = 385 nm, 3.4 V, 350 mA, 1.015 W light flux). All chemicals and solvents were obtained from commercial sources if not otherwise stated below. Specifically, Phth-SCF_3 was purchased from TCI Europe; dry acetonitrile was purchased from *Acros Organics* (Acetonitrile, 99.9%, Extra Dry, over Molecular Sieve, AcroSeal®). Solid aldehydes were used as received; liquid ones were purified by distillation under reduced pressure prior to use. Starting materials **1h**[15b], **1i**[15b], **1z**[25] **1ab**[26], **1ai**[27], **1an**[28] were synthesized according to literature procedures. The synthesis of relevant known (**1e**, **1l**) and unknown substrates (**1j**, **1k**) are outlined below.

3.4.2 Optimization of the Reaction Conditions

Table 2: Optimization for cyclohexane (1a). Reactions were run at the respective scales in anhydrous MeCN under irradiation with UV-LEDs (385 nm) and under an N_2-atmosphere for 16 h at 25 °C. The yield was determined by ^{19}F-crude NMR analysis with α,α,α-trifluorotoluene as internal standard. [a]No light. [b]Run at 80 °C. [c]nd = not detected.

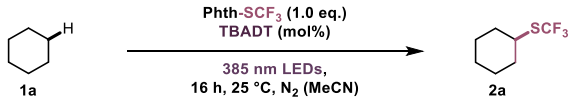

entry	TBADT (mol%)	1a (mmol)	Phth-SCF_3 (mmol)	c (M)	yield (%)
1	0.5	0.2	0.1	0.1	61
2	1.0	0.2	0.1	0.1	66
3	2.5	0.2	0.1	0.1	67
4	5	0.2	0.1	0.1	69
5	5	0.5	0.1	0.1	82
6	5	0.5	0.1	0.2	88
7	5	2.0	0.4	0.2	85
8	**2.5**	**2.0**	**0.4**	**0.2**	**83**
9[a]	2.5	2.0	0.4	0.2	nd[c]
10[a,b]	2.5	2.0	0.4	0.2	nd[c]
11	-	2.0	0.4	0.2	nd[c]

General Procedure A: A crimp cap vial was charged with tetra-*n*-butylammonium decatungstate (TBADT, 33.2 mg. 0.01 mmol, 2.5 mol%), *N*-(trifluoromethylthio)phthalimide (Phth-SCF_3, 98.9 mg, 0.40 mmol, 1.0 equiv), solid substrate (2.00 mmol, 5.0 equiv) and a stirring bar. The vial was sealed, flushed with dry nitrogen (3×), and charged with dry acetonitrile (2 mL, 0.2 M) and liquid substrates (2.00 mmol, 5.0 equiv). The mixture was degassed by three *freeze-pump-backfill-thaw* cycles and subsequently irradiated with LEDs (385 nm) for 16 h at 25 °C. The mixture was transferred into a round bottom flask and concentrated under reduced pressure. The residue was purified by automated column chromatography with indicated solvent mixtures. Products, which are more polar than the phthalimide by-product might require a second chromatographic purification. If the product was suspected to be volatile, the reaction was concentrated by passing a gentle stream of nitrogen through the vial. The residue was absorbed on silica and purified with pentane, diethyl ether, or dichloromethane.

Table 3: Optimization for 4-bromoanisole (1m). Reactions were run at the respective scales in an anhydrous solvent under irradiation with UV-LEDs (385 nm) and under an N_2-atmosphere for 16 h at 25 °C. The yield was determined by ^{19}F-crude NMR analysis with α,α,α-trifluorotoluene as internal standard. [a]No light. [b]Run at 70 °C. [c]nd = not detected.

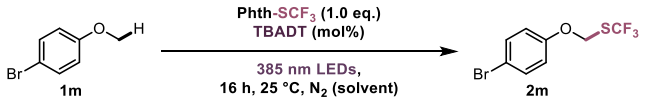

entry	TBADT (mol%)	1m (mmol)	Phth-SCF_3 (mmol)	c (M)	solvent	yield (%)
1	2.5	0.2	0.13	0.13	$PhCF_3$	nd[c]
2	2.5	0.2	0.13	0.13	DCE	traces
3	2.5	0.2	0.13	0.13	C_6D_6	nd[c]
4	2.5	0.2	0.13	0.13	acetone	61
5	2.5	0.2	0.13	0.13	MeCN	62
6	2.5	0.2	0.13	0.2	MeCN	66
7	5	0.2	0.13	0.2	MeCN	66
8	2.5	0.6	0.4	0.4	MeCN	71
9	2.5	1.0	0.4	0.4	MeCN	83
10	2.5	2.0	0.4	0.4	MeCN	86
11[a,b]	2.5	0.15	0.1	0.1	MeCN	nd[c]
12	-	0.15	0.1	0.1	MeCN	nd[c]

General Procedure B: A crimp cap vial was charged with tetra-*n*-butylammonium decatungstate (TBADT, 33.2 mg. 0.01 mmol, 2.5 mol%), *N*-(trifluoromethylthio)phthalimide (Phth-SCF_3, 98.9 mg, 0.40 mmol, 1.0 equiv), solid substrate (1.00 mmol, 2.5 equiv) and a stirring bar. The vial was sealed, flushed with dry nitrogen (3×), and charged with dry acetonitrile (1 mL, 0.4 M) and liquid substrates (2.00 mmol, 2.5 equiv). The mixture was degassed by three *freeze-pump-backfill-thaw* cycles and subsequently irradiated with LEDs (385 nm) for 16 h at 25 °C. The mixture was transferred into a round bottom flask and concentrated under reduced pressure. The residue was purified by automated column chromatography with indicated solvent mixtures or distilled.

Table 4: Optimization for 4-hydroxybenzaldehyde (2s). Reactions were run at the respective scales in anhydrous MeCN under irradiation with UV-LEDs (385 nm) and under an N_2-atmosphere for 3-6 h at 25 °C. The yield was determined by ^{19}F-crude NMR analysis with α,α,α-trifluorotoluene as internal standard. [a]No light. [b]nd = not detected.

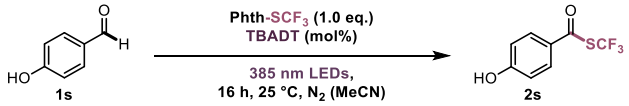

entry	TBADT (mol%)	1s (mmol)	Phth-SCF_3 (mmol)	c (M)	time (h)	yield (%)
1	1	0.15	0.1	0.1	3	83
2	2.5	0.15	0.1	0.1	3	82
3	5	0.15	0.1	0.1	3	83
4	2.5	0.4	0.6	0.1	3	54
5	2.5	0.4	0.6	0.1	6	74
5	2.5	0.4	0.6	0.1	8	77
7	2.5	0.6	0.4	0.1	3	75
8	2.5	0.6	0.4	0.1	6	80
9	2.5	0.6	0.4	0.1	8	80
10	**2.5**	**0.6**	**0.4**	**0.2**	**6**	**92**
11	2.5	0.6	0.4	0.4	6	92
12[a]	2.5	0.6	0.4	0.4	6	nd[b]
13	-	0.6	0.4	0.4	6	30

General Procedure C: A crimp cap vial was charged with tetra-*n*-butylammonium decatungstate (TBADT, 33.2 mg. 0.01 mmol, 2.5 mol%), *N*-(trifluoromethylthio)phthalimide (Phth-SCF_3, 98.9 mg, 0.40 mmol, 1.0 equiv), solid substrate (0.60 mmol, 1.5 equiv) and a stirring bar. The vial was sealed, flushed with dry nitrogen (3×), and charged with dry acetonitrile (2 mL, 0.2 M) and liquid substrates (0.60 mmol, 1.5 equiv). The mixture was degassed by three *freeze-pump-backfill-thaw* cycles and subsequently irradiated with LEDs (385 nm) for 6 h at 25 °C. The mixture was transferred into a round bottom flask and concentrated under reduced pressure. The residue was purified by automated column chromatography with indicated solvent mixtures.

3.4.3 Synthesis of Starting Materials

tert-butyl 7,9-dioxo-8-azaspiro[4.5]decane-8-carboxylate (1e)

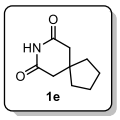

Based on a literature reported procedure,[29] a Schlenk flask equipped with a magnetic stirring bar was charged with di-*tert*-butyl dicarbonate (2.4 g, 0.011 mol, 1.1 equiv) and DMAP (61 mg, 0.50 mmol, 5 mol%) in MeCN (10 mL) and was placed under a nitrogen atmosphere. To this mixture, a solution of tetramethylene glutarimide (1.7 g, 0.01 mol, 1.0 equiv) in MeCN (5 mL) was added at room temperature. The reaction mixture was stirred overnight and was then concentrated in vacuo. Afterward, H_2O (15 mL) was added, and the aqueous layer was extracted with DCM (3 × 20 mL). The combined organics were washed with brine, dried over Na_2SO_4, filtered over Celite, and finally, the solvent was removed in vacuo. Purification by flash column chromatography (10-40% EtOAc in PE) yielded **1e** as a white solid (1.4 g, 5.2 mmol, 52%). **^{1}H NMR** (400 MHz, $CDCl_3$) δ (ppm) 2.55 (s, 4H), 1.73 – 1.66 (m, 4H), 1.54 – 1.51 (m, 13H). **^{13}C NMR** (101 MHz, $CDCl_3$) δ (ppm) 169.9, 149.0, 86.2, 43.9, 40.1, 37.6, 27.5, 24.1. **HRMS (APCI+)** Calc. for $C_{14}H_{25}N_2O_4$ $[M^+NH_4]^+$: 285.1809. Found: 285.1810. **FTIR** (ν / cm^{-1}): 2967, 2870, 1781, 1722, 1684, 1356, 1244, 1140, 1058, 842. **MP.:** 99.7–101.6 °C.

4-methylpentyl benzenesulfonate (1j)

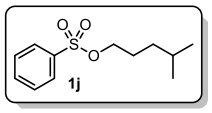

Adapting literature procedure for the benzoylation of 4-methylpentanol,[15b] a mixture of 4-methylpentan-1-ol (1.26 mL, 10.0 mmol, 1.0 equiv), 4-dimethylaminepyridine (244 mg, 2.00 mmol, 0.2 equiv) and Et_3N (2.09 mL, 15.0 mmol, 1.5 equiv) in DCM (50 mL) was cooled down to 0 °C (50 mL) and treated with benzenesulfonyl chloride (1.53 mL, 12.0 mmol, 1.2 equiv). The reaction mixture was stirred at room temperature over night, quenched with water (50 mL), extracted with DCM (2 × 20 mL), dried over Na_2SO_4 and concentrated. The crude product was purified by column chromatography (50 g SiO_2, PE/EA = 80/20 → 40/60) to afford the title compound as a colorless oil (1.84 g, 7.59 mmol, 76%). **^{1}H NMR** (400 MHz, $CDCl_3$) δ (ppm) 7.95 – 7.88 (m, 2H), 7.70 – 7.60 (m, 1H), 7.60 – 7.51 (m, 2H), 4.04 (t, *J* = 6.6 Hz, 2H), 1.70 – 1.58 (m, 2H), 1.53 – 1.42 (m, 1H), 1.22 – 1.12 (m, 2H), 0.83 (d, *J* = 6.6 Hz, 6H). **^{13}C NMR** (101 MHz, $CDCl_3$) δ (ppm) 136.5, 133.8, 129.4, 128.0, 71.4, 34.5, 27.6, 26.9, 22.5. **HRMS** (ESI+) Calc. for $C_{12}H_{19}O_3S^+$ $[M+H^+]$: 243.1049. Found: 243.1051. **FTIR** (ν / cm^{-1}): 2955, 2870, 1468, 1448, 1356, 1185, 1095, 954, 913, 752.

methyl (4-methylpentyl) oxalate (1k)

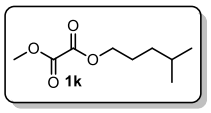

Adapting literature procedure for the benzoylation of 4-methylpentanol,[15b] a mixture of 4-methylpentan-1-ol (1.26 mL, 10.0 mmol, 1.0 equiv), 4-dimethylaminepyridine (244 mg, 2.00 mmol, 0.2 equiv) and Et_3N (2.09 mL, 15.0 mmol, 1.5 equiv) and treated with methyl 2-chloro-2-oxoacetate (1.10 mL, 12.0 mmol, 1.2 equiv). The reaction mixture was stirred at room temperature over night, quenched with water (50 mL), extracted with DCM (2 × 20.0 mL), dried over Na_2SO_4 and concentrated. The crude product was purified by column chromatography (50g SiO_2, PE/EA = 80/20 → 40/60) to afford the title compound as a colorless oil (1.12 g, 5.95 mmol, 60%). **^{1}H NMR** (400 MHz, $CDCl_3$) δ (ppm) 4.27 (t, *J* = 6.9 Hz, 2H), 3.90 (s, 3H), 1.79 – 1.67 (m, 2H), 1.65 – 1.49 (m, 1H), 1.30 – 1.20 (m, 2H), 0.89 (d, *J* = 6.6 Hz, 6H). **^{13}C NMR** (101 MHz, $CDCl_3$) δ (ppm) 158.4, 157.8, 67.7, 53.7, 34.8, 27.8, 26.3, 22.5. **HRMS** (ESI+) Calc. for $C_9H_{20}NO_4^+$ [M+NH_4^+] : 206.1387. Found: 206.1384. **FTIR** (ν / cm^{-1}): 2959, 2873, 1770, 1744, 1468, 1319, 1200, 1155, 957, 775.

diethyl 2-ethyl-2-isopentylmalonate (1l)

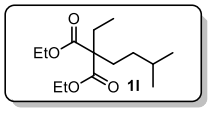

Adapting literature procedure for the alkylation of 2-ethylmalonates[30], diethyl 2-ethylmalonate (10.0 mmol, 1.88 g, 1.87 ml, 1.0 equiv) was dissolved in dry DMF (15 mL), cooled to 0 °C, treated with sodium hydride (60% dispersion in mineral oil, 479 mg, 12.0 mmol, 1.2 equiv) and stirred for 1.5 h. Then 1-bromo-3-methylbutane (12.0 mmol, 1.20 mL, 1.2 equiv) was added and the reaction was stirred overnight. The reaction was quenched by the addition of saturated aqueous NH_4Cl solution (50 mL) and the product was extracted with ether (3 × 25 mL). The combined organic phase was dried over Na_2SO_4 and concentrated. The crude product was purified by column chromatography (50 SiO_2, PE/EA = 80/20 → 50/50) to afford the title compound as a colorless oil (1.91 g, 7.39 mmol, 74%). **^{1}H NMR** (300 MHz, $CDCl_3$) δ (ppm) δ 4.17 (q, *J* = 7.2 Hz, 4H), 1.97 – 1.80 (m, 4H), 1.56 – 1.44 (m, 1H), 1.23 (t, *J* = 7.1 Hz, 6H), 1.06 – 0.95 (m, 2H), 0.88 (d, *J* = 6.5 Hz, 6H), 0.80 (t, *J* = 7.5 Hz, 3H). **^{13}C NMR** (75 MHz, $CDCl_3$) δ (ppm) δ 172.1, 61.1, 58.0, 32.9, 29.4, 28.4, 25.0, 22.6, 14.3, 8.5. **HRMS** (ESI+) Calc. for $C_{14}H_{27}O_4^+$ [M+H^+]: 259.1904. Found: 259.1904. **FTIR** (ν / cm^{-1}): 2959, 2873, 1729, 1464, 1386, 1304, 1252, 1218, 1133, 1028.

3.4.4 Characterization Data of the Products

cyclohexyl(trifluoromethyl)sulfane (2a)

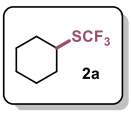

Following procedure A, **2a** was obtained from cyclohexane (216 µL, 2.00 mmol, 5.0 equiv) and Phth-SCF_3 (98.9 mg, 0.40 mmol, 1.0 equiv) in 83% NMR-Yield with trifluoro toluene as internal standard. **^{19}F NMR** (377 MHz, CD_3CN) δ (ppm) = -38.5. **MS** (EI, 70 eV): *m/z* (%) = 184 (19.8), 115 (11.7), 83 (100), 82 (21.8), 81 (8.9), 69 (17.4), 67 (24.2), 55 (81.7), 54 (12.1), 15 (9.1). The data match reported literature values. [15b]

cycloheptyl(trifluoromethyl)sulfane (2b)

Following the procedure A, **2b** was obtained from cyclohexane (262 µL, 2.00 mmol, 5.0 equiv) and Phth-SCF_3 (98.9 mg, 0.40 mmol, 1.0 equiv) in 85% NMR-Yield with trifluoro toluene as internal standard. **^{19}F NMR** (377 MHz, CD_3CN) δ (ppm) = -39.1. **MS** (EI, 70 eV): *m/z* (%) = 198 (1.7), 129 (42.7), 97 (81.9), 96 (11.7), 81 (22.9), 69 (23.9), 68 (11.7), 67 (24.8), 55 (100), 54 (13.5). The data match reported literature values.[15b]

cyclooctyl(trifluoromethyl)sulfane (2c)

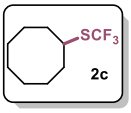

Following the procedure A, **2c** was obtained from cyclohexane (269 µL, 2.00 mmol, 5.0 equiv) and Phth-SCF_3 (98.9 mg, 0.40 mmol, 1.0 equiv) in 83% NMR-Yield with trifluoro toluene as internal standard. **^{19}F NMR** (377 MHz, CD_3CN) δ (ppm) = -39.0 **MS** (EI, 70 eV): *m/z* (%) = 212.1 (0.1), 143.1 (51.8), 128.0 (5.7), 111.1 (26.5), 82.1 (12.8), 81.1 (9.9), 69.1 (100), 67.1 (20.9), 55.1 (30.9), 41.1 (20.3), 39.0 (6.4). The data match reported literature values.[18c, 18d]

2-((trifluoromethyl)thio)-8-oxaspiro[4.5]decane-7,9-dione (2d)

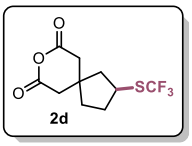

Following procedure A, **2d** was obtained from 8-oxaspiro[4.5]decane-7,9-dione (336 mg, 2.00 mmol, 5.0 equiv) and Phth-SCF_3 (98.9 mg, 0.40 mmol, 1.0 equiv) as a colorless amorphous solid (75.3 mg, 0.28 mmol, 70%). The product was purified by automated column chromatography (*Biotage® SNAP Ultra* 25 g column, pentane/Et_2O = 80/20 → 20/80). **^{1}H NMR** (400 MHz, $CDCl_3$) δ (ppm) 3.70 (p, *J* = 7.6 Hz, 1H), 2.82 – 2.75 (m, 2H), 2.71 (s, 2H), 2.43 – 2.27 (m, 1H), 2.18 (dd, *J* = 14.0, 7.9 Hz, 1H), 1.94 – 1.78 (m, 2H), 1.75 – 1.63 (m, 2H). **^{13}C NMR** (101 MHz, $CDCl_3$) δ (ppm) 165.4, 165.4, 130.5 (q, *J* = 306.8 Hz), 45.3, 42.6, 42.2, 41.1 (q, *J* = 1.8 Hz), 39.5, 36.6, 32.8. **^{19}F NMR** (377 MHz, $CDCl_3$) δ (ppm) -40.0. **HRMS** (EI+) Calc. for $C_{10}H_{11}F_3O_3S^{\bullet+}$ [$M^{\bullet+}$]: 268.0376. Found: 268.0376. **FTIR** (ν / cm^{-1}): 2929, 2855, 1714, 1453, 1416, 1151, 1118.

tert-butyl 7,9-dioxo-2-((trifluoromethyl)thio)-8-azaspiro[4.5]decane-8-carboxylate (2e)

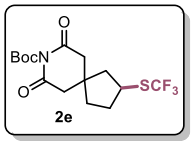

Following procedure A, **2e** was obtained from *tert*-butyl 7,9-dioxo-8-azaspiro[4.5]decane-8-carboxylate (294 mg, 0.80 mmol, 2.0 equiv) and Phth-SCF_3 (98.9 mg, 0.40 mmol, 1.0 equiv) as a colorless solid (78.0 mg, 0.21 mmol, 53%). The product was purified twice by automated column chromatography (*Biotage® SNAP Ultra* 25 g column, PE/EA = 90/10 → 80/20 and *Biotage® Sfär Silica HC D* 10 g column, P/Et_2O = 65/35). Tough separation of the product from phthalimide caused the isolated yield to be significant lower compared to the ^{19}F NMR yield (76%) of the crude reaction with $PhCF_3$ as internal standard. **^{1}H NMR** (400 MHz, $CDCl_3$) δ (ppm) 3.68 (p, *J* = 7.8 Hz, 1H), 2.64 (d, *J* = 27.6 Hz, 4H), 2.37 – 2.26 (m, 1H), 2.18 (dd, *J* = 13.9, 7.9 Hz, 1H), 1.90 – 1.78 (m, 2H), 1.67 (dd, *J* = 13.5, 7.9 Hz, 2H), 1.56 (s, 9H). **^{13}C NMR** (101 MHz, $CDCl_3$) δ (ppm) 168.9, 148.6, 130.6 (q, *J* = 306.5 Hz), 86.7, 45.3, 44.5, 44.0, 41.1, 40.0, 36.6, 32.8, 27.6. **^{19}F NMR** (376 MHz, $CDCl_3$) δ (ppm) -41.0. **HRMS** (ESI+) Calc. for $C_{15}H_{24}F_3N_2O_4S^+$ $[M+NH_4^+]$: 385.1403. Found: 385.1409. **X-Ray Structure CCDC:** 2046602. **FTIR** (ν / cm^{-1}): 2959, 2926, 2855, 1766, 1729, 1692, 1461, 1244, 1107, 842. MP.: 122.4–125.1°C.

2-((trifluoromethyl)thio)-8-azaspiro[4.5]decane-7,9-dione (2f)

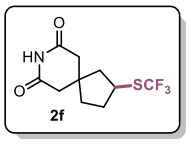

tert-butyl 7,9-dioxo-2-((trifluoromethyl)thio)-8-azaspiro[4.5]decane-8-carboxylate (**2e**, 78.0 mg, 0.21 mmol) was dissolved in DCM (1 mL) and TFA (0.2 mL) was added. The solution was stirred for 2 h at room temperature until complete conversion as monitored by TLC. The solvent was evaporated, the crude mixture was again redissolved in DCM, and was washed with sat. $NaHCO_3$ solution (3x). Evaporation of the solvent yielded **2f** as a white solid (47.6 mg, 0.18 mmol, 86%); mp 129.7-130.3 °C. **^{1}H NMR** (400 MHz, $CDCl_3$) δ (ppm) 8.44 (s, 1H), 3.68 (p, *J* = 7.7 Hz, 1H), 2.63 (s, 2H), 2.56 (s, 2H), 2.37 – 2.26 (m, 1H), 2.17 (dd, *J* = 13.9, 7.9 Hz, 1H), 1.91 – 1.76 (m, 2H), 1.73 – 1.60 (m, 2H). **^{13}C NMR** (101 MHz, $CDCl_3$) δ (ppm) 171.5, 130.6 (q, *J* = 306.7 Hz), 45.5, 44.4, 43.9, 41.1 (q, *J* = 1.8 Hz), 40.7, 36.8, 32.8. **^{19}F NMR** (376 MHz, $CDCl_3$) δ (ppm) -41.0. **HRMS** (ESI+) Calc. for $C_{10}H_{16}F_3N_2O_2S^+$ $[M^+NH_4]^+$: 285.0879. Found: 285.0878. **FTIR** (ν / cm^{-1}): 3190, 3090, 2952, 2866, 1729, 1673, 1379, 1267, 1095, 849.

8-((trifluoromethyl)thio)-3-oxaspiro[5.5]undecane-2,4-dione (2g) and 9-((trifluoromethyl)thio)-3-oxaspiro[5.5]undecane-2,4-dione (2g')

Following procedure A, **2g** and **2g'** were obtained from 3-oxaspiro[5.5]undecane-2,4-dione (364 mg, 2.00 mmol, 5.0 equiv) and Phth-SCF_3 (98.9 mg, 0.40 mmol, 1.0 equiv) as a colorless oil (**2g**, 28.9 mg, 0.10 mmol, 26%) and colorless solid (**2g'**, 31.5 mg, 0.11 mmol, 28 %), respectively. The

products were purified by automated column chromatography twice (*Biotage® SNAP Ultra* 25 g column, P/Et_2O = 80/20 → 20/80 and B*iotage® Sfär Silica* 10 g column, P/Et_2O = 80/20 → 30/70).

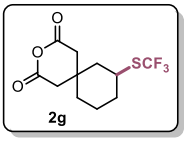

^{1}H NMR (400 MHz, $CDCl_3$) δ (ppm) 3.26 (tt, *J* = 12.3, 3.9 Hz, 1H), 2.87 (dd, *J* = 17.3, 1.3 Hz, 1H), 2.68 (d, 1H), 2.62 (s, 2H), 2.24 – 2.15 (m, 1H), 2.01 – 1.93 (m, 1H), 1.89 – 1.79 (m, 1H), 1.66 – 1.50 (m, 3H), 1.41 – 1.30 (m, 2H). **^{13}C NMR** (101 MHz, $CDCl_3$) δ (ppm) 165.2, 165.2, 130.7 (q, *J* = 306.9 Hz), 44.6, 43.5, 39.0, 38.3, 34.3, 33.8, 32.8, 21.4. **^{19}F NMR** (376 MHz, $CDCl_3$) δ (ppm) -39.3. **HRMS** (EI+) Calc. for $C_{11}H_{13}F_3O_3S^{\bullet+}$ [$M^{\bullet+}$]: 282.0532. Found: 282.05235. **FTIR** (ν / cm^{-1}): 2937, 2870, 1703, 1446, 1408, 1293, 1215, 1110.

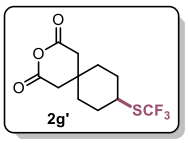

^{1}H NMR (400 MHz, $CDCl_3$) δ (ppm) 3.28 (ddt, *J* = 13.0, 8.6, 3.4 Hz, 1H), 2.73 (d, *J* = 1.2 Hz, 2H), 2.62 (d, *J* = 1.2 Hz, 2H), 2.12 – 2.03 (m, 2H), 1.75 – 1.61 (m, 4H), 1.57 – 1.46 (m, 2H). **^{13}C NMR** (101 MHz, $CDCl_3$) δ (ppm) 165.6, 165.5, 130.9 (q, *J* = 306.5 Hz), 42.9, 42.0, 39.4, 34.6, 31.6, 28.4. **^{19}F NMR** (376 MHz, $CDCl_3$) δ (ppm) -39.6. **HRMS** (EI+) Calc. for $C_{11}H_{13}F_3O_3S^{\bullet+}$ [$M^{\bullet+}$]: 282.0532. Found: 282.0526. **FTIR** (ν / cm^{-1}): 2929, 2862, 1811, 1759, 1707, 1453, 1237, 1103, 1058, 946. **MP.:** 84.6–87.7 °C.

3-methyl-3-((trifluoromethyl)thio)butyl benzoate (2h)

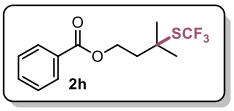

Following procedure A, **2h** was obtained from isopentyl benzoate (385 mg, 2.00 mmol, 5.0 equiv) and Phth-SCF_3 (98.9 mg, 0.40 mmol, 1.0 equiv) as a colorless oil (67.4 mg, 0.23 mmol, 58%, r.r. = 88/12). The product was purified by chromatography (*Biotage® SNAP Ultra* 25 g column, P/Et_2O = 97/3). **^{1}H NMR** (400 MHz, $CDCl_3$) δ (ppm) 8.06 – 8.00 (m, 2H), 7.61 – 7.53 (m, 1H), 7.45 (t, *J* = 7.7 Hz, 2H), 4.52 (t, *J* = 6.7 Hz, 2H), 2.21 (t, *J* = 6.7 Hz, 2H), 1.56 (s, 6H). **^{13}C NMR** (101 MHz, $CDCl_3$) δ (ppm) 166.6, 133.2, 130.9 (d, *J* = 307.8 Hz), 130.2, 129.7, 128.6, 61.8, 50.5, 41.5, 29.9 (q, *J* = 1.7 Hz). **^{19}F NMR** (376 MHz, $CDCl_3$) δ (ppm) -36.2. **HRMS** (EI+) Calc. for $C_{13}H_{19}F_3NO_2S$ [$M^{\bullet+}$]: 292.0739. Found: 292.0743. The data match reported literature values.[15b]

4-methyl-4-((trifluoromethyl)thio)pentyl benzoate (2i)

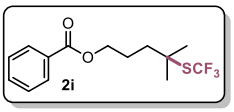

Following procedure A, **2i** was obtained from 4-methylpentyl benzoate (413 mg, 2.00 mmol, 5.0 equiv) and Phth-SCF_3 (98.9 mg, 0.40 mmol, 1.0 equiv) as a colorless oil (73.3 mg, 0.24 mmol, 60%, r.r. = 93/7). The product was purified by column chromatography (*Biotage® SNAP Ultra* 25 g column, P/Et_2O = 95/5). **^{1}H NMR** (400 MHz, $CDCl_3$) δ (ppm) 8.13 – 7.85 (m, 1H), 7.66 – 7.48 (m, 1H), 7.45 (dd, *J* = 8.4, 7.1 Hz, 1H), 4.34 (t, *J* = 6.2 Hz, 1H), 2.01 – 1.88 (m, 1H), 1.87 – 1.78 (m, 1H). **^{13}C NMR** (101 MHz, $CDCl_3$)

δ (ppm) 166.7, 133.1, 131.1 (q, J = 307.6 Hz)130.4, 129.7, 128.5, 64.8, 51.8, 39.6, 29.6 (q, *J* = 1.9 Hz), 24.5. **^{19}F NMR** (376 MHz, $CDCl_3$) δ (ppm) -36.3. **HRMS (APCI+)** Calc. for $C_{14}H_{21}F_3NO_2S$ [M+NH_4^+]: 324.1245. Found: 324.1242. The data match reported literature values.[15b]

4-methyl-4-((trifluoromethyl)thio)pentyl benzenesulfonate (2j)

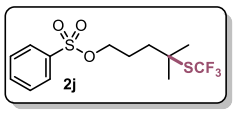

Following procedure A, **2j** was obtained from 4-methylpentyl benzenesulfonate (484 mg, 2.00 mmol, 5.0 equiv) and Phth-SCF_3 (98.9 mg, 0.40 mmol, 1.0 equiv) as a colorless oil (85.5 mg, 0.25 mmol, 62%, r.r. = 90/10). The product was purified by automated column chromatography (*Biotage® SNAP Ultra* 25 g column, P/Et_2O = 95/5 → 80/20). **^{1}H NMR** (300 MHz, $CDCl_3$) δ (ppm) 7.95 – 7.87 (m, 2H), 7.74 – 7.61 (m, 1H), 7.62 – 7.51 (m, 2H), 4.06 (q, *J* = 6.2 Hz, 2H), 1.79 (tdd, *J* = 9.8, 4.8, 1.6 Hz, 2H), 1.72 – 1.59 (m, 2H), 1.40 (d, *J* = 1.0 Hz, 5H). **^{13}C NMR** (75 MHz, $CDCl_3$) δ (ppm) 136.2, 134.0, 130.9 (d, *J* = 307.7 Hz), 129.4, 128.0, 70.7, 51.4, 39.0, 29.5 (d, *J* = 1.7 Hz), 24.7. **^{19}F NMR** (282 MHz, $CDCl_3$) δ -36.32, -41.68. **HRMS** (EI+) Calc. for $C_{13}H_{17}F_3NaO_2S_2^+$ [M+Na^+]: 365.0463. Found: 365.0466. **FTIR** (ν / cm^{-1}): 2970, 2933, 1475, 1449, 1360, 1185, 1095, 969, 916, 752.

methyl (4-methyl-4-((trifluoromethyl)thio)pentyl) oxalate (2k)

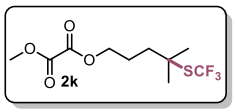

Following procedure A, **2k** was obtained from methyl (4-methylpentyl) oxalate (376 mg, 2.00 mmol, 5.0 equiv) and Phth-SCF_3 (98.9 mg, 0.40 mmol, 1.0 equiv) as a colorless oil (73.0 mg, 0.25 mmol, 63%, r.r. = 93/1/6). The product was purified by chromatography (25 g SiO_2, P/Et_2O = 95/5 → 80/20). **^{1}H NMR** (300 MHz, $CDCl_3$) δ (ppm) 4.30 (t, *J* = 6.4 Hz, 2H), 3.90 (s, 3H), 1.99 – 1.85 (m, 2H), 1.79 – 1.70 (m, 2H), 1.45 (q, *J* = 0.8 Hz, 6H). **^{13}C NMR** (75 MHz, $CDCl_3$) δ (ppm) 158.2, 157.7, 131.0 (q, *J* = 307.5 Hz), 66.9, 53.7, 51.5, 39.1 (d, *J* = 1.8 Hz), 29.5 (d, *J* = 1.7 Hz), 24.0. **^{19}F NMR** (282 MHz, $CDCl_3$) δ (ppm) δ -36.34, -40.03, -41.71. **HRMS** (EI+) Calc. for $C_{10}H_{15}F_3NaO_4S^+$ [M+Na^+]: 311.0535. Found: 311.0538. **FTIR** (ν / cm^{-1}): 2970, 1770, 1744, 1468, 1319, 1095, 965, 723.

diethyl 2-ethyl-2-(3-methyl-3-((trifluoromethyl)thio)butyl)malonate (2l)

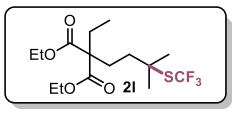

Following procedure A, **2l** was obtained from diethyl 2-ethyl-2-isopentylmalonate (517 mg, 2.00 mmol, 5.0 equiv) and Phth-SCF_3 (98.9 mg, 0.40 mmol, 1.0 equiv) as a colorless oil (65.7 mg, 0.18 mmol, 46%, r.r. = 95/5). The product was purified by automated column chromatography (*Biotage® SNAP Ultra* 25 g column, P/Et_2O = 80/20 → 60/40). **^{1}H NMR** (400 MHz, $CDCl_3$) δ (ppm) 4.18 (q, *J* = 7.1 Hz, 4H), 2.06 – 1.97 (m, 2H), 1.92 (q, *J* = 7.6 Hz, 2H), 1.57 – 1.48 (m, 2H), 1.45 (d, *J* = 0.9 Hz, 6H), 1.24 (t, *J* = 7.1 Hz, 6H), 0.82 (t, *J* = 7.6 Hz, 3H). **^{13}C NMR** (101 MHz, $CDCl_3$) δ (ppm) 171.6, 131.1 (d, *J* = 307.6 Hz), 61.3, 57.6,

51.6, 37.4, 29.4 (q, *J* = 1.3 Hz), 26.8, 25.3, 14.2, 8.4. **^{19}F NMR** (377 MHz, $CDCl_3$) δ (ppm) -36.18. **HRMS** (ESI+) Calc. for $C_{14}H_{21}F_3NO_2S$ [M+NH_4^+]: 324.1245. Found: 324.1242. **FTIR** (ν / cm^{-1}): 2948, 2873, 1811, 1759, 1449, 1237, 1103, 1058, 946, 756.

((3-bromophenoxy)methyl)(trifluoromethyl)sulfane (2m)

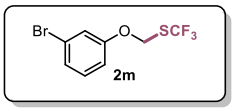

Following procedure B, **2m** was obtained from 1-bromo-3-methoxybenzene (127 µL, 187 mg, 1.00 mmol, 2.5 equiv) and Phth-SCF_3 (98.9 mg, 0.40 mmol, 1.0 equiv) as a colorless oil (47.1 mg, 0.16 mmol, 41%). The product was purified by automated column chromatography (*Biotage® SNAP Ultra* 10 g column, pentane) to obtain a mixture of product and starting material, which was subsequently separated by Kugelrohr distillation (7 mbar, 65 °C). **^{1}H NMR** (400 MHz, $CDCl_3$) δ (ppm) 7.24 – 7.17 (m, 2H), 7.12 – 7.09 (m, 1H), 6.87 (dt, *J* = 6.6, 2.4 Hz, 1H), 5.49 (s, 2H). **^{13}C NMR** (101 MHz, $CDCl_3$) δ (ppm) 156.8, 131.0, 130.1 (q, *J* = 308.2 Hz), 126.3, 123.13, 120.0, 115.2, 68.3 (q, *J* = 2.7 Hz). **^{19}F NMR** (376 MHz, $CDCl_3$) δ (ppm) -40.8. **HRMS** (EI+) Calc. for $C_8H_6{}^{79}BrF_3OS^{\bullet+}$ [$M^{\bullet+}$]: 285.9269. Found: 285.9261. **FTIR** (ν / cm^{-1}): 2970, 2926, 2855, 1461, 1379, 1162, 1080, 1021.

((4-bromophenoxy)methyl)(trifluoromethyl)sulfane (2n)

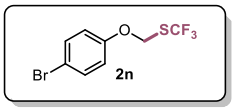

Following procedure B, **2n** was obtained from 1-bromo-4-methoxybenzene (125 µL, 187 mg, 1.00 mmol, 2.5 equiv) and Phth-SCF_3 (98.9 mg, 0.40 mmol, 1.0 equiv) as a colorless oil (51.4 mg, 0.18 mmol, 45%). The product was purified by automated column chromatography (*Biotage® SNAP Ultra* 10 g column, pentane) to obtain a mixture of product and starting material, which was subsequently separated by Kugelrohr distillation (7 mbar, 70 °C). **^{1}H NMR** (400 MHz, $CDCl_3$) δ (ppm) 7.50 – 7.41 (m, 2H), 6.89 – 6.76 (m, 2H), 5.48 (s, 2H). **^{13}C NMR** (101 MHz, $CDCl_3$) δ (ppm) 155.1, 132.8, 130.1 (q, *J* = 308.2 Hz), 118.4, 115.7, 68.5 (q, *J* = 2.8 Hz). **^{19}F NMR** (376 MHz, $CDCl_3$) δ (ppm) -40.7. **HRMS** (EI+) Calc. for $C_8H_6{}^{79}BrF_3OS^{\bullet+}$ [$M^{\bullet+}$]: 285.9269. Found: 285.9270. **FTIR** (ν / cm^{-1}): 1584, 1483, 1442, 1326, 1207, 1103, 1025, 820, 756, 678.

(1-phenoxybutyl)(trifluoromethyl)sulfane (2o)

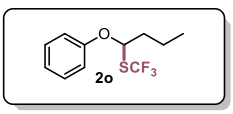

Following procedure B, **2o** was obtained from butoxybenzene (162 µL, 150 mg, 1.00 mmol, 2.5 equiv) and Phth-SCF_3 (98.9 mg, 0.40 mmol, 1.0 equiv) as a colorless oil (78.8 mg, 0.31 mmol, 79%). The product was purified by automated column chromatography (*Biotage® SNAP Ultra* 10 g column, pentane) **^{1}H NMR** (400 MHz, $CDCl_3$) δ (ppm) 7.37 – 7.30 (m, 2H), 7.08 (t, *J* = 7.4 Hz, 1H), 7.05 – 6.93 (m, 2H), 5.66 (dd, *J* = 7.3, 5.4 Hz, 1H), 2.21 (dq, *J* = 14.4, 7.0 Hz, 1H), 2.13 – 2.02 (m, 1H), 1.69 – 1.54 (m, 2H), 1.01 (t, *J* = 7.4 Hz, 3H).

^{13}C NMR (101 MHz, $CDCl_3$) δ (ppm) 156.5, 130.5 (q, *J* = 307.6 Hz), 129.8, 123.3, 117.6, 84.4 (q, *J* = 1.8 Hz), 39.4, 19.3, 13.6. **^{19}F NMR** (376 MHz, $CDCl_3$) δ (ppm) -38.0. **HRMS** (EI+) Calc. for $C_{11}H_{13}F_3OS^{\bullet+}$ [$M^{\bullet+}$]: 250.0634. Found: 250.0627. **FTIR** (ν / cm^{-1}): 2955, 2922, 2855, 1722, 1461, 1379, 1274, 1080, 969 cm^{-1}.

1-(3-(((trifluoromethyl)thio)methoxy)phenyl)propan-2-one (2p)

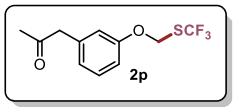

Following procedure B, **2p** was obtained from 1-(3-methoxyphenyl)propan-2-one (153 µL, 164 mg, 2.00 mmol, 2.5 equiv) and Phth-SCF_3 (98.9 mg, 0.40 mmol, 1.0 equiv) as a colorless oil (87.3 mg, 0.33 mmol, 83%). The product was purified by automated column chromatography (*Biotage® SNAP Ultra* 10 g column, PE/EA = 90/10 → 80/20). **^{1}H NMR** (400 MHz, $CDCl_3$) δ (ppm) 7.30 (t, *J* = 7.9 Hz, 1H), 6.92 (d, *J* = 7.9 Hz, 1H), 6.84 (dd, *J* = 8.2, 2.4 Hz, 1H), 6.80 – 6.77 (m, 1H), 5.51 (s, 2H), 3.69 (s, 2H), 2.17 (s, 3H). **^{13}C NMR** (101 MHz, $CDCl_3$) δ (ppm) 205.9, 156.3, 136.2, 130.2 (q, *J* = 308.1 Hz), 130.1, 124.2, 117.7, 114.9, 68.3 (q, *J* = 2.8 Hz), 50.9, 29.5. **^{19}F NMR** (376 MHz, $CDCl_3$) δ (ppm) -40.8. **HRMS** (EI+) Calc. for $C_{11}H_{11}F_3O_2S^{\bullet+}$ [$M^{\bullet+}$]: 264.0426. Found: 264.0418. **FTIR** (ν / cm^{-1}): 2929, 2855, 1699, 1587, 1490, 1453, 1114, 1036, 756, 678.

methyl 2-(3-(((trifluoromethyl)thio)methoxy)phenyl)acetate (2q)

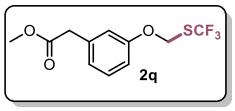

Following procedure B, **2q** was obtained from methyl 2-(3-methoxyphenyl)acetate (161 µL, 180 mg, 1.00 mmol, 2.5 equiv) and Phth-SCF_3 (98.9 mg, 0.40 mmol, 1.0 equiv) as a colorless oil (111 mg, 0.40 mmol, 99%,). The product was purified by automated column chromatography (*Biotage® SNAP Ultra* 25 g column, P/DCM = 50/50). **^{1}H NMR** (400 MHz, $CDCl_3$) δ (ppm) 7.29 (t, *J* = 7.9 Hz, 1H), 7.03 – 6.96 (m, 1H), 6.89 – 6.87 (m, 1H), 6.85 (dd, *J* = 8.2, 2.3 Hz, 1H), 5.53 – 5.48 (m, 2H), 3.70 (s, 3H), 3.62 (s, 2H). **^{13}C NMR** (101 MHz, $CDCl_3$) δ (ppm) 171.7, 156.2, 136.0, 130.3 (q, *J* = 308.0 Hz), 129.9, 124.0, 117.5, 115.0, 68.2 (q, *J* = 2.8 Hz), 52.2, 41.2. **^{19}F NMR** (376 MHz, $CDCl_3$) δ (ppm) -40.8. **HRMS** (EI+) Calc. for $C_{11}H_{11}F_3O_3S^{\bullet+}$ [$M^{\bullet+}$]: 280.0375. Found: 280.0374. **FTIR** (ν / cm^{-1}): 2955, 1736, 1587, 1490, 1438, 1259, 1103, 1036, 756, 678.

***S*-(trifluoromethyl) benzothioate (2r)**

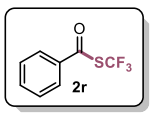

Following procedure C, **2r** was obtained from benzaldehyde (61.2 µL, 0.60 mmol, 1.5 equiv) and Phth-SCF_3 (98.9 mg, 0.40 mmol, 1.0 equiv) as a colorless oil (75.3 mg, 0.28 mmol, 55%, NMR-Yield: 76%). The product was purified by automated column chromatography (*Biotage® SNAP Ultra* 25 g column, pentane). The compound is volatile, evaporation of the solvent at room temperature is recommended. **^{1}H NMR** (400 MHz, $CDCl_3$) δ (ppm) 7.89

– 7.83 (m, 2H), 7.73 – 7.63 (m, 1H), 7.57 – 7.46 (m, 2H). **^{13}C NMR** (101 MHz, $CDCl_3$) δ (ppm) δ 183.4, 135.3 (q, *J* = 2.9 Hz), 135.2, 129.4, 128.2 (q, *J* = 309.6 Hz), 127.8. **^{19}F NMR** (377 MHz, $CDCl_3$) δ (ppm) -40.2. **HRMS** (APCI) Calc. for $C_8H_9F_3NOS^+$ [M+NH_4^+]: 224.0351. Found: 224.0353. The data match reported literature values.[15a]

S-(trifluoromethyl) 4-hydroxybenzothioate (2s)

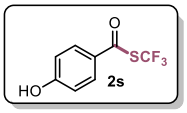

Following procedure C, **2s** was obtained from 4-hydroxybenzaldehyde (73.3 mg, 0.6 mmol, 1.5 equiv) and Phth-SCF_3 (98.9 mg, 0.40 mmol, 1.0 equiv) as a slightly yellow solid (80.0 mg, 0.360 mmol, 90%) after purification by automated column chromatography (25 g SiO_2, PE/EA = 90/10 → 84/16). **^{1}H NMR** (300 MHz, $CDCl_3$) δ (ppm) 7.79 (d, *J* = 8.8 Hz, 2H), 6.94 (d, *J* = 8.9 Hz, 2H), 6.47 (br, 1H). **^{13}C NMR** (75 MHz, $CDCl_3$) δ (ppm) δ 182.9, 162.1, 130.6, 128.2 (q, *J* = 309.4 Hz), 127.9 (q, *J* = 2.8 Hz), 116.2. **^{19}F NMR** (282 MHz, $CDCl_3$) δ (ppm) -39.9. **HRMS** (EI+) Calc. for $C_8H_5F_3O_2S^{\bullet+}$ [$M^{\bullet+}$]: 221.9957. Found: 221.9957. **FTIR** (ν / cm^{-1}): 3444, 2926, 2855, 1677, 1610, 1580, 1510, 1442, 1297, 1211, 1140, 1095, 887, 846. **MP.:** 82.9–84.0 °C.

S-(trifluoromethyl) 4-methylbenzothioate (2t)

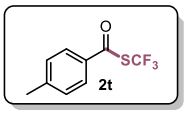

Following procedure C, 2t was obtained from 4-methylbenzaldehyde (70.7 µL, 0.6 mmol, 1.5 equiv) and Phth-SCF_3 (98.9 mg, 0.40 mmol, 1.0 equiv) as a colorless oil (59.2 mg, 0.27 mmol, 67%) after purification by automated column chromatography (10g SiO_2, pentane). As the product is quite volatile, evaporation of the solvent at room temperature is recommended. **^{1}H NMR** (400 MHz, $CDCl_3$) δ (ppm) 7.75 (d, *J* = 8.3 Hz, 1H), 7.30 (d, *J* = 8.1 Hz, 1H), 2.44 (s, 2H). **^{13}C NMR** (101 MHz, $CDCl_3$) δ (ppm) 182.9, 146.6, 132.7 (q, *J* = 2.7 Hz), 130.0, 128.3 (q, *J* = 309.3 Hz), 127.9, 21.9. **^{19}F NMR** (377 MHz, $CDCl_3$) δ (ppm) -40.1. **HRMS** (APCI) Calc. for $C_9H_{11}F_3NOS^+$ [M+NH_4^+]: 238.0508. Found: 238.0511. The data match reported literature values.[15a]

S-(trifluoromethyl) 4-(methylthio)benzothioate (2u)

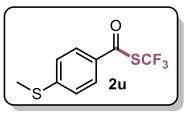

Following procedure C, **2u** was obtained from 4-(methylthio)benzaldehyde (91.3 mg, 0.6 mmol, 1.5 equiv) and Phth-SCF_3 (98.9 mg, 0.40 mmol, 1.0 equiv) as a colorless amorphous solid (43.0 mg, 0.17 mmol, 42%) after purification by automated column chromatography (10g SiO_2, PE/EA = 100/0 → 95/05). **^{1}H NMR** (400 MHz, $CDCl_3$) δ (ppm) 7.71 (d, *J* = 8.6 Hz, 2H), 7.44 – 7.06 (m, 2H), 2.50 (s, 3H). **^{13}C NMR** (101 MHz, $CDCl_3$) δ (ppm) 182.2, 149.3, 131.2 (q, *J* = 2.8 Hz), 128.2 (q, *J* = 309.3 Hz), 128.1, 125.3, 14.7. **^{19}F NMR** (377 MHz, $CDCl_3$) δ (ppm) -39.9. **HRMS** (APCI) Calc. for $C_9H_{11}F_3NOS_2^+$ [M+NH_4^+]: 270.0229. Found: 270.0232. **FTIR** (ν / cm^{-1}): 3373, 2929, 1692, 1580, 1487, 1438, 1401, 1222, 1118, 1088, 820, 719.

S-(trifluoromethyl) [1,1'-biphenyl]-4-carbothioate (2v)

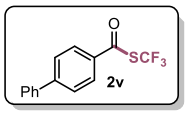

Following procedure C, **2v** was obtained from 4-phenylbenzaldehyde (109 mg, 0.6 mmol, 1.5 equiv) and Phth-SCF_3 (98.9 mg, 0.40 mmol, 1.0 equiv) as a colorless solid (95.0 mg, 0.34 mmol, 84%) after purification by automated column chromatography (*Biotage® SNAP Ultra* 10 g column, PE/EA = 100/0 → 98/02). Alternatively, **2v** was was obtained from 4-phenylbenzaldehyde (327 mg, 1.8 mmol, 1.5 equiv) and Phth-SCF_3 (297 mg, 1.2 mmol, 1.0 equiv) with TBADT (99.6 mg, 0.03 mmol, 2.5 mol%) after irradiation overnight in MeCN (3 mL, 0.4 M) in 74% yield (250 mg, 0.88 mmol). **^{1}H NMR** (400 MHz, $CDCl_3$) δ (ppm) 7.96 – 7.90 (m, 2H), 7.73 (d, *J* = 8.3 Hz, 2H), 7.66 – 7.60 (m, 2H), 7.54 – 7.41 (m, 3H). **^{13}C NMR** (101 MHz, $CDCl_3$) δ 182.8, 148.0, 139.2, 133.8 (q, *J* = 2.6 Hz), 129.2, 128.9, 128.4, 128.2 (q, *J* = 309.7 Hz), 127.9, 127.4. **^{19}F NMR** (377 MHz, $CDCl_3$) δ (ppm) -40.0. **HRMS** (EI+) Calc. for $C_{14}H_9F_3OS^{\bullet+}$ [$M^{\bullet+}$]: 282.0321. Found: 282.0318. **MP.:** 61.1–65.8°C. The data match reported literature values.[15a]

S-(trifluoromethyl) 4-chlorobenzothioate (2w)

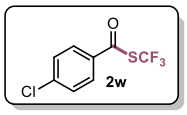

Following procedure C, **2w** was obtained from 4-chlorobenzaldehyde (118 mg, 0.6 mmol, 1.5 equiv) and Phth-SCF_3 (98.9 mg, 0.40 mmol, 1.0 equiv) as a colorless amorphous solid (66.0 mg, 0.27 mmol, 69%) after purification by automated column chromatography (10g SiO_2, 100% pentane). Albeit solid at room temperature, the product was found to be volatile at 40 °C under reduced pressure. Evaporation of the solvent at room temperature is recommended. **^{1}H NMR** (400 MHz, $CDCl_3$) δ (ppm) 7.84 – 7.77 (m, 2H), 7.53 – 7.46 (m, 2H). **^{13}C NMR** (101 MHz, $CDCl_3$) δ (ppm) 182.3, 141.9, 133.6 (q, *J* = 2.8 Hz), 129.7, 129.1, 127.95 (q, *J* = 309.9 Hz). **^{19}F NMR** (377 MHz, $CDCl_3$) δ (ppm) -40.1. **HRMS** (EI+) Calc. for $C_8H_4ClF_3OS^{\bullet+}$ [$M^{\bullet+}$]: 239.9618. Found: 239.9624. The data match reported literature values.[15a]

S-(trifluoromethyl) 3,4,5-trimethoxybenzothioate (2x)

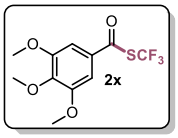

Following procedure C, **2x** was obtained from 3,4,5-trimethoxybenzaldehyde (118 mg, 0.6 mmol, 1.5 equiv) and Phth-SCF_3 (98.9 mg, 0.40 mmol, 1.0 equiv) as a colorless solid (79.6 mg, 0.27 mmol, 67%) after purification by automated column chromatography (25 g SiO_2, PE/EA = 95/05 → 91/09). **^{1}H NMR** (400 MHz, $CDCl_3$) δ (ppm) 7.26 (s, 2H), 4.11 (s, 3H), 4.08 (s, 6H). **^{13}C NMR** (101 MHz, $CDCl_3$) δ (ppm) 182.3, 153.6, 144.3, 130.1 (q, *J* = 2.8 Hz), 128.1 (q, *J* = 309.5 Hz), 105.2, 61.2. **^{19}F NMR** (377 MHz, $CDCl_3$) δ (ppm) -40.2. **HRMS** (EI+) Calc. for $C_{11}H_{11}F_3O_4S^{\bullet+}$ [$M^{\bullet+}$]: 296.0325. Found: 296.0316. **FTIR** (ν / cm^{-1}): 2944, 2840, 1699, 1580, 1498, 1464, 1416, 1319, 1248, 1125, 1088, 991, 760. **MP**.: 53.8–56.8°C.

S-(trifluoromethyl) 4-acetamidobenzothioate (2y)

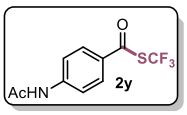

Following procedure C, **2y** was obtained from *N*-(4-formylphenyl)acetamide (97.9 mg, 0.6 mmol, 1.5 equiv) and Phth-SCF_3 (98.9 mg, 0.40 mmol, 1.0 equiv) as a colorless solid (94.2 mg, 0.357 mmol, 89%) after purification by automated column chromatography (25 g SiO_2, PE/EA = 90/10 → 84/16). **^{1}H NMR** (400 MHz, $CDCl_3$) δ (ppm) 7.83 (d, *J* = 8.8 Hz, 2H), 7.67 (d, *J* = 8.8 Hz, 2H), 7.52 (br, 1H), 2.23 (s, 3H). **^{13}C NMR** (101 MHz, $CDCl_3$) δ (ppm) δ 182.0, 168.7, 144.1, 130.6, 129.4, 128.2 (d, *J* = 309.3 Hz), 119.3, 24.5. **^{19}F NMR** (377 MHz, $CDCl_3$) δ (ppm) -40.0. **HRMS** (EI+) Calc. for $C_{10}H_8F_3NO_2S^{\bullet+}$ [$M^{\bullet+}$]: 263.0222. Found: 263.0229. **FTIR** (ν / cm^{-1}): 3246, 3179, 3108, 3049, 2363, 1699, 1587, 1539, 1408, 1323, 1155, 1099, 879, 682. **MP**.: 162.5–165.1°C.

4-(((trifluoromethyl)thio)carbonyl)phenyl benzoate (2z)

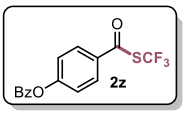

Following procedure C, **2z** was obtained from 4-formylphenyl benzoate (136 mg, 0.6 mmol, 1.5 equiv) and Phth-SCF_3 (98.9 mg, 0.40 mmol, 1.0 equiv) as a colorless solid (105 mg, 0.32 mmol, 80%) after purification by automated column chromatography (*Biotage® SNAP Ultra* 10 g column, PE/DCM = 95/5). **^{1}H NMR** (400 MHz, $CDCl_3$) δ (ppm) 8.20 (dd, *J* = 8.4, 1.4 Hz, 2H), 7.96 (d, *J* = 8.8 Hz, 2H), 7.68 (ddt, *J* = 8.7, 7.0, 1.2 Hz, 1H), 7.58 – 7.51 (m, 2H), 7.44 – 7.38 (m, 2H). **^{13}C NMR** (101 MHz, $CDCl_3$) δ (ppm) 182.2, 164.4, 156.3, 134.3, 132.7 (q, *J* = 2.8 Hz), 130.4, 129.5, 128.9, 128.8, 128.1 (q, *J* = 309.7 Hz), 122.8. **^{19}F NMR** (377 MHz, $CDCl_3$) δ (ppm) -40.1. **HRMS** (APCI) Calc. for $C_{15}H_{13}F_3NO_3S^+$ [$M+NH_4^+$]: 344.0563. Found: 344.0566. **FTIR** (ν / cm^{-1}): 1736, 1695, 1595, 1502, 1267, 1218, 1162, 1125, 1058, 872. **MP**.: 95.6–97.3°C

S-(trifluoromethyl) 4-(pentafluoro-λ⁶-sulfaneyl)benzothioate (2aa)

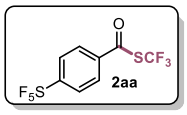

Following procedure C, **2aa** was obtained from 4-(pentafluorosulfaneyl)benzaldehyde (99.5 µL, 139 mg, 0.6 mmol, 1.5 equiv) and Phth-SCF_3 (98.9 mg, 0.40 mmol, 1.0 equiv) as a colorless amorphous solid (69.8 mg, 0.13 mmol, 53%) after purification by automated column chromatography (10g SiO_2, pentane). **^{1}H NMR** (400 MHz, $CDCl_3$) δ (ppm) 7.99 – 7.89 (m, 4H). **^{13}C NMR** (101 MHz, $CDCl_3$) δ (ppm) 182.3, 158.3 (t, *J* = 18.7 Hz), 137.4, 128.2, 127.7 (q, *J* = 310.4 Hz), 127.3 (p, *J* = 4.8 Hz). **^{19}F NMR** (377 MHz, $CDCl_3$) δ (ppm) 81.0 (q, *J* = 150.5 Hz), 61.7 (d, *J* = 150.5 Hz), -40.1. **HRMS** (EI+) Calc. for $C_8H_4F_7OS_2^{\bullet+}$ [$M^{\bullet+}$–$F^{\bullet}$]: 312.9586. Found: 312.9581.

S-(trifluoromethyl) 4-(tosyloxy)benzothioate (2ab)

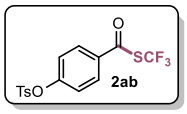

Following procedure C, **2ab** was obtained from 4-formylphenyl 4-methylbenzenesulfonate (166 mg, 0.6 mmol, 1.5 equiv) and Phth-SCF_3 (98.9 mg, 0.40 mmol, 1.0 equiv) as a yellowish amorphous solid (116 mg, 0.31 mmol, 77%) after purification by column chromatography (*Biotage® SNAP Ultra* 10 g column, PE/DCM = 95/5). **^{1}H NMR** (400 MHz, $CDCl_3$) δ (ppm) 7.85 – 7.77 (m, 2H), 7.75 – 7.68 (m, 2H), 7.37 – 7.31 (m, 2H), 7.18 – 7.13 (m, 2H). **^{13}C NMR** (101 MHz, $CDCl_3$) δ (ppm) 182.1, 154.5, 146.2, 133.6 (q, *J* = 2.6 Hz), 132.0, 130.2, 129.6, 128.6, 127.9 (d, *J* = 310.0 Hz), 123.3, 21.9. **^{19}F NMR** (377 MHz, $CDCl_3$) δ (ppm) -40.1. **HRMS** (ESI+) Calc. for $C_{15}H_{11}F_3NaO_4S_2^+$ [M+Na^+]: 398.9943. Found: 398.9943 The data match reported literature values.[20a]

S-(trifluoromethyl) 4-(((*tert*-butoxycarbonyl)amino)methyl)benzothioate (2ac)

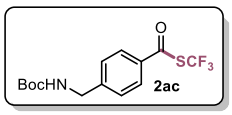

Following procedure C, **2ac** was obtained from *tert*-butyl (4-formylbenzyl)carbamate (141 mg, 0.6 mmol, 1.5 equiv) and Phth-SCF_3 (98.9 mg, 0.40 mmol, 1.0 equiv) as a colorless solid (55.6 mg, 0.17 mmol, 41%) after purification by automated column chromatography (*Biotage® SNAP Ultra* 10 g column, PE/EA = 95/05 → 75/25). **^{1}H NMR** (400 MHz, $CDCl_3$) δ (ppm) 7.81 (d, *J* = 8.3 Hz, 2H), 7.41 (d, *J* = 8.1 Hz, 2H), 5.04 (s, 1H), 4.38 (d, *J* = 5.3 Hz, 2H), 1.45 (s, 9H). **^{13}C NMR** (101 MHz, $CDCl_3$) δ (ppm) 182.9, 156.0, 147.2, 134.2 (q, *J* = 2.4 Hz), 128.1 (q, *J* = 309.6 Hz), 128.1, 127.9, 80.2, 44.3, 28.5. **^{19}F NMR** (377 MHz, $CDCl_3$) δ (ppm) -40.1. **HRMS** (ESI+) Calc. for $C_{14}H_{16}F_3NNaO_3S^+$ [M+Na^+]: 358.0695. Found: 358.0696. **FTIR** (ν / cm^{-1}): 3358, 1684, 1513, 1077, 790. **MP**.: 129.0–131.1°C.

S-(trifluoromethyl) 3-((*tert*-butoxycarbonyl)amino)benzothioate (2ad)

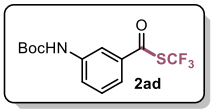

Following procedure C, **2ad** was obtained from *tert*-butyl (3-formylphenyl)carbamate (133 mg, 0.6 mmol, 1.5 equiv) and Phth-SCF_3 (98.9 mg, 0.40 mmol, 1.0 equiv) as a colorless solid (80.3 mg, 0.25 mmol, 62%) after purification by automated column chromatography (*Biotage® SNAP Ultra* 10 g column, PE/EA = 95/05 → 90/10). **^{1}H NMR** (400 MHz, $CDCl_3$) δ (ppm) 7.91 (t, *J* = 2.0 Hz, 1H), 7.67 (d, *J* = 8.1 Hz, 1H), 7.50 (ddd, *J* = 7.8, 1.8, 1.1 Hz, 1H), 7.41 (t, *J* = 7.9 Hz, 1H), 6.76 (s, 1H), 1.53 (s, 9H). **^{13}C NMR** (101 MHz, $CDCl_3$) δ (ppm) 183.3, 152.6, 139.7, 135.9 (q, *J* = 2.7 Hz), 130.0, 128.1 (q, *J* = 309.7 Hz), 124.7, 122.0, 117.1, 81.6, 28.4. **^{19}F NMR** (377 MHz, $CDCl_3$) δ (ppm) -40.3. **HRMS** (EI+) Calc. for $C_{13}H_{14}F_3NNaO_3S^+$ [M+Na$^+$]: 344.0539. Found: 344.0543. **FTIR** (ν / cm^{-1}): 3339, 2974, 1699, 1587, 1543, 1431, 1244, 1155, 1099, 887, 693. **MP**.: 111.7–114.1°C.

S-(trifluoromethyl) naphthalene-2-carbothioate (2ae)

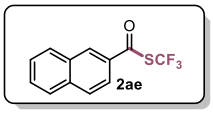

Following procedure C, **2ae** was obtained from 2-naphthaldehyde (93.7 mg, 0.6 mmol, 1.5 equiv) and Phth-SCF_3 (98.9 mg, 0.40 mmol, 1.0 equiv) as a yellow amorphous solid (54.5 mg, 0.21 mmol, 53%) after purification by automated column chromatography (25 g SiO_2, PE/EA = 100/0 → 98/02). **^{1}H NMR** (400 MHz, $CDCl_3$) δ (ppm) 8.38 (d, *J* = 1.8 Hz, 1H), 7.96 (d, *J* = 8.1 Hz, 1H), 7.90 (t, *J* = 8.8 Hz, 2H), 7.84 (dd, *J* = 8.7, 1.9 Hz, 1H), 7.67 (ddd, *J* = 8.2, 6.8, 1.4 Hz, 1H), 7.60 (ddd, *J* = 8.2, 6.9, 1.4 Hz, 1H). **^{13}C NMR** (101 MHz, $CDCl_3$) δ (ppm) 183.3, 132.5 (q, *J* = 2.7 Hz), 130.0, 129.8, 128.3 (q, *J* = 309.6 Hz), 129.7, 129.4, 128.1, 127.7, 122.6. **^{19}F NMR** (377 MHz, $CDCl_3$) δ (ppm) -40.0. **HRMS** (EI+) Calc. for $C_{12}H_7F_3OS^{\bullet+}$ [M$^{\bullet+}$]: 256.0164. Found: 256.0161. The data match reported literature values.[20a]

S-(trifluoromethyl) 6-methoxynaphthalene-2-carbothioate (2af)

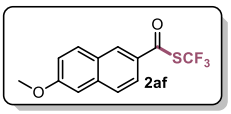

Following procedure C, **2af** was obtained from 6-methoxy-2-naphthaldehyde (109 mg, 0.6 mmol, 1.5 equiv) and Phth-SCF_3 (98.9 mg, 0.40 mmol, 1.0 equiv) as a yellow solid (60.7 mg, 0.21 mmol, 53%) after purification by chromatography (25 g SiO_2, PE/EA = 100/0 → 97/03). **^{1}H NMR** (400 MHz, $CDCl_3$) δ (ppm) 8.31 (d, *J* = 1.7 Hz, 1H), 7.90 – 7.69 (m, 3H), 7.25 (dd, *J* = 8.9, 2.4 Hz, 1H), 7.16 (d, *J* = 2.5 Hz, 1H), 3.96 (s, 3H). **^{13}C NMR** (101 MHz, $CDCl_3$) δ (ppm) 182.8, 160.8, 138.5, 131.5, 130.44 (q, *J* = 2.7 Hz), 129.9, 128.4 (q, *J* = 309.1 Hz), 127.9, 127.7, 123.5, 120.7, 106.0, 55.7. **^{19}F NMR** (377 MHz, $CDCl_3$) δ (ppm) -39.9. **HRMS** (EI+) Calc. for $C_{13}H_9F_3O_2S^{\bullet+}$ [M$^{\bullet+}$]: 286.0270. Found: 286.0277. **FTIR** (ν / cm^{-1}): 2940, 2847, 1703, 1621, 1479, 1390, 1271, 1151, 1099, 1025, 689. **MP**.: 78.4–80.4°C

S-(trifluoromethyl) 3-phenylpropanethioate (2ag)

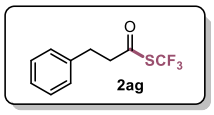

Following procedure C, **2ag** was obtained from 3-phenylpropanal (79.7 µL, 80.5 mg, 0.6 mmol, 1.5 equiv) and Phth-SCF_3 (98.9 mg, 0.40 mmol, 1.0 equiv) as a colorless oil (59.4 mg, 0.25 mmol, 63%) after purification by automated column chromatography (*Biotage® SNAP Ultra* 10 g column, pentane). As the product is quite volatile, evaporation of the solvent at room temperature is recommended. **^{1}H NMR** (300 MHz, $CDCl_3$) δ (ppm) δ 7.37 – 7.29 (m, 2H), 7.29 – 7.24 (m, 1H), 7.20 (m, 2H), 3.09 – 2.99 (m, 2H), 2.98 – 2.90 (m, 2H). **^{13}C NMR** (75 MHz, $CDCl_3$) δ (ppm) 189.7, 138.9, 128.9, 128.4, 127.7 (q, *J* = 310.2 Hz), 126.9, 46.2 (q, *J* = 2.7 Hz), 30.6. **^{19}F NMR** (282 MHz, $CDCl_3$) δ (ppm) -40.9. **HRMS** (EI+) Calc. for $C_{10}H_9F_3OS^{\bullet+}$ [$M^{\bullet+}$]: 234.0321. Found: 234.0315.

S-(trifluoromethyl) 3-(4-methoxyphenyl)propanethioate (2ah)

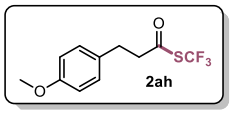

Following procedure C, **2ah** was obtained from 3-(4-methoxyphenyl)propanal (95.0 µL, 98.5 mg, 0.6 mmol, 1.5 equiv) and Phth-SCF_3 (98.9 mg, 0.40 mmol, 1.0 equiv) as a colorless oil (65.0 mg, 0.25 mmol, 62%) after purification by automated column chromatography (*Biotage® SNAP Ultra* 10 g column, pentane). As the product might quite volatile, evaporation of the solvent at room temperature is recommended. **^{1}H NMR** (400 MHz, $CDCl_3$) δ (ppm) 7.10 (d, *J* = 8.6 Hz, 2H), 6.85 (d, *J* = 8.6 Hz, 2H), 3.79 (s, 3H), 2.99 – 2.87 (m, 4H). **^{13}C NMR** (101 MHz, $CDCl_3$) δ (ppm) 189.7, 158.6, 130.9, 129.4, 127.7 (q, *J* = 310.0 Hz), 114.3, 55.4, 46.5 (q, *J* = 2.7 Hz), 29.8. **^{19}F NMR** (376 MHz, $CDCl_3$) δ (ppm) -40.7. **HRMS** (EI+) Calc. for $C_{11}H_{11}F_3O_2S^{\bullet+}$ [$M^{\bullet+}$]: 264.0426. Found: 264.0423. **FTIR** (ν / cm^{-1}): 3004, 2937, 2840, 1736, 1613, 1513, 1464, 1244, 1148, 1103, 1028, 954.

S-(trifluoromethyl) 4-(1,3-dioxoisoindolin-2-yl)butanethioate (2ai)

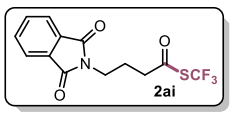

Following procedure C, **2ai** was obtained from 4-(1,3-dioxoisoindolin-2-yl)butanal (130 mg, 0.6 mmol, 1.5 equiv) and Phth-SCF_3 (98.9 mg, 0.40 mmol, 1.0 equiv) as a colorless solid (121 mg, 0.378 mmol, 95%) after purification by chromatography (10 g SiO_2, PE/DCM = 80/20 → 0/100). **^{1}H NMR** (300 MHz, $CDCl_3$) δ (ppm) 7.87 – 7.79 (m, 2H), 7.75 – 7.68 (m, 2H), 3.74 (t, *J* = 6.6 Hz, 2H), 2.71 (t, *J* = 7.3 Hz, 2H), 2.14 – 2.00 (m, 2H). **^{13}C NMR** (75 MHz, $CDCl_3$) δ (ppm) 189.5, 168.4, 134.3, 132.0, 127.6 (q, *J* = 310.1 Hz), 123.5, 42.0 (q, *J* = 2.8 Hz), 36.7, 23.6. **^{19}F NMR** (282 MHz, $CDCl_3$) δ (ppm) -40.66. **HRMS** (APCI) Calc. for $C_{13}H_{11}F_3NO_3S^+$ [$M+H^+$]: 318.0406. Found: 318.0410. **FTIR** (ν / cm^{-1}): 2940, 2911, 1781, 1699, 1442, 1397, 1341, 1110, 1058, 950, 883, 715. **MP**.: 64.3–66.7 °C.

S-(trifluoromethyl) 7-hydroxy-3,7-dimethyloctanethioate (2aj)

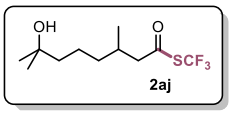

Following procedure C, **2aj** was obtained from 7-hydroxy-3,7-dimethyloctanal (103 mg, 0.6 mmol, 1.5 equiv) and Phth-SCF_3 (98.9 mg, 0.40 mmol, 1.0 equiv) as a colorless oil (88.8 mg, 0.33 mmol, 82%) after column chromatography (*Biotage® SNAP Ultra* 10g, PE/DCM = 80/20 → 0/100). **^{1}H NMR** (400 MHz, $CDCl_3$) δ (ppm) 2.61 (dd, *J* = 15.2, 6.0 Hz, 1H), 2.43 (dd, *J* = 15.2, 7.9 Hz, 1H), 2.15 – 1.94 (m, 2H), 1.51 – 1.23 (m, 4H), 1.21 (s, 6H), 1.00 (d, *J* = 6.7 Hz, 3H). **^{13}C NMR** (75 MHz, $CDCl_3$) δ (ppm) 190.0, 127.8 (q, *J* = 309.9 Hz), 71.0, 51.8 (d, *J* = 2.6 Hz), 43.8, 36.9, 30.9, 29.4 (d, *J* = 6.9 Hz), 21.6, 19.5. **^{19}F NMR** (376 MHz, $CDCl_3$) δ (ppm) δ -40.8. **HRMS** (EI+) Calc. for $C_{11}H_{23}F_3NO_2S^+$ [M+NH_4^+]: 290.1396. Found: 290.1398. **IR** (neat): 3377, 2937, 2967, 1744, 1710, 1461, 1379, 1151, 1110, 987, 931, 760 cm^{-1}.

S-(trifluoromethyl) 3,7-dimethyloct-6-enethioate (2ak)

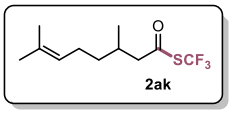

Following procedure C, **2ak** was obtained from 3,7-dimethyloct-6-enal (92.5 mg, 0.6 mmol, 1.5 equiv) and Phth-SCF_3 (98.9 mg, 0.40 mmol, 1.0 equiv) as a colorless oil (72.1 mg, 0.28 mmol, 71%) after purification by automated column chromatography (*Biotage® SNAP Ultra* 10 g column, pentane). As the product is quite volatile, evaporation of the solvent at room temperature is recommended. **^{1}H NMR** (400 MHz, $CDCl_3$) δ (ppm) 5.07 (tt, *J* = 7.1, 1.4 Hz, 1H), 2.62 (dd, *J* = 15.2, 5.8 Hz, 1H), 2.41 (dd, *J* = 15.2, 8.1 Hz, 1H), 2.09 – 1.94 (m, 3H), 1.69 (q, *J* = 1.3 Hz, 3H), 1.60 (s, 3H), 1.43 – 1.33 (m, 1H), 1.31 – 1.21 (m, 1H), 0.99 (d, *J* = 6.7 Hz, 3H). **^{13}C NMR** (101 MHz, $CDCl_3$) δ (ppm) 190.0, 132.3, 127.9 (q, *J* = 309.8 Hz), 123.8, 51.8 (q, *J* = 2.7 Hz), 36.5, 30.5, 25.8, 25.4, 19.5, 17.8. **^{19}F NMR** (376 MHz, $CDCl_3$) δ (ppm) -40.8. **HRMS** (EI+) Calc. for $C_{10}H_{17}O^+$ [M-SCF_3]$^+$ 153.1274. Found: 153.1272. **FTIR** (ν / cm^{-1}): 2926, 2855, 1710, 1461, 1379, 1159, 1114, 984.

SCF_3-Sclareoide (2al)

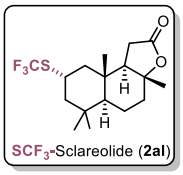

Following procedure A, **2al** was obtained from Sclareoide (501 mg, 2.0 mmol, 5 equiv) and Phth-SCF_3 (98.9 mg, 0.40 mmol, 1.0 equiv) as a colorless amorphous solid (76.9 mg, 0.22 mmol, 55%) after purification by automated column chromatography (*Biotage® SNAP Ultra* 25 g column, PE/EtOAc = 95/5 → 80/20). **^{1}H NMR** (400 MHz, $CDCl_3$) δ (ppm) 3.52 (tt, *J* = 12.8, 3.8 Hz, 1H), 2.50 – 2.37 (m, 1H), 2.26 (dd, *J* = 16.2, 6.5 Hz, 1H), 2.10 (dt, *J* = 12.0, 3.3 Hz, 1H), 1.99 (dd, *J* = 14.7, 6.5 Hz, 1H), 1.94 – 1.83 (m, 3H), 1.70 (td, *J* = 12.5, 4.1 Hz, 1H), 1.41 – 1.30 (m, 5H), 1.23 (d, *J* = 13.0 Hz, 1H), 1.10 (dd, *J* = 12.6, 2.4 Hz, 1H), 0.97 (d, *J* = 10.4 Hz, 6H), 0.92 (s, 3H). **^{13}C NMR** (101 MHz, $CDCl_3$) δ (ppm) 176.1, 131.1 (q, *J* = 306.6 Hz), 85.9, 58.7, 55.9, 49.2, 46.8, 38.6, 37.6, 37.3, 37.2, 35.1, 33.0, 28.7, 21.8, 21.3, 20.4, 15.7. **^{19}F NMR**

(377 MHz, $CDCl_3$) δ (ppm) -39.3. **HRMS** (APCI) Calc. for $C_{17}H_{29}F_3NO_2S^+$ $[M+NH_4]^+$: 368.1866. Found: 368.1869. The data match reported literature values.[18b]

SCF_3-Ambroxide (2am)

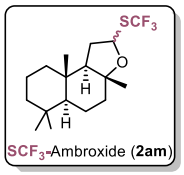

Following procedure B, **2am** was obtained from (-)-Ambroxide (236 mg, 1.0 mmol, 2.5 equiv) and Phth-SCF_3 (98.9 mg, 0.40 mmol, 1.0 equiv) as a colorless amorphous solid (90.6 mg, 0.27 mmol, 67%, d.r.: 60/40) after purification by automated column chromatography (*Biotage® SNAP Ultra* 25 g column, P/Et_2O = 98/2 → 97/3). **Mixture diastereomers: ^{1}H NMR** (400 MHz, $CDCl_3$) δ (ppm) 5.73 – 5.66 (m, 1H), 2.41 – 2.25 (m, 1H), 2.00 (ddt, *J* = 11.3, 7.8, 3.1 Hz, 1H), 1.90 – 1.74 (m, 2H), 1.70 – 1.60 (m, 1H), 1.58 – 1.28 (m, 6H), 1.25 – 1.12 (m, 4H), 1.10 – 1.02 (m, 1H), 1.01 – 0.93 (m, 1H), 0.89 – 0.81 (m, 9H). **^{13}C NMR** (101 MHz, $CDCl_3$) δ (ppm) 130.58 (q, *J* = 307.1 Hz), 130.52 (q, *J* = 307.1 Hz), 85.1, 84.1, 81.5 (q, *J* = 2.1 Hz), 80.9 (q, *J* = 2.0 Hz), 60.3, 58.5, 57.2, 57.1, 42.4, 40.1, 40.0, 40.0, 39.9, 36.4, 36.3, 33.6, 33.2, 31.7, 31.1, 22.7, 22.4, 21.19, 21.17, 20.9, 20.5, 18.4, 15.5, 15.3. **^{19}F NMR** (376 MHz, $CDCl_3$) δ (ppm) -39.6 (*minor diastereomer*), -40.4 (*major diastereomer*). **HRMS** (APCI) Calc. for $C_{17}H_{31}F_3NOS^+$ $[M+NH_4]^+$: 354.2073. Found: 354.2075. The data matches the literature reported data.[15b]

4-(((trifluoromethyl)thio)carbonyl)phenyl (*R*)-4-((5*S*,8*R*,9*S*,10*S*,13*R*,14*S*,17*R*)-10,13-dimethyl-3,7,12-trioxohexadecahydro-1*H*-cyclopenta[a]phenanthren-17-yl)pentanoate (2an)

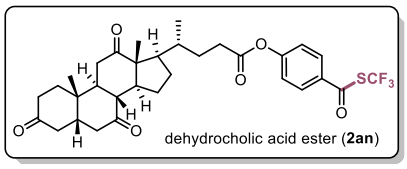

Following procedure C, **2an** was obtained from 4-formylphenyl (*R*)-4-((5*S*,8*R*,9*S*,10*S*,13*R*,14*S*,17*R*)-10,13 - dimethyl - 3,7,12 -trioxohexadecahydro-1*H*-cyclopenta[a]phenanthren-17-yl)pentanoate (**1an**, 304 mg, 0.6 mmol, 1.5 equiv) and Phth-SCF_3 (98.9 mg, 0.40 mmol, 1.0 equiv) as a colorless solid (109 mg, 0.18 mmol, 45%) after purification by automated column chromatography (*Biotage® SNAP Ultra* 25 g column, PE/EtOAc = 80/20 → 0/100); mp 207.2-212.3 °C. **^{1}H NMR** (400 MHz, $CDCl_3$) δ (ppm) 7.89 (d, *J* = 8.7 Hz, 2H), 7.25 (d, *J* = 8.8 Hz, 2H), 2.95 – 2.81 (m, 3H), 2.68 (ddd, *J* = 16.2, 9.3, 5.3 Hz, 1H), 2.55 (ddd, *J* = 16.1, 9.0, 7.1 Hz, 1H), 2.40 – 1.79 (m, 15H), 1.69 – 1.47 (m, 3H), 1.40 (s, 3H), 1.30 – 1.24 (m, 1H), 1.09 (s, 3H), 0.92 (d, *J* = 6.7 Hz, 3H). **^{13}C NMR** (101 MHz, $CDCl_3$) δ (ppm) 212.0, 209.1, 208.8, 182.2, 171.8, 156.07, 132.5 (q, *J* = 3.1 Hz), 129.4, 128.0 (q, *J* = 309.6 Hz), 122.6, 57.0, 51.9, 49.1, 46.9, 45.7, 45.1, 42.9, 38.8, 36.6, 36.1, 35.6, 35.4, 31.6, 30.3, 27.8, 25.2, 22.0, 18.8, 12.0. **^{19}F NMR** (376 MHz, $CDCl_3$) δ (ppm) -40.0. **HRMS** (ESI+) Calc. for $C_{32}H_{37}F_3NaO_6S^+$ $[M+Na^+]$: 629.2155. Found: 629.2153. **FTIR** (ν / cm^{-1}): 2959, 1770, 1699, 1599, 1502, 1427, 1215, 1159, 1099, 887.

SCF_3-Amobarbital (3l)

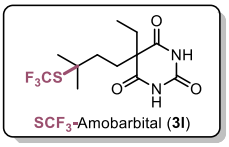

Adapting literature procedure for the synthesis of barbiturates,[30] a suspension of urea (60.1 mg, 1.00 mmol, 10.0 equiv) in dry DMF (2 mL) was treated with sodium hydride (60% dispersion in mineral oil, 24.0 mg, 0.60 mmol, 6.0 equiv) at 0 °C and stirred for 1 hour. A solution of **2l** (0.1 mmol) in dry DMF (1 mL) was added, the mixture was stirred overnight, and the reaction was quenched by the addition of saturated aqueous ammonium chloride solution (5 mL). The product was extracted into ether (3 × 10 mL), which was dried over anhydrous Na_2SO_4 and subsequently evaporated under reduced pressure. The title compound was purified by automated column chromatography (*Biotage® SNAP Ultra* 10 g column, PE/EtOAc = 60/40 → 0/100) to yield a colorless solid (13.6 mg, 41.7 µmol, 42%). **^{1}H NMR** (400 MHz, $CDCl_3$) δ (ppm) 8.52 (s, 2H), 2.20 – 2.11 (m, 2H), 2.07 (q, *J* = 7.5 Hz, 2H), 1.60 – 1.52 (m, 2H), 1.42 (d, *J* = 1.0 Hz, 6H), 0.92 (t, *J* = 7.5 Hz, 3H). **^{13}C NMR** (101 MHz, $CDCl_3$) δ (ppm) 171.8, 148.4, 130.7 (d, *J* = 308.1 Hz), 56.7, 50.8, 37.9, 33.1, 32.8, 29.1, 9.3. **^{19}F NMR** (376 MHz, $CDCl_3$) δ (ppm) -36.2. **HRMS** (ESI+) Calc. for $C_{12}H_{17}F_3N_2NaO_3S^+$ $[M+Na]^+$: 349.0810. Found: 349.0804. **FTIR** (ν / cm^{-1}): 3220, 3108, 2926, 2855, 1699, 1423, 1353, 1304, 1095, 756. **MP**.: 132.6–138.7°C

8-(4-bromobutyl)-2-((trifluoromethyl)thio)-8-azaspiro[4.5]decane-7,9-dione (3f)

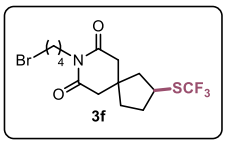

Adapting literature procedure,[31] a crimp capped vial (20 mL) equipped with **2f** (20 mg, 0.075 mmol, 1.0 equiv), DMAP (2 mol% 0.2 mg), and K_2CO_3 (31.1 mg, 0.23 mmol, 3.0 equiv) was set under a nitrogen atmosphere. 1.4-dibromobutane (11.2 µL, 0.094 mmol, 1.25 equiv) was added via a syringe, followed by MeCN (0.5- 1 mL, anhydrous) and the reaction mixture was heated overnight at 95 °C. The next day, the reaction was filtered, concentrated and purified by column chromatography (Pe/EtOAc = 75/25 → 60/40) to yield **3f** as clear oil (27.8 mg, 0.069 mmol, 92%). **^{1}H NMR** (400 MHz, $CDCl_3$) δ (ppm) 3.78 (t, *J* = 7.2 Hz, 2H), 3.66 (p, *J* = 7.8 Hz, 1H), 3.40 (t, *J* = 6.7 Hz, 2H), 2.68 (s, 2H), 2.62 (s, 2H), 2.34 – 2.24 (m, 1H), 2.11 (dd, *J* = 13.8, 7.8 Hz, 1H), 1.89 – 1.72 (m, 4H), 1.71 – 1.57 (m, 4H). **^{13}C NMR** (101 MHz, $CDCl_3$) δ (ppm) 171.2, 130.6 (q, *J* = 306.7 Hz). 45.5, 45.4, 44.9, 41.2 (q, *J* = 1.8 Hz) 39.5, 38.8, 36.6, 33.1, 32.9, 30.2, 26.8. **^{19}F NMR** (377 MHz, $CDCl_3$) δ (ppm) -41.0. **HRMS** (ESI+) Calc. for $C_{14}H_{20}{}^{79}BrF_3NO_2S^+$ $[M^+H]^+$: 402.0345. Found: 402.0347. **FTIR** (ν / cm^{-1}): 2955, 2866, 1729, 1669, 1435, 1390, 1353, 1267, 1233, 1110, 756.

SCF_3-Buspirone (4f)

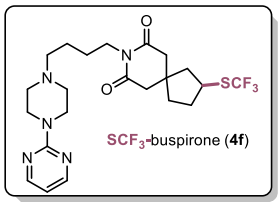

Adapting literature procedure,[31] a crimp capped vial (20 mL) equipped with **3f** (27.6 mg, 68.6 µmol), KI (0.6 mg, 5 mol%), 1-(2-pyrimidyl)piperazine (11.3 mg, 9.8 µL, 0.069 mmol, 1.0 equiv) and K_2CO_3 (28.6 mg, 0.21 mmol, 3.0 equiv) was set under a nitrogen atmosphere and MeCN (1 mL, anhydrous) was added via a syringe. The reaction mixture was heated overnight at 95 °C. The next day, the reaction was filtered while hot, concentrated and purified by column chromatography (5% MeOH in DCM) to yield Buspirone-SCF_3 as white amorphous solid (29.4 mg, 61 µmol, 89%). The ^{1}H NMR spectrum shows an impurity (at 8.20 ppm, ~ 6%), which was identified by HRMS as the *p*-chloro derivative, probably originating in the use of chlorinated solvents. **^{1}H NMR** (400 MHz, $CDCl_3$) δ (ppm) 8.29 (d, *J* = 4.7 Hz, 2H), 6.49 (t, *J* = 4.7 Hz, 1H), 3.92 (s, 4H), 3.78 (t, *J* = 7.0 Hz, 2H), 3.65 (p, *J* = 7.8 Hz, 1H), 2.69 (s, 3H), 2.62 (s, 5H), 2.51 (s, 2H), 2.34 – 2.22 (m, 1H), 2.10 (dd, *J* = 13.8, 7.8 Hz, 1H), 1.87 – 1.71 (m, 2H), 1.66 – 1.49 (m, 6H). **^{13}C NMR** (101 MHz, $CDCl_3$) δ (ppm) 171.3, 161.6, 157.9, 130.6 (q, *J* = 306.8 Hz), 110.3, 58.1, 52.9, 45.4, 45.4, 44.9, 43.0, 41.2 (q, *J* = 1.7 Hz), 39.5, 39.3, 36.6, 32.9, 25.9, 23.5. **^{19}F NMR** (376 MHz, $CDCl_3$) δ (ppm) -41.0. **HRMS** (ESI+) Calc. for $C_{22}H_{31}F_3N_5O_2S^+$ [M+H$^+$]: 486.2145. Found: 486.2146. **HRMS** (ESI+) Calc. for $C_{22}H_{30}ClF_3N_5O_2S^+$ [M_{Cl}+H$^+$] 520.17555. Found: 520.1756. **FTIR** (ν / cm^{-1}): 2922, 2851, 2363, 1722, 1669, 1625, 1587, 1554, 1438, 1349, 1267, 1207, 1103, 969, 793, 760.

3.5 References

[1] (a) Trost, B. M., *Angew. Chem. Int. Ed.* **1995**, *34*, 259-281; (b) Newhouse, T.; Baran, P. S.; Hoffmann, R. W., *Chem. Soc. Rev.* **2009**, *38*, 3010-3021.

[2] (a) Capaldo, L.; Ravelli, D., *Eur. J. Org. Chem.* **2017**, *2017*, 2056-2071; (b) Capaldo, L.; Quadri, L. L.; Ravelli, D., *Green Chem.* **2020**, *22*, 3376-3396.

[3] Xue, X. S.; Ji, P.; Zhou, B.; Cheng, J. P., *Chem. Rev.* **2017**, *117*, 8622-8648.

[4] (a) Tzirakis, M. D.; Lykakis, I. N.; Orfanopoulos, M., *Chem. Soc. Rev.* **2009**, *38*, 2609-2621; (b) Ravelli, D.; Protti, S.; Fagnoni, M., *Acc. Chem. Res.* **2016**, *49*, 2232-2242; (c) Crespi, S.; Fagnoni, M., *Chem. Rev.* **2020**, *120*, 9790-9833.

[5] Ravelli, D.; Fagnoni, M.; Fukuyama, T.; Nishikawa, T.; Ryu, I., *ACS Catal.* **2017**, *8*, 701-713.

[6] (a) Perry, I. B.; Brewer, T. F.; Sarver, P. J.; Schultz, D. M.; DiRocco, D. A.; MacMillan, D. W. C., *Nature* **2018**, *560*, 70-75; (b) Laudadio, G.; Deng, Y.; van der Wal, K.; Ravelli, D.; Nuno, M.; Fagnoni, M.; Guthrie, D.; Sun, Y.; Noel, T., *Science* **2020**, *369*, 92-96; (c) Cao, H.; Kuang, Y.; Shi, X.; Wong, K. L.; Tan, B. B.; Kwan, J. M. C.; Liu, X.; Wu, J., *Nat. Commun.* **2020**, *11*, 1956; (d) Sarver, P. J.; Bacauanu, V.; Schultz, D. M.; DiRocco, D. A.; Lam, Y. H.; Sherer, E. C.; MacMillan, D. W. C., *Nat. Chem.* **2020**, *12*, 459-467.

[7] (a) Kuang, Y.; Cao, H.; Tang, H.; Chew, J.; Chen, W.; Shi, X.; Wu, J., *Chem. Sci.* **2020**, *11*, 8912-8918; (b) Dong, J.; Wang, X.; Wang, Z.; Song, H.; Liu, Y.; Wang, Q., *Chem. Sci.* **2020**, *11*, 1026-1031.

[8] (a) Halperin, S. D.; Fan, H.; Chang, S.; Martin, R. E.; Britton, R., *Angew. Chem. Int. Ed.* **2014**, *53*, 4690-4693; (b) Meanwell, M.; Lehmann, J.; Eichenberger, M.; Martin, R. E.; Britton, R., *Chem. Commun.* **2018**, *54*, 9985-9988.

[9] See reference 20c.

[10] Toulgoat, F.; Alazet, S.; Billard, T., *Eur. J. Org. Chem.* **2014**, *2014*, 2415-2428.

[11] (a) Leroux, F.; Jeschke, P.; Schlosser, M., *Chem. Rev.* **2005**, *105*, 827-856; (b) Landelle, G.; Panossian, A.; Leroux, F. R., *Curr. Top. Med. Chem.* **2014**, *14*, 941-951; (c) Boiko, V. N., *Beilstein J. Org. Chem.* **2010**, *6*, 880-921.

[12] Chachignon, H.; Cahard, D., *Chin. J. Chem.* **2016**, *34*, 445-454.

[13] (a) Liang, T.; Neumann, C. N.; Ritter, T., *Angew. Chem. Int. Ed.* **2013**, *52*, 8214-8264; (b) Tlili, A.; Billard, T., *Angew. Chem. Int. Ed.* **2013**, *52*, 6818-6819; (c) Yang, X.; Wu, T.; Phipps, R. J.; Toste,

F. D., *Chem. Rev.* **2015**, *115*, 826-870; (d) Barata-Vallejo, S.; Bonesi, S.; Postigo, A., *Org. Biomol. Chem.* **2016**, *14*, 7150-7182; (e) Xu, X. H.; Matsuzaki, K.; Shibata, N., *Chem. Rev.* **2015**, *115*, 731-764.

[14] (a) Ghiazza, C.; Billard, T.; Tlili, A., *Chem. Eur. J.* **2019**, *25*, 6482-6495; (b) Yerien, D. E.; Barata-Vallejo, S.; Postigo, A., *J. Fluor. Chem.* **2020**, *240*, 109652; (c) Nobile, E.; Castanheiro, T.; Besset, T., *Angew. Chem. Int. Ed.* **2021**, *60*, 12170-12191; (d) Zhang, F. G.; Wang, X. Q.; Zhou, Y.; Shi, H. S.; Feng, Z.; Ma, J. A.; Marek, I., *Chem. Eur. J.* **2020**, *26*, 15378-15396.

[15] (a) Mukherjee, S.; Patra, T.; Glorius, F., *ACS Catal.* **2018**, *8*, 5842-5846; (b) Mukherjee, S.; Maji, B.; Tlahuext-Aca, A.; Glorius, F., *J. Am. Chem. Soc.* **2016**, *138*, 16200-16203.

[16] Xu, W.; Ma, J.; Yuan, X. A.; Dai, J.; Xie, J.; Zhu, C.,*Angew Chem Int Ed Engl* **2018**, *57*, 10357-10361.

[17] Xu, W.; Wang, W.; Liu, T.; Xie, J.; Zhu, C., *Nat Commun* **2019**, *10*, 4867.

[18] (a) Wang, D.; Carlton, C. G.; Tayu, M.; McDouall, J. J. W.; Perry, G. J. P.; Procter, D. J., *Angew. Chem. Int. Ed.* **2020**, *59*, 15918-15922; (b) Guo, S.; Zhang, X.; Tang, P., *Angew. Chem. Int. Ed.* **2015**, *54*, 4065-4069; (c) Wu, H.; Xiao, Z.; Wu, J.; Guo, Y.; Xiao, J. C.; Liu, C.; Chen, Q. Y., *Angew. Chem. Int. Ed.* **2015**, *54*, 4070-4074; (d) Zhao, Y.; Lin, J. H.; Hang, X. C.; Xiao, J. C., *J. Org. Chem.* **2018**, *83*, 14120-14125; (e) Xia, Y.; Wang, L.; Studer, A., *Angew. Chem. Int. Ed.* **2018**, *57*, 12940-12944; (f) Modak, A.; Pinter, E. N.; Cook, S. P., *J. Am. Chem. Soc.* **2019**, *141*, 18405-18410.

[19] Munavalli, S.; Rohrbaugh, D. K.; Rossman, D. I.; Berg, F. J.; Wagner, G. W.; Durst, H. D., *Synth. Commun.* **2000**, *30*, 2847-2854.

[20] (a) Wang, M. Y.; Zhu, X. Q.; Zhang, X. L.; Guo, R. L.; Jia, Q.; Wang, Y. Q., *Org. Biomol. Chem.* **2020**, *18*, 5918-5926; (b) Dong, J.; Yue, F.; Wang, X.; Song, H.; Liu, Y.; Wang, Q., *Org. Lett.* **2020**, *22*, 8272-8277; (c) During the first submission of our manuscript, a DT-based protocol for the synthesis of trifluoromethylthioesters from aromatic aldehydes was published: 8 mol% TBADT (instead of 2.5 mol%), 3 equiv. of $PhthSCF_3$ (instead of 1.5 equiv ArCHO (inverse stoichiometry)) and 1.5 equiv Na_2HPO_4 (instead of base-free) are required to achieve comparable yields (e.g. **2v** (78% instead of 84%), **2ae** (55% instead of 53%)) after 96h (instead of 6h). Neither aliphatic aldehydes nor alkanes are functionalized in this report: Wang, X.; Dong, J.; Liu, Y.; Song, H.; Wang, Q., *Chin. Chem. Lett.* **2021**.

[21] Topcu, G.; Ulubelen, A.; Tam, T. C.-M.; Che, C.-T., *J. Nat. Prod.* **1996**, *59*, 113-116.

[22] Fahlbusch, K.-G.; Hammerschmidt, F.-J.; Panten, J.; Pickenhagen, W.; Schatkowski, D.; Bauer, K.; Garbe, D.; Surburg, H., *Ullmann's Encyclopedia of Industrial Chemistry*, Wiley-VCH, Weinheim, Germany, **2000**.

[23] Pearson, C. M.; Parks, A.; Landazuri, P., in *Neurosurgical Neuropsychology* (Eds.: C. M. Pearson, E. Ecklund-Johnson, S. D. Gale), Academic Press, San Diego, **2019**, pp. 99-112.

[24] (a) Fulmer, G. R.; Miller, A. J. M.; Sherden, N. H.; Gottlieb, H. E.; Nudelman, A.; Stoltz, B. M.; Bercaw, J. E.; Goldberg, K. I., *Organometallics* **2010**, *29*, 2176-2179; (b) Gottlieb, H. E.; Kotlyar, V.; Nudelman, A., *J. Org. Chem.* **1997**, *62*, 7512-7515.

[25] Nasri, S.; Zahou, I.; Turowska-Tyrk, I.; Roisnel, T.; Loiseau, F.; Saint-Amant, E.; Nasri, H., *Eur. J. Inorg. Chem.* **2016**, *2016*, 5004-5019.

[26] Andersen, T. L.; Donslund, A. S.; Neumann, K. T.; Skrydstrup, T., *Angew. Chem. Int. Ed.* **2018**, *57*, 800-804.

[27] Pansuwan, H.; Ditmangklo, B.; Vilaivan, C.; Jiangchareon, B.; Pan-In, P.; Wanichwecharungruang, S.; Palaga, T.; Nuanyai, T.; Suparpprom, C.; Vilaivan, T., *Bioconjug. Chem.* **2017**, *28*, 2284-2292.

[28] Schwarz, J. L.; Huang, H.-M.; Paulisch, T. O.; Glorius, F., *ACS Catal.* **2019**, *10*, 1621-1627.

[29] Kurimoto, Y.; Nasu, T.; Fujii, Y.; Asano, K.; Matsubara, S., *Org. Lett.* **2019**, *21*, 2156-2160.

[30] Calamai, E.; Dall'Angelo, S.; Koss, D.; Domarkas, J.; McCarthy, T. J.; Mingarelli, M.; Riedel, G.; Schweiger, L. F.; Welch, A.; Platt, B.; Zanda, M., *Chem. Commun.* **2013**, *49*, 792-794.

[31] Bonacorsi, S. J.; Burrell, R. C.; Luke, G. M.; DePue, J. S.; Kent Rinehart, J.; Balasubramanian, B.; Christopher, L. J.; Iyer, R. A. S., *J. Label. Compd. Rad.* **2007**, *50*, 65-71.

[32] (a) Sheldrick, G. M., *Acta Cryst. C* **2015**, *71*, 3-8; (b) Sheldrick, G. M., *Acta Cryst. A* **2015**, *71*, 3-8.

[33] Dolomanov, O. V.; Bourhis, L. J.; Gildea, R. J.; Howard, J. A. K.; Puschmann, H., *J. Appl. Cryst.* **2009**, *42*, 339-341.

CHAPTER IV

Mesoporous Graphitic Carbon Nitride as Heterogeneous Photocatalyst in the Dual Catalytic Arylation of Alkyl Silicates

Author Contributions:

Tobias Schirmer developed the project, optimized the reaction conditions, isolated the aryl bromide scope (**3a**-**3j**), the silicate scope (**3p**-**3y**), and compiled the draft below. Mehdi Abdellaoui (Sorbonne University, Paris) isolated the alkenyl bromide scope (**3k**-**3o**). The mpg-CN photocatalyst was provided by our cooperation partners Dr. Aleksandr Savateev and Prof. Dr. Markus Antonietti from the Max Planck Institute of Colloids and Interface, Potsdam. Dr. Cyril Ollivier (Sorbonne University, Paris), Prof. Dr. Louis Fensterbank (Sorbonne University, Paris), and Prof. Dr. Burkhard König supervised the project. The project was carried out in the laboratories of Prof. Fensterbank at *Sorbonne Université - Campus Pierre et Marie Curie,* Paris.

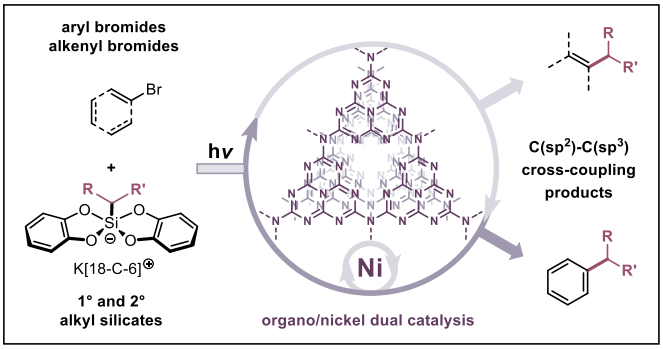

ABSTRACT

Mesoporous Graphitic Carbon Nitride is introduced as a heterogeneous photocatalyst for the single electron transmetalation of alkyl silicates. The synergy between this recyclable photocatalyst and a broadly applied homogenous nickel diimine complex gives access to $C(sp^2)$–$C(sp^3)$ cross-coupling products of aryl and alkenyl bromides in a sustainable fashion.

4.1 Introduction

Since MacMillan's[1] and Molander's[2] seminal reports, photoredox/nickel dual catalysis has attracted broad interest in the scientific community, in turn leading to the development of a multitude of new single-electron transmetalation based transformations.[3] The number of compatible radical precursors increased rapidly, followed by the discovery of alternative photocatalysts that can promote such a transformation, thereby broadening the scope of possible modes of substrate activation.[4] This development went hand in hand with the quest for more sustainable alternatives to the common iridium- and ruthenium-based catalysts.[5]

In this context, mesoporous graphitic carbon nitride (mpg-CN) and derivatives thereof[6] emerged as a viable alternative to metal-based photocatalysts, not only in photoredox chemistry itself,[7] but also in photoredox/nickel dual catalytic applications. Initially, mpg-CN/nickel dual catalysis was employed to couple aryl halides with N-,[8] O-,[9] and S-nucleophiles[9d] in a more sustainable manner (Scheme 1). More recently, our group demonstrated that mpg-CN could also be employed to initiate α-arylation of amides by C(sp^3)-H activation.[10] Further, single-electron transmetalation of organotrifluoroborates is achievable through mpg-CN and nickel catalysis. However, the latter methodology remains limited to benzylic and allylic radicals.[11]

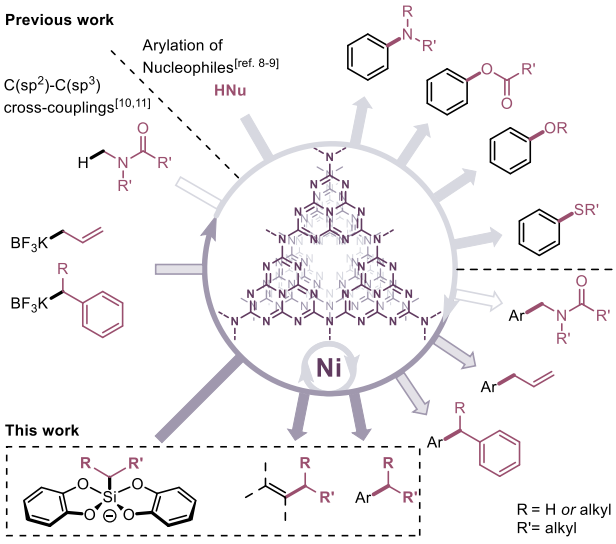

Scheme 1: mpg-CN/nickel dual catalytic transformations.

To broaden the scope of mpg-CN-nickel catalyzed C(sp^2)–C(sp^3) cross-couplings, we envisioned the use of alkyl silicates as radical precursors. Since their introduction as radical sources,[12] silicates have proven to be reliable reagents in cross-coupling applications.[13] Both their low oxidation

potential (< 0.9 V vs. SCE for alkyl silicates)[12a] and their accessibility from commercial starting materials grant access to a variety of primary, secondary and tertiary radicals.

The combination with mpg-CN, its low price, its robustness, and facile recycling would offer a valuable extension to the current C(sp^2)–C(sp^3) cross-coupling toolbox. Such a transformation would start with the photoexcitation of the semiconductor material, generating an electron-hole pair (e^- and) on its surface (Scheme 2) with an oxidation potential of (+1.2 V vs. SCE) and a reduction potential of (–1.5 V vs. SCE).[8a] The first potential is sufficient to oxidize alkyl silicates and thereby induce the fragmentation to the alkyl radicals, while the latter potential can easily reduce the nickel(II) precatalyst and the nickel(I) intermediate to its active nickel(0) oxidation state, which would readily undergo oxidative addition with aryl bromides to furnish a nickel(II) complex. It serves as a radical trap for the previously generated alkyl radical. Reductive elimination to the C(sp^2)–C(sp^3) cross-coupling product and subsequent single-electron-reduction of the resulting nickel(I) complex by mpg-CN are closing the cycle.

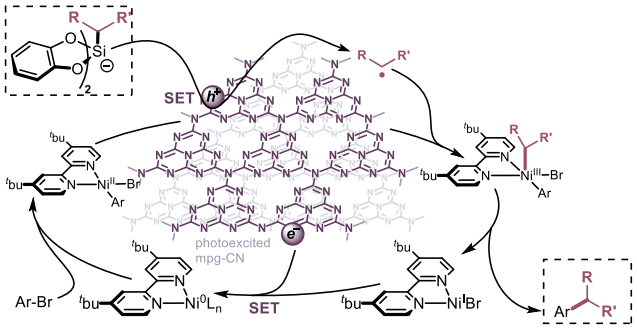

Scheme 2: Mechanistic hypothesis.

4.2 Results and Discussion

We began our investigation with 4-bromobenzotrifluoride (**1**) and potassium [18-C-6] acetoxypropyl silicate (**2**) as model substrates. The initial conditions were chosen according to our previous works, which repeatedly found a substrate concentration of 0.2 M and an mpg-CN loading of 10 mg/ml to be optimal,[10-11] whereas DMF is the preferred solvent for most mpg-CN catalyzed reactions as well as for photo-nickel catalyzed cross-couplings of silicates. The optimization began with a screening of different bipyridyl ligands (Table 1, entry 1–4) on the nickel(II)-bromide precatalyst. With unsubstituted bipyridyl (bpy), a yield of 58% was achieved (entry 1), which could be improved to 63% by using 4,4' dimethyl bipyridyl as a ligand (entry 2). The yield decreased to 44% when the position of the methyl groups was changed to 5,5'-position of the ligand (entry 3). However, upon using 4,4′-di-*tert*-butyl-2,2′-dipyridyl (dtbbpy) as ligand, the product was obtained in

70% NMR-yield (entry 4). The increase of either the photocatalyst or the nickel salt loading slightly improved the yield to 71% and 72%, respectively (entries 5 and 6). Finally, increasing the equivalents of alkyl silicate furnished the desired product **3a** in 71% isolated yield (entry 7). Most economical conditions with slightly decreased yield are found in entry 4. Control reactions confirmed the essential role of both catalysts and light (entry 8–10).

Table 1: Optimization and control reactions. Reactions were run in anhydrous DMF (0.2 M) under irradiation with blue LEDs (451 nm) and under an Ar-atmosphere for 24 h at 25 °C. [a]Yield was determined by 19F-crude NMR analysis with 4-fluoroanisole as internal standard. [b]Isolated yield. [c]nd = not detected. [d]no light.

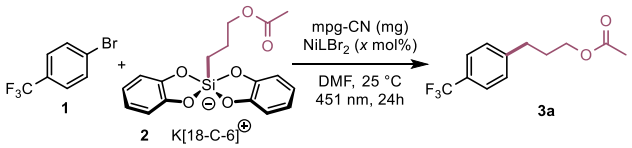

entry	L	x	mpg-CN (mg)	silicate (equiv)	yield[a] (%)
1	bpy	5.0%	10	1.5	58
2	4,4' -Me_2bpy	5.0%	10	1.5	63
3	5,5' -Me_2bpy	5.0%	10	1.5	44
4	**dtbbpy**	**5.0%**	**10**	**1.5**	**70**
5	dtbbpy	10%	10	1.5	71
6	dtbbpy	5.0%	20	1.5	72
7	**dtbbpy**	**5.0%**	**20**	**2.0**	**76, (71)[b]**
8			20	2.0	nd[c]
9	dtbbpy	5.0%		2.0	nd[c]
10[d]	dtbbpy	5.0%	20	2.0	nd[c]

With the optimized conditions in hand, we explored the scope of our methodology. Differently substituted aryl bromide acceptors were readily alkylated in between 69% and 95% yield (**3a**-**3d**), demonstrating that esters, ketones, and nitriles are well tolerated under these conditions. Bromobenzene as an electron neutral example was coupled in 75% yield (**3g**). Upon increasing the aromatic system from benzene to naphthalene, the yield slightly decreased to 70% (**3f**). The trend continued with 9-bromophenanthrene, which yielded the respective product **3e** in 63% yield. The same tendency was observed for heteroarenes: While 2-fluoro-4-bromopyridine could be converted to the product **3i** in 88% yield, 3-bromoquinoline merely furnished half of the theoretical yield possible (**3j**). Electron-rich 4-bromoanisole, previously reported as a rather challenging substrate for mpg-CN nickel dual-catalysis,[8b] yielded only 28% of the corresponding product **3h**. Next, we

expanded the scope of our mpg-CN/nickel cross-coupling to alkenyl bromides, which were previously shown to undergo cross-coupling under dual catalytic conditions.[13b, 14]

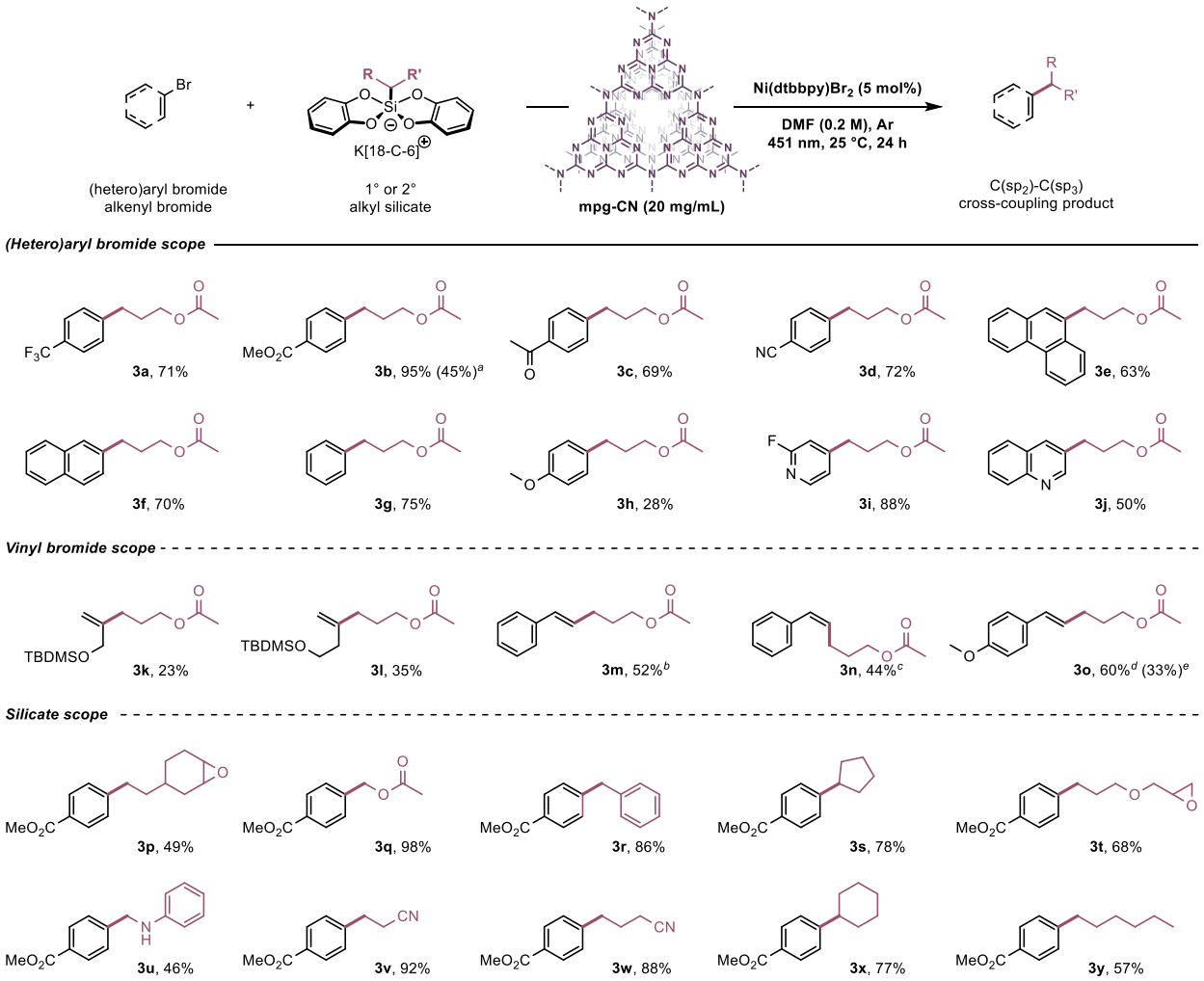

Scheme 3: Substrate scope. Reactions were run at a 0.2 mmol scale in anhydrous DMF (0.2 M) under irradiation with blue LEDs (451 nm) and under an Argon atmosphere for 24 h at 25 °C. Isolated yields are given. [a]1.0 mmol scale (see the experimental section for details). [b]Received as an isomeric mixture (E/Z = 85/15) from the commercial starting material (E/Z = 90/10). [c]Received as an isomeric mixture (E/Z = 22/78) from the (*Z*)-vinyl bromide (E/Z = 02/98). [d]Received as an isomeric mixture (E/Z = 93/7) from the (*E*)-vinyl bromide. [e]Vinyl chloride is used as starting material.

Starting from geminal substituted vinyl bromides, **3k** and **3l** were obtained in 23% and 35% yield, respectively. A commercial mixture of *β*-bromostyrene (E/Z = 90/10) was cross-coupled in 52% yield with a slight decrease of the diastereomeric ratio (**3m**, E/Z = 92/08). *Vice versa*, (*Z*)-*β*-bromostyrene (E/Z = 02/98) yielded product **3n** in 44% yield with an increased amount of the thermodynamically favored E-isomer (E/Z = 22/78). An improved yield of 60% was observed when 4-methoxybromostyrene was subjected to our cross-coupling protocol (**3o**). Further, its alkenyl chloride

derivative could be employed in the reaction, albeit furnishing **3o** with around half the yield compared to the bromide.

Last, we explored the scope of the silicate radical precursors. Both primary and secondary silicates could be employed in this transformation. As an example for the latter ones, cyclohexyl and cyclopropyl silicate were transformed into respective products **3s** and **3x** in 77% and 78% yield. We then turned our attention to the more abundant primary silicates. Radicals derived from benzyl silicate and acetoxymethyl silicate were coupled in 86% and 95% yield (**3q** and **3r**), while methylanilino silicate was converted in only 46% yield to product **3u**. Both cyanoethyl- and propyl silicate were competent coupling partners that reacted to the products **3v** and **3w** in 92% and 88% yield, respectively. A significantly lower amount of product was formed when the parent silicate contained an epoxide, leading to 49% and 68% of product **3t** and **3p**. Lastly, *n*-hexyl benzoate **3y** was synthesized in 57% yield. Recycling experiments demonstrate the reusability of recovered mpg-CN in this reaction (see experimental section).

4.3 Conclusion

We introduced mpg-CN as a sustainable photocatalyst in the dual catalytic cross-coupling of alkyl silicates. A variety of aryl bromides and alkyl silicates, readily accessible from commercially available silanes, reacted to their $C(sp^2)$–$C(sp^3)$ cross-coupling products under the developed conditions. Additionally, alkenyl bromides are competent coupling partners in this transformation. A recycling experiment demonstrates the reusability of the recovered mpg-CN catalyst. Further studies of the recycled material are ongoing.

4.4 Experimental Section

4.4.1 General Information

All NMR spectra were recorded at room temperature using one of the following devices: Bruker Avance 300 (300 MHz for ^{1}H, 75 MHz for ^{13}C, 282 MHz for ^{19}F), Bruker Avance 400 (400 MHz for ^{1}H, 100 MHz for ^{13}C, 376 MHz for ^{19}F). All chemical shifts are reported on the δ-scale in parts per million (ppm) (multiplicity, coupling constant *J* in Hertz (Hz), number of protons) relative to the solvent residual peaks as the internal standard.[15] Abbreviations used for signal multiplicity are br = broad, s = singlet, d = doublet, t = triplet, q = quartet, m = multiplet and combinations thereof. High-resolution mass spectra (HRMS) were obtained from the institute's central analytic mass spectrometry department. Analytical TLC was performed on silica gel-coated alumina plates (MN TLC plates ALUGRAM® Xtra SIL G/UV254). Detection was done by UV light (254 or 366 nm). Infrared spectra were recorded neatly on an Agilent Cary 630 FT-IR Spectrometer; melting points were measured in open capillary tubes by a Stanford Research System OptiMelt MPA 100 and are uncorrected. Compounds were purified by column chromatography with silica gel 60 M (40-63 µm, 230-440 mesh, Machery Nagel). Reactions were irradiated from the bottom (distance ca. 1 cm) with 451 nm LEDs (OSRAM OSLON® SSL 80 GD CS8PM1.14 LEDs, λ= 451 nm (± 15 nm), 5 W optical power) If not otherwise stated below, all chemicals and solvents were obtained from commercial sources. Commercial catechol was recrystallized from chloroform prior to use. DMF was distilled under reduced pressure and stored under argon atmosphere over a molecular sieve. Alkyl silicates and vinyl halides were synthesized according to the literature procedure.[12a, 13a-c, 14a] The nickel catalysts were synthesized as previously described.[16] The mpg-CN catalyst was received from our cooperation partner.

4.4.2 General procedure

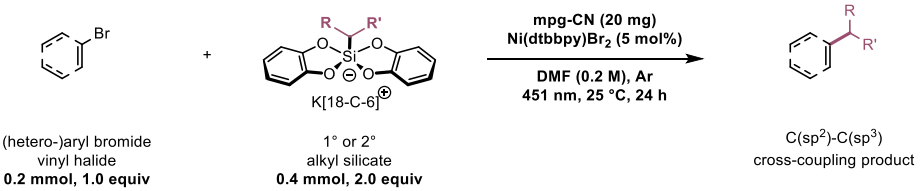

A crimp cap vial was charged with mpg-CN (20 mg), Ni(dtbbpy)Br_2 (4.8 mg, 0.01 mmol, 5 mol%), alkyl silicate (0.40 mmol, 2.0 equiv), solid bromide (0.2 mmol, 1 equiv), and a magnetic stirring bar. The vial was sealed, flushed with argon (3×) before dry DMF (1 mL, 0.2 M) was added. At this point, liquid aryl bromide substrates were added by syringe through the septum. The mixture was

degassed by three *freeze-pump-backfill-thaw* cycles and subsequently irradiated with LEDs (451 nm) for 24 h at 25 °C. The mixture was transferred into a falcon tube, diluted with ethyl acetate (approximately 10 – 15 mL), and centrifuged (5 min, 5000 rpm). The clear supernatant was transferred into a separation funnel while the remaining solid was suspended in ethyl acetate (15 mL) once more and centrifuged again. The mpg-CN pellet can be recovered at this point. The combined supernatants were extracted with saturated aqueous sodium carbonate solution (3 × 25 mL) and brine (1 × 25 mL). The organic phase was dried over sodium sulfate, filtered, and concentrated. The residue was purified by column chromatography (5 g SiO_2) with indicated solvent mixtures. Upon co-elution of bis(catecholato)silane, the fractions were combined in a separation funnel and extracted with saturated aqueous sodium carbonate solution (which turns purple) until a colorless aqueous phase was received.

4.4.3 Recycling Experiments

The recovered mpg-CN pellet was suspended in a minimum (1-3 mL) of ethyl acetate and transferred to a new reaction vial. The falcon tube was washed several times with ethyl acetate to ensure the complete transfer of the heterogeneous material. The solvent was removed and the remaining solid dried in a high vacuum. The new reaction was set up according to the procedure above. The attempt to determine the initial rate of the reaction was hampered by irregular induction periods upon the usage of recovered mpg-CN.

Table 2: Recycling experiments. Reactions were run as described above.

entry	cycle	yield (%)
1	1st (fresh mpg-CN)	74
2	2nd (recovered once)	76
3	3rd (recovered twice)	77
4	4th (recovered thrice)	43

4.4.4 Characterization Data

3-(4-(trifluoromethyl)phenyl)propyl acetate (3a)

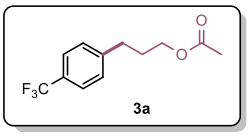

Following the general procedure, the title compound was obtained from 4-bromobenzotrifluoride (27.6 µL, 0.20 mmol, 1.0 equiv) and potassium [18-Crown-6] bis(catecholato)-acetoxypropylsilicate (260 mg, 0.4 mmol, 2.0 equiv) as a colorless oil (35.2 mg, 0.14 mmol, 71%) after purification by column chromatography (5 g SiO_2, P/Et_2O = 90/10) and concentration at 45 °C/150 mbar. The compound was found to evaporate in high vacuum. **^{1}H NMR** (400 MHz, $CDCl_3$) δ (ppm) 7.54 (d, *J* = 8.0 Hz, 2H), 7.36 – 7.27 (m, 2H), 4.09 (t, *J* = 6.5 Hz, 2H), 2.85 – 2.57 (m, 2H), 2.05 (s, 3H), 2.03 – 1.92 (m, 2H). **^{13}C NMR** (101 MHz, $CDCl_3$) δ (ppm) 171.2, 145.5, 128.8, 128.6 (q, *J* = 32.6 Hz), 125.5 (q, *J* = 3.8 Hz), 124.4 (q, *J* = 271.8 Hz), 63.7, 32.2, 30.0, 21.0. **^{19}F NMR** (376 MHz, $CDCl_3$) δ (ppm) -62.4. **HRMS** (APCI): Calc. for $C_{12}H_{13}F_3O_2H^+$ $[M+H]^+$: 247.0940. Found: 247.0941. The data match reported literature values.[13c, 13f]

methyl 4-(3-acetoxypropyl)benzoate (3b)

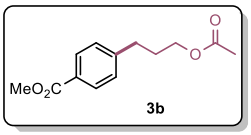

Following the general procedure, the title compound was obtained from methyl 4-bromobenzoate (43.0 mg, 0.20 mmol, 1.0 equiv) and potassium [18-Crown-6] bis(catecholato)-acetoxypropylsilicate (260 mg, 0.4 mmol, 2.0 equiv) as a colorless oil (44.7 mg, 0.19 mmol, 95%) after purification by column chromatography (5 g SiO_2, P/Et_2O = 80/20) and removal of coeluated bis(catecholato)silane by extraction with saturated aqueous sodium carbonate solution. Alternatively, (100 mg mpg-CN, 24 mg Ni(dtbbpy)Br_2), the title compound was obtained from methyl 4-bromobenzoate (213 mg, 1.00 mmol, 1.0 equiv) and potassium [18-Crown-6] bis(catecholato)-acetoxypropylsilicate (1.3 g, 2.00 mmol, 2.0 equiv) as a colorless oil (107.0 mg, 0.45 mmol, 45%; 83% brsm) using mpg-CN (100 mg) and Ni(dtbbpy)Br_2 (24 mg, 5 mol%) after 4 d. 46% of the starting material was recovered. **^{1}H** NMR (400 MHz, $CDCl_3$) δ (ppm) 7.95 (d, *J* = 8.3 Hz, 2H), 7.24 (d, *J* = 8.3 Hz, 2H), 4.07 (t, *J* = 6.5 Hz, 2H), 3.89 (s, 3H), 2.73 (dd, *J* = 8.7, 6.7 Hz, 2H), 2.03 (s, 3H), 1.97 (ddt, *J* = 9.2, 7.6, 6.4 Hz, 2H). **^{13}C NMR** (101 MHz, $CDCl_3$) δ 171.2, 167.1, 146.8, 129.9, 128.5, 128.2, 63.7, 52.1, 32.4, 29.9, 21.0. **HRMS** (ESI): Calc. for $C_{13}H_{16}O_4Na^+$ $[M+Na]^+$: 259.0941. Found: 259.0941. The data match reported literature values.[17]

3-(4-acetylphenyl)propyl acetate (3c)

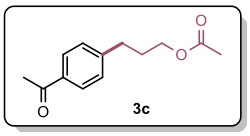

Following the general procedure, the title compound was obtained from 4-bromoacetophenone (39.8 mg, 0.20 mmol, 1.0 equiv) and potassium [18-Crown-6] bis(catecholato)-acetoxypropylsilicate (260 mg, 0.4 mmol, 2.0 equiv) as a yellow oil (30.4 mg, 0.14 mmol, 69%) after purification by column chromatography (5 g SiO_2, P/Et_2O = 70/30) and removal of coeluated bis(catecholato)silane by extraction with saturated aqueous sodium carbonate solution. **^{1}H NMR** (400 MHz, $CDCl_3$) δ (ppm) 7.94 – 7.87 (m, 2H), 7.29 (d, *J* = 8.0 Hz, 2H), 4.10 (t, *J* = 6.5 Hz, 2H), 2.77 (dd, *J* = 8.7, 6.8 Hz, 2H), 2.60 (s, 3H), 2.07 (s, 3H), 2.04 – 1.94 (m, 2H). **^{13}C NMR** (101 MHz, $CDCl_3$) δ (ppm) 197.9, 171.2, 147.1, 135.4, 128.7, 128.7, 63.7, 32.3, 29.9, 26.7, 21.0. **HRMS** (ESI): Calc. for $C_{13}H_{16}O_3Na^+$ $[M+Na]^+$: 243.0992. Found: 243.0991. The data match reported literature values.[13c, 13f]

3-(4-cyanophenyl)propyl acetate (3d)

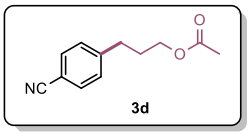

Following the general procedure, the title compound was obtained from 4-bromobenzonitrile (36.4 mg, 0.20 mmol, 1.0 equiv) and potassium [18-Crown-6] bis(catecholato)-acetoxypropylsilicate (260 mg, 0.4 mmol, 2.0 equiv) as a yellow oil (29.3 mg, 0.14 mmol, 72%) after purification by column chromatography (5 g SiO_2, P/Et_2O = 80/20) and removal of coeluated bis(catecholato)silane by extraction with saturated aqueous sodium carbonate solution. **^{1}H NMR** (300 MHz, $CDCl_3$) δ (ppm) 7.58 (d, *J* = 8.0 Hz, 2H), 7.44 – 7.16 (m, 2H), 4.08 (t, *J* = 6.5 Hz, 2H), 3.23 – 2.42 (m, 2H), 2.04 (s, 3H), 2.04 – 1.89 (m, 2H). **^{13}C NMR** (75 MHz, $CDCl_3$) δ (ppm) 171.1, 147.0, 132.4, 129.3, 119.1, 110.2, 63.5, 32.5, 29.8, 21.0. **HRMS** (APCI): Calc. for $C_{12}H_{13}NO_2H^+$ $[M+H]^+$: 204.1019. Found: 204.1019. The data match reported literature values.[13f]

3-(phenanthren-9-yl)propyl acetate (3e)

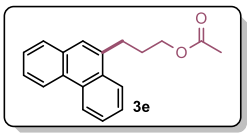

Following the general procedure, the title compound was obtained from 9-bromophenanthrene (51.4 mg, 0.20 mmol, 1.0 equiv) and potassium [18-Crown-6] bis(catecholato)-acetoxypropylsilicate (260 mg, 0.4 mmol, 2.0 equiv) as a colorless solid (34.9 mg, 0.13 mmol, 63%) after purification by column chromatography (5 g SiO_2, P/Et_2O = 90/10). **^{1}H NMR** (400 MHz, $CDCl_3$) δ (ppm) 8.80 – 8.72 (m, 1H), 8.67 (ddd, *J* = 8.0, 1.4, 0.7 Hz, 1H), 8.14 – 8.06 (m, 1H), 7.87 – 7.81 (m, 1H), 7.72 – 7.55 (m, 5H), 4.24 (t, *J* = 6.5 Hz, 2H), 3.25 – 3.16 (m, 2H), 2.24 – 2.13 (m, 2H), 2.11 (s, 3H). **^{13}C NMR** (101 MHz, $CDCl_3$) δ (ppm) 171.3, 135.4, 131.9, 131.2, 130.9, 129.9, 128.2, 126.8, 126.7, 126.4, 126.4, 126.2, 124.3, 123.4, 122.6,

64.3, 29.8, 29.1, 21.1. **HRMS** (APCI): Calc. for $C_{19}H_{18}O_2H^+$ [M+H]$^+$: 279.1380. Found: 279.1384. The data match reported literature values.[13b]

3-(naphthalen-2-yl)propyl acetate (3f)

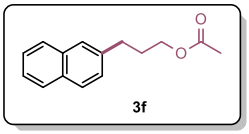

Following the general procedure, the title compound was obtained from 2-bromonaphthalene (41.4 mg, 0.20 mmol, 1.0 equiv) and potassium [18-Crown-6] bis(catecholato)-acetoxypropylsilicate (260 mg, 0.4 mmol, 2.0 equiv) as a colorless oil (32.0 mg, 0.14 mmol, 70%) after purification by column chromatography (5 g SiO_2, P/Et_2O = 90/10). Coeluated 3-bromopropyl acetate was removed in high vacuum. **^{1}H NMR** (300 MHz, $CDCl_3$) δ (ppm) 7.85 – 7.76 (m, 3H), 7.64 (dd, *J* = 2.0, 1.0 Hz, 1H), 7.51 – 7.39 (m, 2H), 7.34 (dd, *J* = 8.4, 1.8 Hz, 1H), 4.14 (t, *J* = 6.6 Hz, 2H), 2.15 – 2.00 (m, 5H). **^{13}C NMR** (101 MHz, $CDCl_3$) δ (ppm) 171.3, 138.8, 133.7, 132.2, 128.2, 127.7, 127.6, 127.3, 126.6, 126.1, 125.4, 64.0, 32.5, 30.2, 21.1. **HRMS** (APCI): Calc. for $C_{15}H_{16}O_2H^+$ [M+H]$^+$: 229.1223. Found: 229.1222.

3-phenylpropyl acetate (3g)

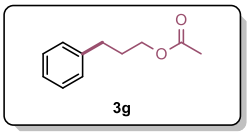

Following the general procedure, the title compound was obtained from bromobenzene (21.3 µL, 0.20 mmol, 1.0 equiv) and potassium [18-Crown-6] bis(catecholato)-acetoxypropylsilicate (260 mg, 0.4 mmol, 2.0 equiv) as a colorless oil (26.7 mg, 0.15 mmol, 75%) after purification by column chromatography (5 g SiO_2, P/Et_2O = 90/10). **^{1}H NMR** (400 MHz, $CDCl_3$) δ (ppm) 7.35 – 7.27 (m, 2H), 7.24 – 7.15 (m, 3H), 4.09 (t, *J* = 6.6 Hz, 2H), 2.69 (dd, *J* = 8.6, 6.8 Hz, 2H), 2.05 (s, 3H), 2.02 – 1.91 (m, 2H). **^{13}C NMR** (101 MHz, $CDCl_3$) δ 171.3, 141.4, 128.6, 128.5, 126.2, 64.0, 32.3, 30.3, 21.1. **HRMS** (APCI): Calc. for $C_{11}H_{14}O_2H^+$ [M+H]$^+$: 179.1067. Found: 179.1066. The data match reported literature values.[13b]

3-(4-methoxyphenyl)propyl acetate (3h)

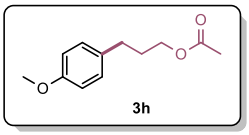

Following the general procedure, the title compound was obtained from 4-bromoanisole (25.0 µL, 0.20 mmol, 1.0 equiv) and potassium [18-Crown-6] bis(catecholato)-acetoxypropylsilicate (260 mg, 0.4 mmol, 2.0 equiv) as a colorless oil (11.8 mg, 0.06 mmol, 28%) after purification by column chromatography (5 g SiO_2, P/Et_2O = 90/10). Coeluated 3-bromopropyl acetate was removed by prolonged concentration at 45 °C/150 mbar. **^{1}H NMR** (300 MHz, $CDCl_3$) δ (ppm) 7.10 (d, *J* = 8.3 Hz, 2H), 6.88 – 6.79 (m, 2H), 4.07 (t, *J* = 6.6 Hz, 2H), 3.79 (s, 3H), 2.63 (t, *J* = 7.7 Hz, 2H), 2.05 (s, 3H), 2.00 – 1.84 (m, 2H). **^{13}C NMR** (101 MHz, $CDCl_3$) δ (ppm) 171.3, 158.1, 133.4, 129.4, 114.0, 64.0, 55.4, 31.4, 30.6, 21.1. **HRMS** (ESI): Calc. for $C_{12}H_{16}O_3Na^+$ [M+Na]$^+$: 231.0992. Found: 231.10993. The data match reported literature values.[13b]

3-(2-fluoropyridin-4-yl)propyl acetate (3i)

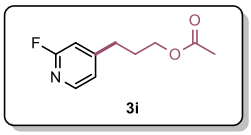

Following the general procedure, the title compound was obtained from 4-bromo-2-fluoropyridine (20.5 µL, 0.20 mmol, 1.0 equiv) and potassium [18-Crown-6] bis(catecholato)-acetoxypropylsilicate (260 mg, 0.4 mmol, 2.0 equiv) as a colorless oil (34.6 mg, 0.18 mmol, 88%) after purification by column chromatography (5 g SiO_2, P/Et_2O = 50/50) and removal of coeluated bis(catecholato)silane by extraction with saturated aqueous sodium carbonate solution. **^{1}H NMR** (400 MHz, $CDCl_3$) δ (ppm) 8.10 (dt, *J* = 5.2, 0.7 Hz, 1H), 7.13 – 6.90 (m, 1H), 6.75 (tt, *J* = 1.5, 0.8 Hz, 1H), 4.09 (t, *J* = 6.4 Hz, 2H), 2.76 – 2.68 (m, 2H), 2.04 (s, 3H), 2.01 – 1.90 (m, 2H). **^{13}C NMR** (101 MHz, $CDCl_3$) δ (ppm) 171.1, 164.3 (d, *J* = 238.4 Hz), 156.3 (d, *J* = 7.8 Hz), 147.6 (d, *J* = 15.3 Hz), 121.7 (d, *J* = 3.8 Hz), 109.2 (d, *J* = 36.9 Hz), 63.4, 31.6 (d, *J* = 2.9 Hz), 29.0, 21.0. **^{19}F NMR** (376 MHz, $CDCl_3$) δ (ppm) -68.8. **HRMS** (ESI): Calc. for $C_{10}H_{12}FNO_2H^+$ $[M+H]^+$: 198.0925. Found: 198.0924. The data match reported literature values.[13b]

3-(quinolin-3-yl)propyl acetate (3j)

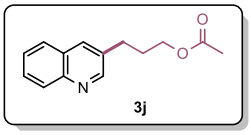

Following the general procedure, the title compound was obtained from 3-bromoquinoline (27.1 µL, 0.20 mmol, 1.0 equiv) and potassium [18-Crown-6] bis(catecholato)-acetoxypropylsilicate (260 mg, 0.4 mmol, 2.0 equiv) as a yellow oil (22.8 mg, 0.10 mmol, 50%) after purification by column chromatography (5 g SiO_2, P/Et_2O = 80/20 → 40/60) and removal of coeluated bis(catecholato)silane by extraction with saturated aqueous sodium carbonate solution. **^{1}H NMR** (400 MHz, $CDCl_3$) δ (ppm) 8.79 (d, *J* = 2.2 Hz, 1H), 8.16 – 8.04 (m, 1H), 7.94 (dd, *J* = 2.3, 1.0 Hz, 1H), 7.77 (dd, *J* = 8.1, 1.4 Hz, 1H), 7.67 (ddd, *J* = 8.5, 6.9, 1.5 Hz, 1H), 7.53 (ddd, *J* = 8.1, 6.8, 1.2 Hz, 1H), 4.15 (t, *J* = 6.4 Hz, 2H), 2.90 (dd, *J* = 8.6, 6.9 Hz, 2H), 2.13 – 2.02 (m, 2H), 2.06 (s, 3H). **^{13}C NMR** (101 MHz, $CDCl_3$) δ (ppm) 171.5, 152.0, 146.9, 134.4, 133.3, 129.4, 128.9, 128.2, 127.5, 126.9, 63.6, 30.0, 29.8, 21.1. **HRMS** (ESI): Calc. for $C_{14}H_{15}NO_2H^+$ $[M+H]^+$: 230.1176. Found: 230.1174. The data match reported literature values.[13b]

4-(((tert-butyldimethylsilyl)oxy)methyl)pent-4-en-1-yl acetate (3k)

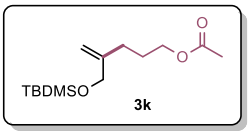

Following the general procedure, the title compound was obtained from ((2-bromoallyl)oxy)(tert-butyl)dimethylsilane (50.3 mg, 0.20 mmol, 1.0 equiv) and potassium [18-Crown-6] bis(catecholato)-acetoxypropylsilicate (260 mg, 0.4 mmol, 2.0 equiv) as a colorless oil (23%) after purification by column chromatography. **^{1}H NMR** (300 MHz, $CDCl_3$) δ (ppm) 5.05 (d, *J* = 1.9 Hz, 1H), 4.89 – 4.76 (m, 1H), 4.21 – 3.89 (m, 4H), 2.10 (m, 2H), 2.04 (s, 3H), 1.80 (dt, *J* = 8.9, 6.7 Hz, 2H), 0.91 (s, 9H), 0.07 (s, 6H).

^{13}C NMR (75 MHz, $CDCl_3$) δ (ppm) 171.1, 147.5, 109.2, 65.9, 64.2, 28.9, 26.7, 25.9, 20.9, 18.4, -5.4. The data match reported literature values.[13b]

6-((tert-butyldimethylsilyl)oxy)-4-methylenehexyl acetate (3l)

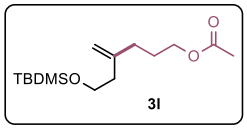

Following the general procedure, the title compound was obtained from ((3-bromobut-3-en-1-yl)oxy)(tert-butyl)dimethylsilane (53.1 mg, 0.20 mmol, 1.0 equiv) and potassium [18-Crown-6] bis(catecholato)-acetoxypropylsilicate (260 mg, 0.4 mmol, 2.0 equiv) as a colorless oil (35%) after purification by column chromatography. **^{1}H NMR** (400 MHz, $CDCl_3$) δ (ppm) 4.77 (dq, *J* = 2.2, 1.3 Hz, 2H), 4.06 (t, *J* = 6.7 Hz, 2H), 3.70 (t, *J* = 7.0 Hz, 2H), 2.24 (td, *J* = 7.0, 1.1 Hz, 2H), 2.14 – 2.06 (m, 2H), 2.04 (s, 3H), 1.83 – 1.71 (m, 2H), 0.89 (s, 9H), 0.05 (s, 6H). **^{13}C NMR** (101 MHz, $CDCl_3$) δ (ppm) 171.3, 145.9, 111.2, 64.3, 62.5, 39.5, 32.9, 26.8, 26.1, 21.1, 18.5, -5.2. **HRMS** (ESI): Calc. for $C_{15}H_{30}O_3SiH^+$ [M+H$^+$]: 287.2037. Found: 287.2038.

(*E*)-5-phenylpent-4-en-1-yl acetate (3m)

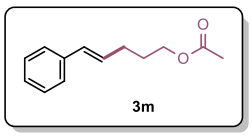

Following the general procedure, the title compound was obtained from commercial (2-bromovinyl)benzene (36.6 mg, 0.20 mmol, 1.0 equiv, E/Z = 90/10) and potassium [18-Crown-6] bis(catecholato)-acetoxypropylsilicate (260 mg, 0.4 mmol, 2.0 equiv) as a colorless oil (52%, E/Z = 85/15) after purification by column chromatography. **^{1}H NMR** (400 MHz, $CDCl_3$) δ (ppm) 7.38 – 7.22 (m, 4H), 7.20 (td, *J* = 5.2, 2.5 Hz, 1H), 6.42 (dt, *J* = 15.9, 1.6 Hz, 1H), 6.20 (dt, *J* = 15.8, 6.9 Hz, 1H), 4.13 (t, *J* = 6.6 Hz, 2H), 2.34 – 2.24 (m, 2H), 2.06 (s, 3H), 1.90 – 1.75 (m, 2H). **^{13}C NMR** (101 MHz, $CDCl_3$) δ (ppm) 171.3, 137.7, 130.8, 129.5, 128.6, 127.2, 126.1, 64.1, 29.5, 28.4, 21.1. The data match reported literature values.[13b]

(*E*)-5-phenylpent-4-en-1-yl acetate (3n)

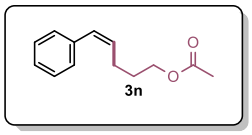

Following the general procedure, the title compound was obtained from (*Z*)-(2-bromovinyl)benzene (36.6 mg, 0.20 mmol, 1.0 equiv, E/Z = 02/98) and potassium [18-Crown-6] bis(catecholato)-acetoxypropylsilicate (260 mg, 0.4 mmol, 2.0 equiv) as a colorless oil (44%, E/Z = 22/78) after purification by column chromatography. **^{1}H NMR** (400 MHz, $CDCl_3$) δ (ppm) 7.40 – 7.10 (m, 5H), 6.49 – 6.42 (m, 1H), 5.64 (dt, *J* = 11.6, 7.3 Hz, 1H), 4.09 (h, *J* = 6.9 Hz, 2H), 2.41 (qd, *J* = 7.4, 1.8 Hz, 2H), 2.00 (s, 3H), 1.78 (m, 2H). The data match reported literature values.[13b]

(*E*)-5-(4-methoxyphenyl)pent-4-en-1-yl acetate (3o)

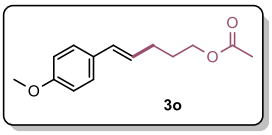

Following the general procedure, the title compound was obtained from (*E*)-1-(2-bromovinyl)-4-methoxybenzene (42.6 mg, 0.20 mmol, 1.0 equiv, E/Z = 02/98) and potassium [18-Crown-6] bis(catecholato)-acetoxypropylsilicate (260 mg, 0.4 mmol, 2.0 equiv) as a colorless oil (60%, E/Z = 93/7) after purification by column chromatography. Alternatively, **3o** was synthesized from (*E*)-1-(2-chlorovinyl)-4-methoxybenzene in 33% yield. (*E*)-isomer (major): **^{1}H NMR** (400 MHz, $CDCl_3$) δ (ppm) 7.33 – 7.26 (m, 2H), 6.88 – 6.82 (m, 2H), 6.38 (dt, *J* = 15.8, 1.6 Hz, 1H), 6.08 (dt, *J* = 15.8, 6.9 Hz, 1H), 4.14 (t, *J* = 6.6 Hz, 2H), 3.82 (s, 3H), 2.33 – 2.24 (m, 2H), 2.08 (s, 3H), 1.91 – 1.77 (m, 2H). **^{13}C NMR** (101 MHz, $CDCl_3$) δ (ppm) 171.3, 158.9, 130.5, 130.2, 127.3, 127.2, 114.1, 64.1, 55.4, 29.5, 28.6, 21.1. (*Z*)-isomer (minor): **^{1}H NMR** (400 MHz, $CDCl_3$) δ (ppm) 7.23 (d, *J* = 8.7 Hz, 2H), 6.90 (d, *J* = 8.8 Hz, 2H), 6.45 – 6.40 (m, 1H), 5.57 (dt, *J* = 11.6, 7.2 Hz, 1H), 4.12 – 4.07 (m, 2H), 3.83 (s, 3H), 2.42 (qd, *J* = 7.4, 1.9 Hz, 2H), 2.03 (s, 3H), 1.90 – 1.75 (m, 2H). The data match reported literature values.[13b]

methyl 4-(2-(7-oxabicyclo[4.1.0]heptan-3-yl)ethyl)benzoate (3p)

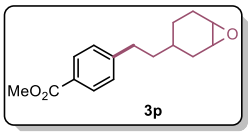

Following the general procedure, the title compound was obtained from methyl 4-bromobenzoate (43.0 mg, 0.20 mmol, 1.0 equiv) and potassium [18-Crown-6] bis(catecholato)-2-(7-oxabicyclo[4.1.0]heptan-3-yl)ethylsilicate (269 mg, 0.4 mmol, 2.0 equiv) as a colorless oil (25.4 mg, 0.10 mmol, 49%) after purification by column chromatography (5 g SiO_2, P/Et_2O = 80/20 → 40/60, 1% triethylamine). The product is an inseparable mixture of diastereoisomeres. **^{1}H NMR** (400 MHz, $CDCl_3$) δ (ppm) 7.96 – 7.92 (m, 2H), 7.22 (d, *J* = 8.3 Hz, 2H), 3.90 (s, 3H), 3.20 – 3.09 (m, 2H), 2.69 – 2.60 (m, 2H), 2.29 – 1.95 (m, 2H), 1.89 – 1.64 (m, 1H), 1.60 – 0.79 (m, 6H). **^{13}C NMR** (101 MHz, $CDCl_3$) δ (ppm) 167.3, 148.3, 148.2, 129.9, 128.5, 128.5, 127.9, 127.9, 53.2, 52.7, 52.1, 52.0, 51.9, 38.3, 38.0, 33.5, 33.2, 32.2, 32.0, 30.7, 29.5, 27.2, 25.3, 24.5, 23.6 (*two carbon signals are missing due to overlap (Ar<u>C</u>-H and O<u>C</u>H$_3$)*. **HRMS** (APCI): Calc. for $C_{16}H_{20}O_3H^+$ $[M+H]^+$: 261.1485. Found: 261.1486. **FTIR** (ν / cm^{-1}): 2924, 1718, 1610, 1433, 1276, 1178, 1109. 1020, 970, 800, 765, 744.

methyl 4-(acetoxymethyl)benzoate (3q)

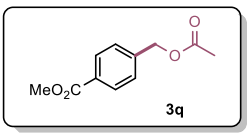

Following the general procedure, the title compound was obtained from methyl 4-bromobenzoate (43.0 mg, 0.20 mmol, 1.0 equiv) and potassium [18-Crown-6] bis(catecholato)-acetoxymethylsilicate (248 mg, 0.4 mmol, 2.0 equiv) as a colorless oil (40.8 mg, 0.19 mmol, 98%) after purification by column chromatography (5 g SiO_2, P/Et_2O = 80/20). **^{1}H NMR** (400 MHz, $CDCl_3$) δ (ppm) 8.03 (d, *J* = 8.4 Hz, 2H), 7.41

(d, *J* = 8.7 Hz, 2H), 5.15 (s, 2H), 3.91 (s, 3H), 2.12 (s, 3H). **^{13}C NMR** (101 MHz, $CDCl_3$) δ (ppm) 170.8, 166.9, 141.1, 130.05, 130.0, 127.8, 65.6, 52.3, 21.0. **HRMS** (ESI): Calc. for $C_{11}H_{12}O_4H^+$ $[M+H]^+$: 209.0808. Found: 209.0808. The data match reported literature values.[18]

methyl 4-benzylbenzoate (3r)

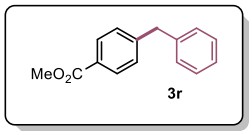

Following the general procedure, the title compound was obtained from methyl 4-bromobenzoate (43.0 mg, 0.20 mmol, 1.0 equiv) and potassium [18-Crown-6] bis(catecholato)-benzylsilicate (256 mg, 0.4 mmol, 2.0 equiv) as a colorless oil (39.1 mg, 0.17 mmol, 86%) after purification by chromatography (5 g SiO_2, P/Et_2O = 90/10). **^{1}H NMR** (400 MHz, $CDCl_3$) δ (ppm) 8.04 – 7.97 (m, 2H), 7.38 – 7.18 (m, 7H), 4.07 (s, 2H), 3.93 (s, 3H). **^{13}C NMR** (101 MHz, $CDCl_3$) δ (ppm) 167.1, 146.6, 140.2, 129.9, 129.1, 128.7, 128.22, 126.5, 52.2, 42.0. **HRMS** (ESI): Calc. for $C_{15}H_{14}O_2H^+$ $[M+H]^+$: 227.1067. Found: 227.1065. The data match reported literature values.[19]

methyl 4-cyclopentylbenzoate (3s)

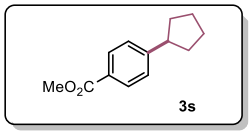

Following the general procedure, the title compound was obtained from methyl 4-bromobenzoate (43.0 mg, 0.20 mmol, 1.0 equiv) and potassium [18-Crown-6] bis(catecholato)-cyclopentylsilicate (247 mg, 0.4 mmol, 2.0 equiv) as a colorless solid (32.0 mg, 0.16 mmol, 78%) after purification by column chromatography (5 g SiO_2, P/Et_2O = 95/05). The isolated sample contains <5% methyl benzoate, which is inseparable by column chromatography.[20] **^{1}H NMR** (400 MHz, $CDCl_3$) δ (ppm) 7.99 – 7.89 (m, 2H), 7.32 – 7.27 (m, 2H), 3.90 (s, 3H), 3.11 – 2.98 (m, 1H), 2.13 – 2.01 (m, 2H), 1.84 – 1.79 (m, 2H), 1.77 – 1.66 (m, 2H), 1.66 – 1.54 (m, 2H). **^{13}C NMR** (101 MHz, $CDCl_3$) δ (ppm) 167.3, 152.3, 129.7, 127.8, 127.3, 52.1, 46.1, 34.6, 25.7. **HRMS** (APCI): Calc. for $C_{13}H_{16}O_2H^+$ $[M+H]^+$: 205.1223. Found: 205.1230. The data match reported literature values.[20]

methyl 4-(3-(oxiran-2-ylmethoxy)propyl)benzoate (3t)

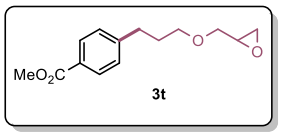

Following the general procedure, the title compound was obtained from methyl 4-bromobenzoate (43.0 mg, 0.20 mmol, 1.0 equiv) and potassium [18-Crown-6] bis(catecholato)-3-glycidyloxypropylsilicate (265 mg, 0.4 mmol, 2.0 equiv) as a yellow oil (34.0 mg, 0.14 mmol, 68%) after purification by column chromatography (5 g SiO_2, P/Et_2O = 80/20) and removal of coeluated bis(catecholato)silane by extraction with saturated aqueous sodium carbonate solution. **^{1}H NMR** (400 MHz, $CDCl_3$) δ (ppm) 7.95 (d, *J* = 8.3 Hz, 2H), 7.26 (d, *J* = 8.2 Hz, 2H), 3.90 (s, 3H), 3.72 (dd, *J* = 11.5, 3.0 Hz, 1H), 3.49 (qt, *J* = 9.4, 6.3 Hz, 2H), 3.36 (dd, *J* = 11.5, 5.9 Hz, 1H), 3.15 (ddt, *J* = 5.8, 4.1, 2.8 Hz, 1H), 2.83 – 2.72 (m,

3H), 2.61 (dd, *J* = 5.0, 2.7 Hz, 1H), 1.98 – 1.87 (m, 2H). **^{13}C NMR** (101 MHz, $CDCl_3$) δ (ppm) 167.3, 147.6, 129.9, 128.6, 128.0, 71.7, 70.5, 52.1, 51.0, 44.4, 32.4, 31.1. **HRMS** (APCI): Calc. for $C_{14}H_{18}O_4H^+$ $[M+H]^+$: 251.1278. Found: 251.1278. **FTIR** (ν / cm^{-1}): 1716, 1608, 1434, 1274, 1020, 966, 904, 856, 835,800, 763, 704.

methyl 4-((phenylamino)methyl)benzoate (3u)

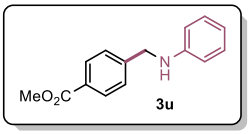

Following the general procedure, the title compound was obtained from methyl 4-bromobenzoate (43.0 mg, 0.20 mmol, 1.0 equiv) and potassium [18-Crown-6]bis(catecholato)-anilinomethylsilicate (262 mg, 0.4 mmol, 2.0 equiv) as a pinkish solid (22.0 mg, 0.09 mmol, 46%) after purification by column chromatography (5 g SiO_2, P/Et_2O = 70/30) and removal of coeluated bis(catecholato)silane by extraction with saturated aqueous sodium carbonate solution. **^{1}H NMR** (400 MHz, $CDCl_3$) δ (ppm) 8.09 – 7.98 (m, 2H), 7.44 (dq, *J* = 7.4, 0.7 Hz, 2H), 7.22 – 7.13 (m, 2H), 6.74 (tt, *J* = 7.4, 1.1 Hz, 1H), 6.65 – 6.58 (m, 2H), 4.41 (s, 2H), 4.15 (s, 1H), 3.92 (s, 3H). **^{13}C NMR** (101 MHz, $CDCl_3$) δ (ppm) 167.1, 147.9, 145.1, 130.1, 129.4, 129.2, 127.3, 118.0, 113.0, 52.2, 48.1. **HRMS** (ESI): Calc. for $C_{15}H_{15}NO_2H^+$ $[M+H]^+$: 242.1176. Found: 242.1175. The data match reported literature values.[21]

methyl 4-(2-cyanoethyl)benzoate (2v)

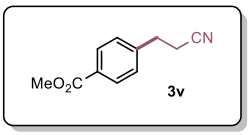

Following the general procedure, the title compound was obtained from methyl 4-bromobenzoate (43.0 mg, 0.20 mmol, 1.0 equiv) and potassium [18-Crown-6] bis(catecholato)-2-cyanoethylsilicate (241 mg, 0.4 mmol, 2.0 equiv) as a colorless solid (35.0 mg, 0.17 mmol, 92%) after purification by column chromatography (5 g SiO_2, P/Et_2O = 90/10) and removal of coeluated bis(catecholato)silane by extraction with saturated aqueous sodium carbonate solution. **^{1}H NMR** (400 MHz, $CDCl_3$) δ (ppm) 8.06 – 7.98 (m, 2H), 7.35 – 7.28 (m, 2H), 3.92 (s, 3H), 3.02 (t, *J* = 7.4 Hz, 2H), 2.65 (t, *J* = 7.4 Hz, 2H). **^{13}C NMR** (101 MHz, $CDCl_3$) δ (ppm) 166.9, 143.2, 130.4, 129.5, 128.5, 118.8, 52.3, 31.6, 19.1. **HRMS** (ESI): Calc. for $C_{11}H_{11}NO_2H^+$ $[M+H]^+$: 190.0863. Found: 190.0862. The data match reported literature values.[22]

methyl 4-(2-cyanopropyl)benzoate (3w)

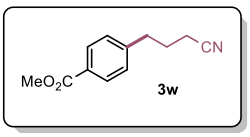

Following the general procedure, the title compound was obtained from methyl 4-bromobenzoate (43.0 mg, 0.20 mmol, 1.0 equiv) and potassium [18-Crown-6] bis(catecholato)-2-cyanopropylsilicate (246 mg, 0.4 mmol, 2.0 equiv) as a colorless solid (35.9 mg, 0.18 mmol, 88%) after purification by column chromatography (5 g SiO_2, P/Et_2O = 90/10) and removal of coeluated bis(catecholato)silane by extraction

with saturated aqueous sodium carbonate solution. **^{1}H NMR** (300 MHz, $CDCl_3$) δ (ppm) 8.05 – 7.96 (m, 2H), 7.25 (d, *J* = 8.1 Hz, 2H), 3.90 (s, 3H), 2.84 (t, *J* = 7.5 Hz, 2H), 2.33 (t, *J* = 7.0 Hz, 2H), 2.00 (p, *J* = 7.2 Hz, 2H). **^{13}C NMR** (75 MHz, $CDCl_3$) δ (ppm) 167.0, 145.2, 130.1, 128.7, 128.6, 119.3, 52.2, 34.5, 26.7, 16.6. **HRMS** (ESI): Calc. for $C_{12}H_{13}NO_2H^+$ $[M+H]^+$: 204.1019. Found: 204.1019. The data match reported literature values.[23]

methyl 4-cyclohexylbenzoate (3x)

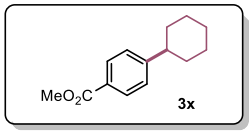

Following the general procedure, the title compound was obtained from methyl 4-bromobenzoate (43.0 mg, 0.20 mmol, 1.0 equiv) and potassium [18-Crown-6] bis(catecholato)-cyclohexylsilicate (252 mg, 0.4 mmol, 2.0 equiv) as a colorless oil (33.6 mg, 0.15 mmol, 77%) after purification by column chromatography (5 g SiO_2, P/Et_2O = 95/05). The isolated sample contains 5% methyl benzoate, which is inseparable by column chromatography. The same is reported for the cyclopentyl derivative.[20] **^{1}H NMR** (400 MHz, $CDCl_3$) δ (ppm) 8.02 – 7.94 (m, 2H), 7.33 – 7.26 (m, 2H), 3.92 (s, 3H), 2.66 – 2.52 (m, 1H), 1.93 – 1.85 (m, 4H), 1.83 – 1.74 (m, 1H), 1.53 – 1.39 (m, 4H), 1.34 – 1.18 (m, 1H). **^{13}C NMR** (101 MHz, $CDCl_3$) δ (ppm) 167.3, 153.6, 129.8, 127.9, 127.0, 52.1, 44.8, 34.3, 26.9, 26.2. **HRMS** (APCI): Calc. for $C_{14}H_{18}O_2H^+$ $[M+H]^+$: 219.1380. Found: 219.1382. The data match reported literature values.[20]

methyl 4-hexylbenzoate (3y)

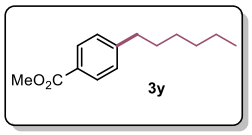

Following the general procedure, the title compound was obtained from methyl 4-bromobenzoate (43.0 mg, 0.20 mmol, 1.0 equiv) and potassium [18-Crown-6] bis(catecholato)-*n*-hexylsilicate (253 mg, 0.4 mmol, 2.0 equiv) as a colorless oil (25.3 mg, 0.11 mmol, 57%) after purification by column chromatography (5 g SiO_2, P/Et_2O = 95/05). **^{1}H NMR** (400 MHz, $CDCl_3$) δ (ppm) 8.10 – 7.60 (m, 2H), 7.36 – 7.14 (m, 2H), 3.90 (s, 3H), 2.82 – 2.49 (m, 2H), 1.74 – 1.57 (m, 2H), 1.35 – 1.23 (m, 6H), 0.95 – 0.80 (m, 3H). **^{13}C NMR** (101 MHz, $CDCl_3$) δ (ppm) 167.4, 148.7, 129.8, 128.6, 127.8, 52.1, 36.2, 31.8, 31.2, 29.1, 22.7, 14.2. **HRMS** (ESI): Calc. for $C_{14}H_{20}O_2H^+$ $[M+H]^+$: 221.1536. Found: 221.1535. The data match reported literature values.[25]

4.5 References

[1] Zuo, Z.; Ahneman, D. T.; Chu, L.; Terrett, J. A.; Doyle, A. G.; MacMillan, D. W., *Science* **2014**, *345*, 437-440.

[2] Tellis, J. C.; Primer, D. N.; Molander, G. A., *Science* **2014**, *345*, 433-436.

[3] (a) Twilton, J.; Le, C.; Zhang, P.; Shaw, M. H.; Evans, R. W.; MacMillan, D. W. C., *Nat. Rev. Chem.* **2017**, *1*; (b) Prier, C. K.; Rankic, D. A.; MacMillan, D. W., *Chem. Rev.* **2013**, *113*, 5322-5363; (c) Badir, S. O.; Molander, G. A., *Chem.* **2020**, *6*, 1327-1339; (d) Milligan, J. A.; Phelan, J. P.; Badir, S. O.; Molander, G. A., *Angew. Chem. Int. Ed.* **2019**, *58*, 6152-6163; (e) Skubi, K. L.; Blum, T. R.; Yoon, T. P., *Chem. Rev.* **2016**, *116*, 10035-10074; (f) Zhu, C.; Yue, H.; Chu, L.; Rueping, M., *Chem. Sci.* **2020**, *11*, 4051-4064.

[4] Mantry, L.; Maayuri, R.; Kumar, V.; Gandeepan, P., *Beilstein J. Org. Chem.* **2021**, *17*, 2209-2259.

[5] Romero, N. A.; Nicewicz, D. A., *Chem. Rev.* **2016**, *116*, 10075-10166.

[6] Rieth, A. J.; Qin, Y.; Martindale, B. C. M.; Nocera, D. G., *J. Am. Chem. Soc.* **2021**, *143*, 4646-4652.

[7] (a) Savateev, A.; Ghosh, I.; Konig, B.; Antonietti, M., *Angew. Chem. Int. Ed.* **2018**, *57*, 15936-15947; (b) Gisbertz, S.; Pieber, B., *ChemPhotoChem* **2020**, *4*, 456-475.

[8] (a) Ghosh, I.; Khamrai, J.; Savateev, A.; Shlapakov, N.; Antonietti, M.; Konig, B., *Science* **2019**, *365*, 360-366; (b) Gisbertz, S.; Reischauer, S.; Pieber, B., *Nat. Catal.* **2020**, *3*, 611-620; (c) Rosso, C.; Gisbertz, S.; Williams, J. D.; Gemoets, H. P. L.; Debrouwer, W.; Pieber, B.; Kappe, C. O., *React. Chem. Eng.* **2020**, *5*, 597-604.

[9] (a) Vijeta, A.; Casadevall, C.; Roy, S.; Reisner, E., *Angew. Chem. Int. Ed.* **2021**, *60*, 8494-8499; (b) Zhao, X.; Deng, C.; Meng, D.; Ji, H.; Chen, C.; Song, W.; Zhao, J., *ACS Catalysis* **2020**, *10*, 15178-15185; (c) Malik, J. A.; Madani, A.; Pieber, B.; Seeberger, P. H., *J. Am. Chem. Soc.* **2020**, *142*, 11042-11049; (d) Cavedon, C.; Madani, A.; Seeberger, P. H.; Pieber, B., *Org. Lett.* **2019**, *21*, 5331-5334; (e) Pieber, B.; Malik, J. A.; Cavedon, C.; Gisbertz, S.; Savateev, A.; Cruz, D.; Heil, T.; Zhang, G.; Seeberger, P. H., *Angew. Chem. Int. Ed.* **2019**, *58*, 9575-9580.

[10] Das, S.; Murugesan, K.; Villegas Rodriguez, G. J.; Kaur, J.; Barham, J. P.; Savateev, A.; Antonietti, M.; Koenig, B., *ACS Catal.* **2021**, *11*, 1593-1603.

[11] Khamrai, J.; Ghosh, I.; Savateev, A.; Antonietti, M.; König, B., *ACS Catal.* **2020**, *10*, 3526-3532.

[12] (a) Corce, V.; Chamoreau, L. M.; Derat, E.; Goddard, J. P.; Ollivier, C.; Fensterbank, L., *Angew. Chem. Int. Ed.* **2015**, *54*, 11414-11418; (b) Jouffroy, M.; Primer, D. N.; Molander, G. A., *J. Am. Chem. Soc.* **2016**, *138*, 475-478.

[13] (a) Levernier, E.; Corcé, V.; Rakotoarison, L.-M.; Smith, A.; Zhang, M.; Ognier, S.; Tatoulian, M.; Ollivier, C.; Fensterbank, L., *Org. Chem. Front.* **2019**, *6*, 1378-1382; (b) Leveque, C.; Chenneberg, L.; Corce, V.; Ollivier, C.; Fensterbank, L., *Chem. Commun.* **2016**, *52*, 9877-9880; (c) Lévêque, C.; Chenneberg, L.; Corcé, V.; Goddard, J.-P.; Ollivier, C.; Fensterbank, L., *Org. Chem. Front.* **2016**, *3*, 462-465; (d) Lin, K.; Wiles, R. J.; Kelly, C. B.; Davies, G. H. M.; Molander, G. A., *ACS Catal.* **2017**, *7*, 5129-5133; (e) Zheng, S.; Primer, D. N.; Molander, G. A., *ACS Catal.* **2017**, *7*, 7957-7961; (f) Patel, N. R.; Molander, G. A., *J. Org. Chem.* **2016**, *81*, 7271-7275; (g) Garcia-Dominguez, A.; Mondal, R.; Nevado, C., *Angew. Chem. Int. Ed.* **2019**, *58*, 12286-12290.

[14] (a) Fensterbank, L.; Ollivier, C.; Abdellaoui, M.; Millanvois, A.; Levernier, E., *Synlett* **2021**, *32*, 1513-1518; (b) Patel, N. R.; Kelly, C. B.; Jouffroy, M.; Molander, G. A., *Org. Lett.* **2016**, *18*, 764-767.

[15] (a) Fulmer, G. R.; Miller, A. J. M.; Sherden, N. H.; Gottlieb, H. E.; Nudelman, A.; Stoltz, B. M.; Bercaw, J. E.; Goldberg, K. I., *Organometallics* **2010**, *29*, 2176-2179; (b) Gottlieb, H. E.; Kotlyar, V.; Nudelman, A., *J. Org. Chem.* **1997**, *62*, 7512-7515.

[16] Schirmer, T. E.; Wimmer, A.; Weinzierl, F. W. C.; Konig, B., *Chem. Commun.* **2019**, *55*, 10796-10799.

[17] Das, A.; Chaudhuri, R.; Liu, R. S., *Chem. Commun.* **2009**, 4046-4048.

[18] Chen, J.; Lin, J. H.; Xiao, J. C., *Chem. Commun.* **2018**, *54*, 7034-7037.

[19] Shen, Y.; Gu, Y.; Martin, R., *J. Am. Chem. Soc.* **2018**, *140*, 12200-12209.

[20] Primer, D. N.; Karakaya, I.; Tellis, J. C.; Molander, G. A., *J. Am. Chem. Soc.* **2015**, *137*, 2195-2198.

[21] Xu, Z.; Wang, D.-S.; Yu, X.; Yang, Y.; Wang, D., *Adv. Synth. Catal.* **2017**, *359*, 3332-3340.

[22] Weweler, J.; Younas, S. L.; Streuff, J., *Angew. Chem. Int. Ed.* **2019**, *58*, 17700-17703.

[23] Suga, T.; Shimazu, S.; Ukaji, Y., *Org. Lett.* **2018**, *20*, 5389-5392.

[24] Martin-Montero, R.; Yatham, V. R.; Yin, H.; Davies, J.; Martin, R., *Org. Lett.* **2019**, *21*, 2947-2951.

Summary

Recent developments in photoredox catalysis provided many new concepts, methodologies, and applications to synthesize organic compounds. One mutual goal for synthetic chemists across different disciplines is to provide facial and straightforward access to the molecule of interest.

One concept to do so in an enantioselective manner is asymmetric ion-pairing catalysis. Despite being part of the chemist's toolbox for quite some time now, its application in the field of photoredox catalysis is relatively scarce. The introductory **Chapter I** provides an overview of current transformations and strategies in counter-ion directed and ion-binding catalysis in the light of photoredox catalysis. The other part of the thesis is dedicated to developing new photochemical methodologies.

Chapter II explores a highly efficient photochemical synthesis of benzophenones. The developed methodology exploits the photophysical properties of the aromatic aldehyde starting material and the diaryl ketone products. Both carbonyl compounds can be photo-excited to their triplet state by UV light and thereby could act as a hydrogen-atom-transfer catalyst to activate the formyl C–H bond. A nickel diimine complex then catalyzes the coupling of the generated acyl radical with various aryl bromides. Through this reactant-focused reaction design, the need for expensive iridium or ruthenium photocatalysts, as well as the additional use of HAT-catalysts, can elegantly be avoided.

Like carbonyl compounds, the decatungstate anion can act as a hydrogen-atom-transfer catalyst upon its excitation with UV light and activate alkanes, which exhibit a rather strong C(sp^3)–H bonds. In **Chapter III**, we applied this exceptional property to synthesize trifluoromethylthiolated compounds. This structural motive is vital in medicinal chemistry, as it adds both lipophilicity and polarity to a compound, properties that generally contradict each other. By identifying the decatungstate anion as a suitable catalyst for the direct transformation of C–H bonds into the C–SCF_3 group, we gained facial access to trifluoromethylthioethers, -acetals, and esters. The applicability of our methodology was demonstrated by the synthesis of SCF_3-derivatives of two drug molecules and the functionalization of several natural products.

Chapter IV revisits photo-nickel dual catalysis and again addresses the quest to replace iridium or ruthenium photocatalysts and run these kinds of cross-coupling reactions more sustainably.

Therefore, the heterogeneous semiconductor material mpg-CN is introduced as an alternative photocatalyst for the cross-coupling of alkyl silicates with aryl and alkenyl bromides. Recycling experiments showed the reusability of the catalyst in this transformation.

Zusammenfassung

In den letzten Jahren wurde eine Vielzahl photochemischer Konzepte und Methoden entwickelt, und in der Synthese organischer Moleküle angewandt. Besonderes Augenmerk liegt dabei auf dem direkten und selektiven Zugang zur Zielstruktur.

Ein bis dato in der Photokatalyse eher selten angewandtes Konzept, um Verbindungen enantioselektiv darzustellen, ist die asymmetrische Ionenpaarkatalyse. Das einleitende **Kapitel I** fasst bisherige Ergebnisse auf diesem Forschungsgebiet zusammen, und geht dabei auf die Unterdisziplinen der Gegenion-vermittelten, und Ionenbindungskatalyse im Zusammenspiel mit photochemischen Prozessen ein. Der andere Teil der vorliegenden Arbeit widmet sich der Entwicklung neuer photochemischer Methoden.

Kapitel II beschreibt die Entwicklung einer effizienten Methode zur Darstellung von Benzophenonen. Die Reaktion basiert auf der Eigenschaft von aromatischen Carbonylverbindungen nach Anregung durch UV-Licht und intersystem crossing in ihren Triplettzustand überzugehen. Das Carbonly im Triplettzustand kann den Formylwasserstoff eines Aldehydausgangsmaterials abstrahieren und das entstandene Acylradical wird dann mit Hilfe eines Nickelkatalysators unter der Bildung einer $C(sp^2)–C(sp^2)$ Bindung mit dem Arylbromid gekuppelt. Durch die Ausnutzung der photophysikalischen Eigenschaften der Edukte und Produkte ist die Zugabe von teuren Ruthenium- und Iridiumkatalysatoren oder die Zugabe eines zusätzlichen HAT-Katalysators nicht notwendig.

Analog den aromatischen Carbonylverbindungen, kann auch das Dekawolframat Anion nach Anregung durch UV-Licht als Wasserstofftransferkatalysator wirken und dabei auch C-H Bindung mit einer hohen Bindungsenergie homolytisch brechen. Basierend auf dieser Eigenschaft wurde in **Kapitel III** eine photochemische Trifluormethylthiolierungsreaktion entwickelt. In der medizinischen Chemie spielen fluorierte Gruppen, darunter die Trifluormethylthiolgruppe, eine wichtige Rolle, da diese gleichzeitig die Lipophiet and die Polarität der Verbindung erhöhen. Das Dekawolframat Anion erwies sich im Rahmen der Studie als geeigneter Photokatalysator für die Darstellung verschiedener Molekülklassen wie Trifluormethylthioether, -acetale und -ester. Die entwickelte Methode ist dabei auch zur Funktionalisierung von Naturstoffen oder zur Synthese von SCF_3-Derivaten verschiedener Wirkstoffe anwendbar.

Kapitel IV beschäftigt sich nochmals mit Photo-Nickel Dualkatalyse und erforscht die Anwendbarkeit des organischen Halbleiters mpg-CN als Photokatalysator in der nickelkatalysierten Arylierung von Alkylsilikaten. Die Anwendung dieses recyclebaren Katalysators macht die Verwendung von metallbasierten Photokatalysatoren überflüssig und die Reaktion daher nachhaltiger.

Appendix

7.1 Abbreviations

°C	degrees Celsius
Å	Ångström (10^{-10}m)
λ	wavelength
4CzIPN	2,4,5,6-Tetrakis(9-carbazol-9-yl) isophthalonitrile
Ar	aryl; arene group
BArf	tetrakis[3,5-bis(trifluoromethyl)phenyl]borate
Bn	benzyl
boc	*tert*-butyloxycarbonyl
BODIPY	dipyrrometheneboron difluoride
BP	benzophenone
bpy	2,2'-bipyridine
bu	butyl
Cbz	benzyloxycarbonyl protectin group
cm	centimeter
Cy	cyclohexyl
DBU	diazabicycloundecene
DCE	dichloroethane
DCM	dichloromethane
DFT	density functional theory
DIPEA	*N*,*N*-diisopropylethylamine
DMA	*N*,*N*-dimethylacetamide
dmbpy	4,4′-dimethyl-2,2′-dipyridyl
DMF	*N*,*N*-dimethylformamide
DMSO	dimethyl sulfoxide
dtbbpy	4,4′-di-*tert*-butyl-2,2′-dipyridyl
EDA	electron donor-acceptor [complex]

e.g.	for example
EI	electron ionization
equiv	equivalent
ESI	electrospray ionization
Et	ethyl
EtOAc	ethyl acetate
eV	electron volt
FID	flame ionization detector
g	gram
GC	gas chromatography
h	hour(s)
HAT	hydrogen atom transfer
HEH	Hantzsch Ester (1,4-dihydro-2,6-dimethyl-3,5-pyridinedicarboxylate)
HRMS	high resolution mass spectrometry
^{i}Pr	isopropyl
K	Kelvin
L	liter
LED	light emitting diode
M	molar (mol/L)
Me	methyl
MeCN	acetonitrile
Mes-Acr	9-mesityl-10-methylacridinium
mg	milligram
mpg-CN	mesoporous graphitic carbon nitride
Ms	methanesulfonyl group
min	minute
mL	milliliter
mM	millimolar (mmol/L)
mmol	millimole
MP.	melting point
MS	mass spectrometry
MTBE	methyl-*tert*-butlyether

n-Bu	*n*-butyl
nm	nanometer
NMR	nuclear magnetic resonance
OAc	acetoxy group
PC	photocatalyst
PE	petroleum ether
Ph	phenyl
phen	1,10-phenanthroline
Phth	phthalimide, phthalimidyl
PMP	*para*-methoxyphenyl
ppy	2-phenylpyridinato
PTC	phase-transfer catalysis/catalyst
R	rest, e.g. alkyl-, aryl- or other functional groups
r.t.	room temperature
s	second
SCE	saturated calomel electrode
SET	single electron transfer
^{t}Bu	*tert*-butyl
TBADT	tetra-*n*-butylammonium decatungstate
TEMPO	(2,2,6,6-tetramethylpiperidin-1-yl)oxyl
Tf	triflyl (trifluoromethanesulfonyl)
THF	tetrahydrofuran
THIQ	tetrahydroisoquinoline
Tip	2,4,6-triisopropylphenyl group
TIPS-EBX	1-[(Triisopropylsilyl)ethynyl]-1,2-benziodoxol-3(1*H*)-one
TLC	thin layer chromatography
TPP	5,10,15,20-Tetraphenylporphyrin
TMS	trimethylsilyl
Ts	toluene sulfonyl group
UV	ultra violet
Vis	visible light
vs.	against

7.2 NMR-Spectra of Unknown and Unpublished Compounds

4-(((tert-butyldimethylsilyl)oxy)methyl)pent-4-en-1-yl acetate (^{1}H NMR, 300 MHz, $CDCl_3$)

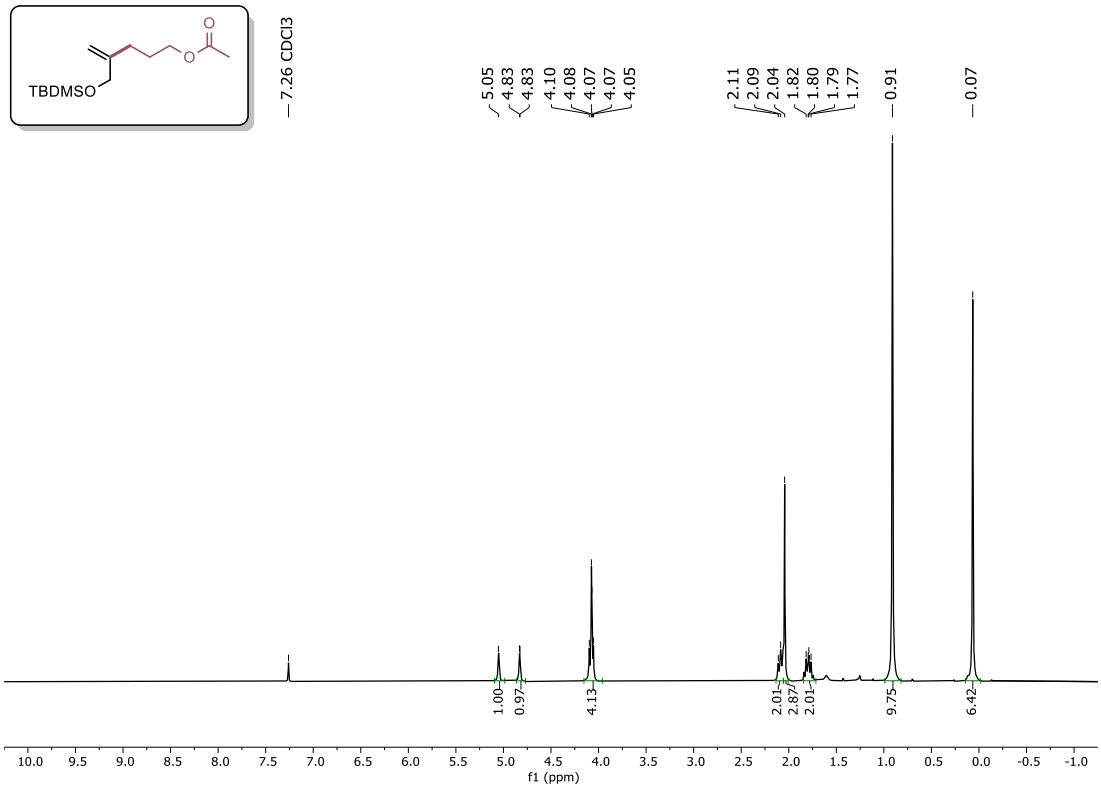

4-(((tert-butyldimethylsilyl)oxy)methyl)pent-4-en-1-yl acetate (^{13}C NMR, 75 MHz, $CDCl_3$)

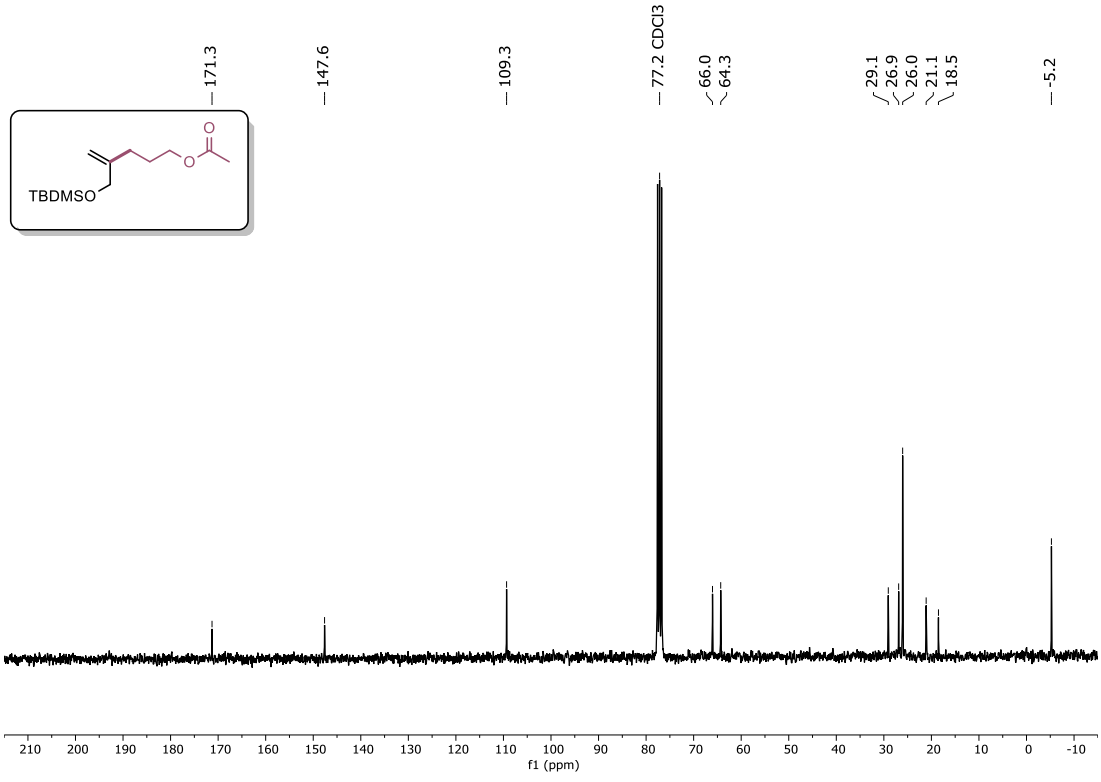

methyl 4-(2-(7-oxabicyclo[4.1.0]heptan-3-yl)ethyl)benzoate (^{1}H NMR, 400 MHz, $CDCl_3$)

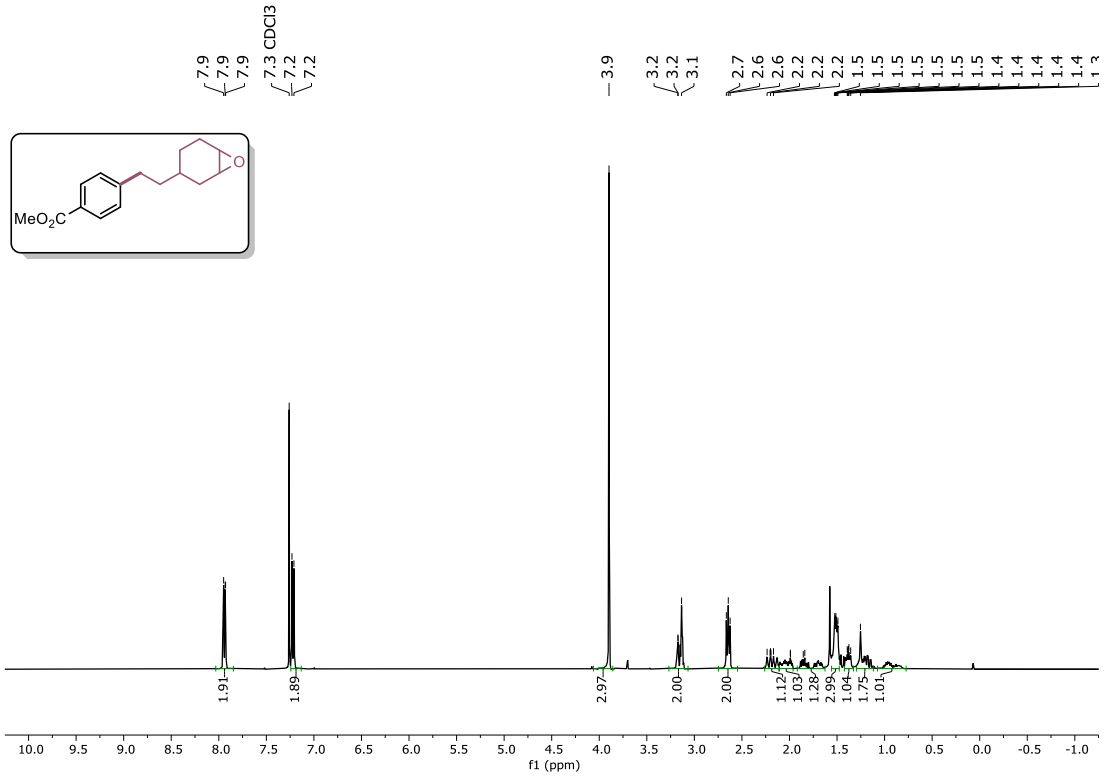

methyl 4-(2-(7-oxabicyclo[4.1.0]heptan-3-yl)ethyl)benzoate (^{13}C NMR, 101 MHz, $CDCl_3$)

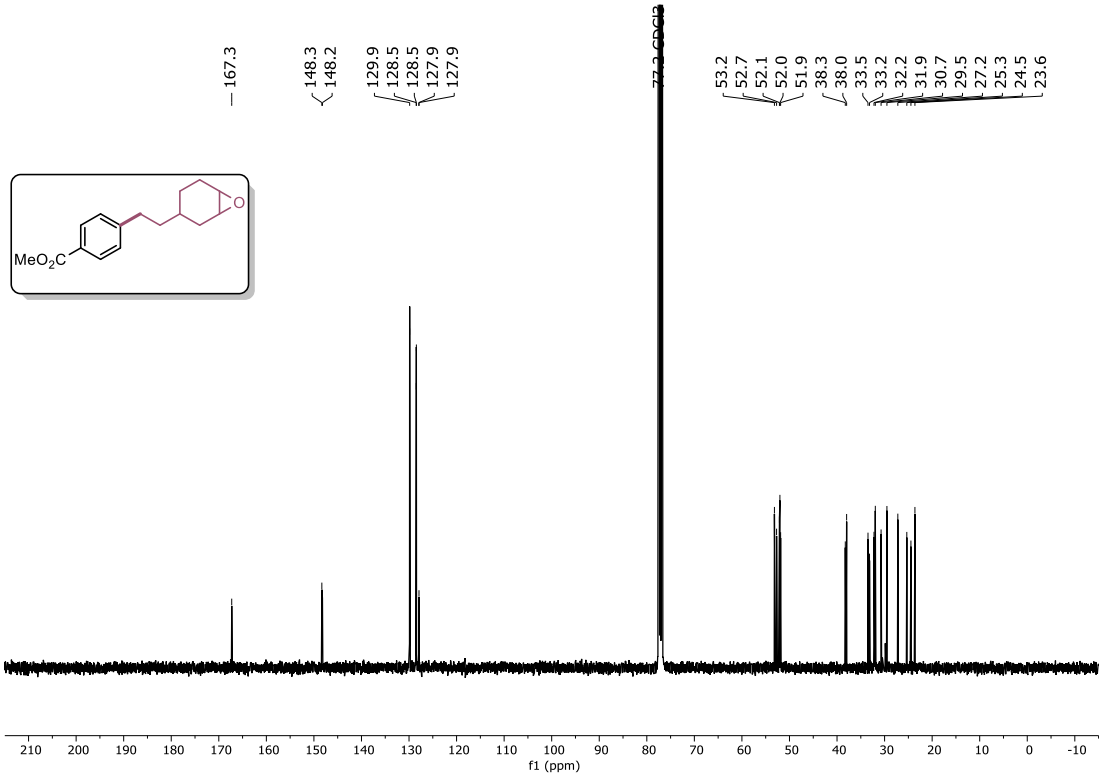

methyl 4-(3-(oxiran-2-ylmethoxy)propyl)benzoate (^{1}H NMR, 400 MHz, $CDCl_3$)

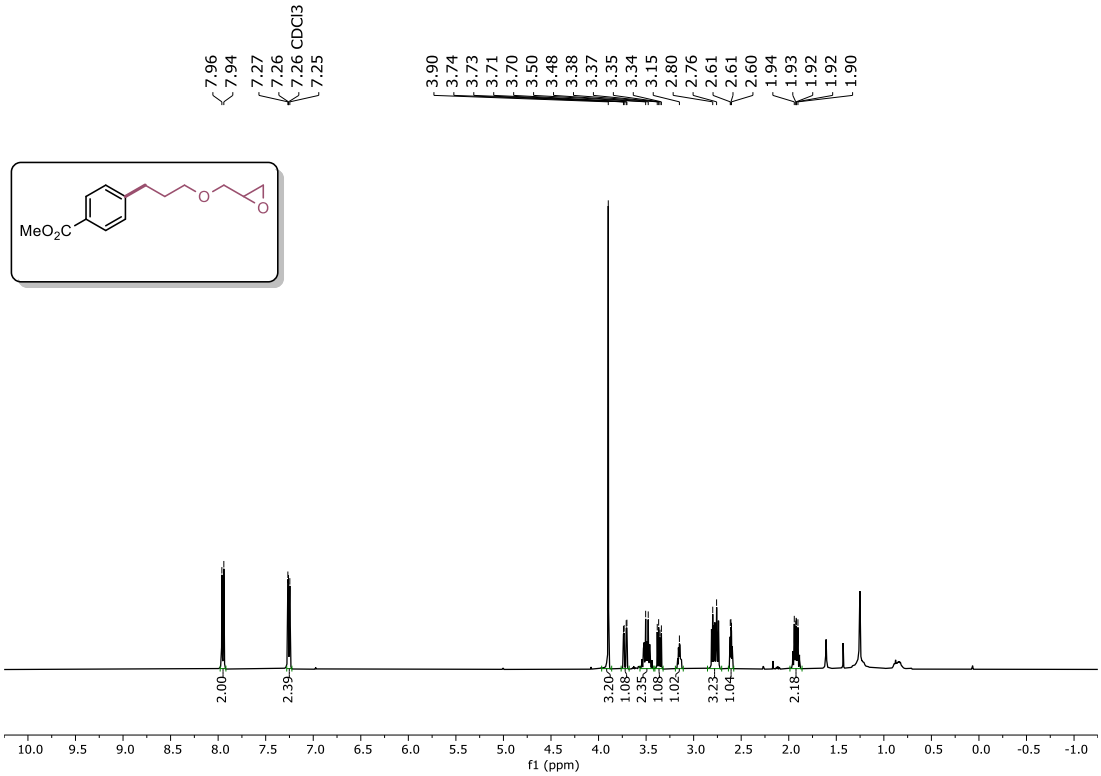

methyl 4-(3-(oxiran-2-ylmethoxy)propyl)benzoate (^{13}C NMR, 101 MHz, $CDCl_3$)

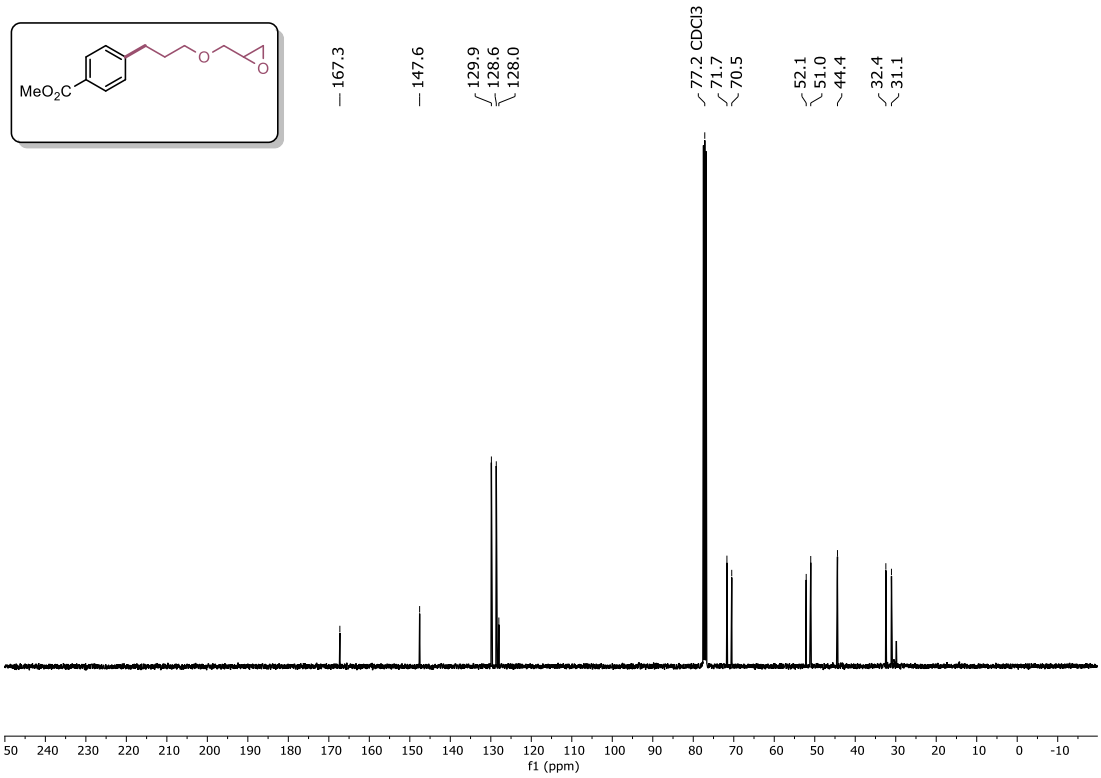

7.3 Curriculum Vitae

PERSONAL DATA

Name:	Tobias Emanuel Schirmer
Nationality:	German
Date and Place of Birth:	19.02.1991 in Starnberg, Germany

ACADEMIC RESEARCH

01/2018 – 12/2021	Doctoral thesis, group of Prof. König, University of Regensburg *Development of Novel Photochemical Transformations*
06/2021 – 12/2021	Visiting Scientist at *Sorbonne Université - Campus Pierre et Marie Curie,* Paris, group of Prof. Fensterbank.
04/2016 – 09/2016	Master's thesis, group of Prof. Bach, TUM: *Towards the Dihydroxylation of 4-Aryl-quinolones*

EDUCATION

10/2014 – 09/2016	Master of Science in Chemistry Major: Organic Chemistry, Minor: Inorganic Chemistry Technical University Munich (TUM)
10/2012 – 09/2014	Bachelor of Science in Chemistry (TUM)
10/2010 – 10/2013	Bachelor of Science in Biochemistry (TUM)

PUBLICATIONS

4. Tobias E. Schirmer, Alessa B. Rolka, Tobias A. Karl, Ferdinand Holzhausen and Burkhard König, Photocatalytic C–H Trifluoromethylthiolation by the Decatungstate Anion. *Org. Lett.* **2021**, *23*, 5729.

3. Tobias E. Schirmer, Alexander Wimmer, Florian W. C. Weinzierl and Burkhard König, Photo-Nickel Dual Catalytic Benzoylation of Aryl Bromides. *Chem. Commun.* **2019**, *55*, 10796-10799.

2. Qing-Yuan Meng, Tobias E. Schirmer, Anna Lucia Berger, Karsten Donabauer and Burkhard König, Photocarboxylation of Benzylic C–H Bonds. *J. Am. Chem. Soc* **2019**, *141*, 11393–11397.

1. Qing-Yuan Meng, Tobias E. Schirmer, Kousuke Katou and Prof. Burkhard König, Controllable Isomerization of Alkenes by Dual Visible-Light-Cobalt Catalysis. *Angew. Chem. Int. Ed.* **2019**, *58*, 5723–5728.

7.4 Eidestattliche Erklärung

Ich erkläre hiermit an Eid statt, dass ich die vorliegende Arbeit ohne unzulässige Hilfe Dritter und ohne Benutzung anderer als der angegebenen Hilfsmittel angefertigt habe; die aus anderen Quellen direkt oder indirekt übernommenen Daten und Konzepte sind unter Angabe des Literaturzitats gekennzeichnet.

Bei der Auswahl und Auswertung folgenden Materials haben mir die nachstehend aufgeführten Personen in der jeweils beschriebenen Weise unentgeltlich geholfen:

1. Chapter II: Gekennzeichnete Experimente wurden von Alexander Wimmer durchgeführt. Forian Weinzierl unterstützte das Projekt als Praktikant.
2. Chapter III: Gekennzeichnete Experimente wurden von Alessa Rolka und Tobias Karl durchgeführt. Ferdinand Holzhausen unterstütze das Projekt als Praktikant.
3. Chapter IV: Gekennzeichnete Experimente wurden von Mehdi Abdellaoui durchgeführt.
4. Die Manuskripte wurden von den in den jeweiligen Kapiteln angegebenen Personen mitverfasst bzw. verbessert oder korrigiert.

Weitere Personen waren an der inhaltlich-materiellen Herstellung der vorliegenden Arbeit nicht beteiligt. Insbesondere habe ich hierfür nicht die entgeltliche Hilfe eines Promotionsberaters oder anderer Personen in Anspruch genommen. Niemand hat von mir weder unmittelbar noch mittelbar geldwerte Leistungen für Arbeiten erhalten, die im Zusammenhang mit dem Inhalt der vorgelegten Dissertation stehen.

Die Arbeit wurde bisher weder im In- noch im Ausland in gleicher oder ähnlicher Form einer anderen Prüfungsbehörde vorgelegt.

Ich versichere an Eides statt, dass ich nach bestem Wissen die reine Wahrheit gesagt und nichts verschwiegen habe.

Acknowledgements

This enterprise would not have been possible without the assistant, support, and encouragement of my supervisors, my fellow researchers, friends, and family, whom I would like to acknowledge in the following.

I am grateful to Prof. Burkhard König for accepting me into his group and for the opportunity to work in the field of photocatalysis. I enjoyed the freedom to pursue my own ideas and was thereby granted the chance to develop into the scientist I am today. I am particularly grateful for his support and encouragement to pursue a research-stay abroad. The research-stay in Paris was a gratifying experience.

It would not have been possible without Prof. Louis Fensterbank, who spontaneously accepted me as visiting researcher in his laboratories. I would like to express my thanks for this and for being the second referee of my thesis.

I thank Prof. Robert Wolf and Prof. Julia Rehbein for joining the examinations board.

My sincere thanks go to my cooperation partners, who strongly contributed to the success of my projects with creative ideas, their expertise, and their practical capabilities. In this context, I would like to thank Alexander Wimmer, Alessa Rolka, Tobias Karl, and Mehdi Abdellaoui, as well as my research students Jose Cammarata, Florian Weinzierl, and Ferdinand Holzhausen.

I warmly thank my labmates Dr. Andi Gramml, Dr. Tanguy Saget, and Dr. Bartosz Bieszczad, who were dear companions during the ups and downs of the thesis and who are now my friends. I am grateful for the constantly positive lab environment that reigned in Lab 26 in their presence. Paris would not have been such a pleasant experience without my great colleagues Pierre de Sevin, Lukas Enders, Dr. Omar Sadek, Dr. Jade Dussart, and Dr. Daisuke Sakomoto, whom I would like to thank as well.

I sincerely thank my mentor and friend, Dr. Qing-Yuan Meng, from whom I learned a lot while he helped me to get started. I also would like to thank Dr. Indrajit Ghosh for his advice, the many discussions over the years, and, most importantly, for his friendship.

I would like to thank Andi, Tobi, Karsten, Alessa, Michela, Matthias, Alex, Anna, Rok, Karin, Saikat, Greg, Shun, Uli, and all other colleagues from the group for all the discussions, evenings spent together; the cooking, the Weißwurstfrühstück, and the door-art competitions.

I also would like to thank Julia Zach, Katharina Nickl, Barbara Bauer, and the glassblower team of the faculty for their incredible support during all those years.

I would like to thank my friends and my family. Without my best friends Jakob, Maxi, Carsten, Benni, Christopher, Malena, Philippe, Jan, and Jonas, I certainly would not be where I am today. For their unconditional and never-ending support, I would like to thank my mother, Barbara, and my sister Mona as well as my grandparents Ingrid and Erich Oppermann. I am deeply grateful to my godmother Irmi, who incredibly generously supported me throughout my studies.

Finally, I would like to thank my dearest Katharina for her patience, for her incredible support throughout the last years, for being such a wonderful person, and for being a part of my life.